Max-Planck-Institut für Metallforschung
Stuttgart

Micro/nanomechanical measurements on insect and plant cuticles

Nato Barbakadze

Dissertation
an der
Universität Stuttgart

Bericht Nr. 172
April 2005

Micro/nanomechanical measurements on insect and plant cuticles

Von der Fakultät für Chemie der Universität Stuttgart
zur Erlangung der Würde eines Doktors der
Naturwissenschaften (Dr. rer. nat.) genehmigte Abhandlung

Vorgelegt von

Dipl.-Ing. Nato Barbakadze

aus Tbilissi

Hauptberichter:	Prof. Dr. phil. Eduard Arzt
Mitberichter:	Prof. Dr. rer. nat. Alexander Wanner
Tag der mündlichen Prüfung:	19.04.2005

Max-Planck-Institut für Metallforschung Stuttgart
Institut für Metallkunde der Universität Stuttgart

2005

ვუძღვნი
ჩემს საყვარელ
დედიკოს და მამიკოს!

To my dear
mammy and daddy!

”ცუდად ხომ მაინც არ ჩაივლის ეს განწირულის სულის კვეთება,
და გზა უვალი, შენგან თელილი, მერანო ჩემო, მაინც დარჩება;
და ჩემს შემდგომად მოძმესა ჩემსა სიძნელე გზისა გაუადვილდეს!”

ნიკოლოზ ბარათაშვილი

”The yearnings of my restless soul will no in vain have glowed,
For, dashing on, my steel has paved a new untrodden road.
He who follows in our wake, a smoother path will find!”

Nikoloz Baratashvili

Danksagung

Die vorliegende Dissertation wurde von Dezember 2001 bis Februar 2005 am Max-Planck-Institut für Metallforschung und am Institut für Metallkunde der Universität Stuttgart durchgeführt.

Herrn Prof. Dr. E. Arzt danke ich herzlich für die Aufnahme als Doktorandin, für seine professionellen Ratschläge und fruchtbare Diskussionen.

Herrn Prof. Dr. A. Wanner danke ich für seine Hilfsbereitschaft und für die freundliche Übernahme des Mitberichts.

Ich danke Frau Dr. S. Enders und Herrn Dr. S. Gorb für die Betreuung der Arbeit. Herrn Dr. S. Gorb danke ich besonders für das große Interesse an dieser Arbeit, seine konstruktive Kritik, das große Vertrauen und seine ständige Hilfsbereitschaft.

Frau Dr. O. Gorb, Frau Dr. U. Wegst, Herrn Prof. Dr. R. Spolenak und Herrn Dr. A. Peressadko danke ich herzlich für ihre Diskussionsbereitschaft sowie vielfältige Unterstützung.

Herrn O. Bullinger danke ich für seine Unterstützung bei Computer Tomographie (IKP).

Ich möchte mich herzlich bei meinen Kolleginnen und Kollegen für die angenehme und freundschaftliche Atmosphäre bedanken. Ulrike, Camilla, Birgit und Chris danke ich besonders für die Unterstützung und ihre Freundschaft.

Meiner Familie: meinen lieben Eltern, Naira und Johndo, sowie meinen Bruder, Artschil und meiner Cousine, Natia möchte ich besonders herzlich für ihre große Geduld und vielfältige Unterstützung danken.

Ich möchte mich bei all meinen Freunden für ihre Geduld bedanken. Ganz herzlich möchte ich meinen lieben Freunden, Laura und Luc, Eva und Gerrit, Lena und Stas, Brigitte und Ralph, Maia, Barbara, Guillaume, Arancha und Dagmar für ihre Unterstützung und Hilfsbereitschaft danken. In großem Vertrauen und Liebe - sie sind meine zweite Familie hier in Stuttgart.

Table of Contents

Symbols

A	contact area	[m²]
α	radius of contact	[m]
β	geometric constant of indenter tip	[]
γ	work of adhesion	[J/m²]
γ_1	surface energy	[J/m²]
γ_2	surface energy	[J/m²]
γ_{12}	interfacial energy	[J/m²]
ε	geometric constant of indenter	[]
E^*	reduced elastic modulus	[Pa]
E	Young's modulus	[Pa]
F	load	[N]
F_{AN}	applied normal load	[N]
F_{max}	peak load	[N]
F_N	normal load	[N]
F_L	attractive force	[N]
$F_{pull\text{-}off}$	pull-off force	[N]
F_T	tangential force	[N]
H	hardness	[Pa]
h	displacement	[m]
h_{max}	depth at peak load	[m]
h_f	final depth after unloading	[m]
h_c	contact depth	[m]

h_{sx}	elastic deflection	[m]
k	geometric constant of indenter tip	[]
μ	friction coefficient	[]
n	number of indents	[]
ν_1	Poisson's ratio	[]
ν_2	Poisson's ratio	[]
R	radius	[m]
R_a	average surface roughness	[m]
R_z	average absolute value of ten-point height	[m]
rms	root mean square	[m]
S_{max}	initial unloading contact stiffness	[Pa]
t	film thickness	[m]

Nato Barbakadze

Micro/nanomechanical measurements on insect and plant cuticles

128 pages, 60 figures, 4 tables

Abstract

Head articulation cuticle of the beetle (*Pachnoda marginata)* designed for friction minimization and wax covered pea (*Pisum sativum)* plant surfaces adapted for insect attachment prevention have been studied. Both insect and plant cuticles are multilayered fiber-composite materials. All samples were tested in fresh and dry conditions to observe the effect of desiccation. To understand the influence of an outer wax/lipid layer, tribo-mechanical experiments on the *gula* cuticle were performed as well in a chemically treated condition. Mechanical properties were determined by nanoindentation. Due to the high damping coefficient and high resonant frequency of the indenter it was possible to determine mechanical properties of materials with low contact stiffness and low damping coefficients. Continuous stiffness measurement (CSM) allowed hardness and elastic modulus to be calculated at every data point acquired during the indentation. The mechanical behavior of all samples was found to be greatly influenced by desiccation. However the effect on hardness and elastic modulus were different for insect and plant cuticles. Desiccation made *gula* cuticle of the beetle harder and stiffer but the plant surface softer and more compliant. Chemical treatment caused further hardening and stiffening of the *gula* cuticle. All fresh plants exhibited the same mechanical behavior apparently due to the influence of cell walls and especially pressure of the cell-fluid. Dry samples with normal wax layer were softer and more compliant than with reduced waxy bloom. Friction properties of the *gula* cuticle were influenced by different factors. Fresh samples were smooth, soft and compliant and exhibited higher friction coefficients than dry ones, which were rough, hard and stiff. Chemically treated cuticles showed the lowest friction coefficient. This study is believed to be one of the first for the mechanical testing of insect cuticles and the very first for wax coated plant surfaces in native condition.

Nato Barbakadze

Mikro/nanomechanische Messungen an Insekten- und Pflanzencuticula

128 Seiten, 60 Abbildungen, 4 Tabellen

Kurzzusammenfassung

Im Rahmen dieser Arbeit wurden die für die Reibungsreduzierung optimierten Cuticulae des Kopfgelenksystems des Rosenkäfers (*Pachnoda marginata*) und die für die Haftprävention adaptierten wachsbeschichteten Pflanzenoberflächen (Erbse *Pisum sativum*) untersucht. Beide, Insekten- und Pflanzencuticulae sind Faserverbundstoffe, welche schichtweise aufgebaut sind. Um den Einfluss des Wassergehaltes zu studieren, wurden die Experimente an allen Proben in frischem und trockenem Zustand durchgeführt. Das tribo-mechanische Verhalten wurde auch an chemisch behandelten Proben der *Gula*-Cuticula untersucht. Für die Ermittlung der lokalen mechanischen Eigenschaften wurden Nanoindentationsexperimente verwendet. Durch einen großen Dämpfungskoeffizient und eine hohe Resonanzfrequenz ermöglichte das Gerät die Durchführung von Messungen an Materialien mit niedriger Kontaktsteifigkeit und kleinem Dämpfungskoeffizient. Die kontinuierliche Steifigkeitsmessung (CSM Methode) erlaubte während des Versuchs die Berechnung der Härte und des Elastizitätsmoduls bei jeder Eindringtiefe. Die mechanischen Eigenschaften der Insekten- und Pflanzencuticulae änderten sich wesentlich in Abhängigkeit vom Feuchtigkeitsverlust. Nach der Austrocknung war die Insektencuticula härter und steifer, während die trockenen Pflanzenoberflächen weicher und nachgiebiger als die frischen waren. Die chemische Behandlung erhöhte die Härte und die Steifigkeit der *Gula*-Cuticula zusätzlich. Auf Grund der Wirkung des Zellflüssigkeitsdruckes und der Zellwände, wiesen alle frischen Pflanzen das gleiche mechanische Verhalten auf. Die trockenen Erbsenproben mit reduzierter Wachsschicht waren härter und steifer als die mit normaler Wachschicht. Die Reibung war von mehreren Faktoren abhängig. Die glatte Oberfläche der frischen, weichen und nachgiebigen *Gula*-Cuticulae zeigte den höchsten Reibungskoeffizient im vergleich zu trockenen, harten und steifen Proben, die eine hohe Oberflächenrauhigkeit aufwiesen. Die chemisch behandelten Cuticulae zeigten den kleinsten Reibungskoeffizienten. Nanoindentationsversuche an biologischen Materialien wurden hierbei erstmalig im natürlichen Zustand durchgeführt.

1 Introduction

An extension of the lifetime of machines is of increasing importance. The breakdown of instruments is often caused by tribological failures, which are friction and wear-related. Maximizing the friction and wear resistance of the contacting pairs by optimizing tribo-mechanical properties of the surface materials plays an important role in different industrial applications (Holmberg, 2001). The miniaturisation of technical systems creates the need for today's science and engineering to assess the tribological properties of small volumes of material. Specific structures and properties across several length scales are fascinating in biological systems (Ball, 2002). Determining the extraordinary properties of natural materials at the nanometer scale is regarded as a very attractive target of materials research. However, tribological systems in biology have not been studied much from a materials science point of view. The majority of work in tribology research has focused on the material properties and working mechanisms of human and animal joints (Fung 1993; Persson 1998). It was found that articular cartilage has a unique quality of lubrication and shock absorption that is mainly due to the multilayer structure (Fung, 1993). Being related to bone, cartilage has a very small coefficient of friction for relative motion between two articular pieces (Fung, 1993). There are considerable data in the literature about ultrastructural architecture and mechanical properties of the arthropod cuticle (Fraenkel and Rudal, 1940; Neville, 1975; Hepburn and Joffe, 1976; Andersen, 1979; Andersen *et al*., 1996; Vincent, 1980; 2002; Binnington and Retnakaran, 1991; Gorb, 1997; Arzt *et al*., 2002; Enders *et al*., 2004; Vincent and Wegst, 2004). It is the most widely distributed high-performance composite material after plant cell and wood (Vincent, 2002). Much work has been published on the correlation of microtribological properties of biological systems with its material structure (Scherge and Gorb 2000; Gorb and Scherege 2000; Gorb *et al*. 2001; Dai *et al*. 2002; Gorb and Perez Goodwyn 2003; Perez Goodwyn and Gorb 2004).

Wax coated plant surfaces were studied in relation to insect attachment systems over the last century (Kerner von Marilaun, 1898). Great work has been done on the structure and the chemical composition of the wax crystals (Hallam and Chambers, 1976; Bianchi *et al*., 1978; Haas and Schonherr, 1979; Baker, 1982; Avato *et al*., 1984; Jeffree, 1986; Baker and Gaskin, 1987; Walton, 1990; Barthlott, 1990; Bianchi, 1995; Barthlott *et al*., 1998; Gorb, 2001;

Eigenbrode and Jetter, 2002; Gorb and Gorb, 2002). However little is known about the mechanical properties of the wax layer.

This study aims to explore mechanical performance of insect and plant cuticle using the material sciences approach. In order to observe the influence of water loss, the mechanical properties were studied in fresh and dry conditions using nanoindentation. The experiments on the insect cuticle were curried out in chemically treated condition as well. Chapter 2 gives the motivation, a brief description of natural materials, the important issues in determining the mechanical properties by nanoindentation and same tribological details. The mechanical properties of insect and plant cuticles determined by nanoindentation are presented in chapter 3 and 5 respectively. Chapter 4 characterizes the tribological behavior of the *gula* cuticle in the beetle *Pachnoda marginata*. The brief summary of the mechanical behavior of biological materials is presented in chapter 6.

2 Motivation and literature review

"Why should engineers be interested in biological materials?
One only has to look to the history of technology, starting from the first use of tools, to see that revolution and progress are driven by the new possibilities which new materials create."

Julian Vincent

The improvement of surface properties and development of new materials with specific functionality play an important role with respect to the introduction to new technologies. The miniaturization of engineering systems requires from modern techniques to evaluate the mechanical properties of materials in very small dimensions. The biological systems, which because of the long evolution period optimally combine the mechanical (stability, elasticity) and tribological (friction, adhesion, wear) properties, are excellent models for the design of new micromechanically applicable materials.

The structural design and the tribo-mechanical performance of biological systems as well as the development of new techniques allowing the testing of soft materials in micro/nanometer range have motivated this study. An attempt to use the modern experimental techniques of material science to determine the mechanical properties of natural materials will contribute to the bridging gap between engineering and biology. The goal of this study is to explore the structural and mechanical design of biological materials and to find interesting properties providing one step forward to enter into the development of novel materials. In this chapter natural materials and tribo-mechanical mechanisms expected to play a role in studying natural materials are introduced. The details related to each biological surface and experimental procedure used in this work will be described in chapters 3, 4 and 5.

2.1 Biological materials

Natural materials have been used in engineering over twelve millennia. The first houses and bridges were built from grass, wood and stone. The first clothes and shoes were made from animal skins. There are still no alternatives to wood and horsehair for many musical instruments (Wegst and Ashby, 2004). We use natural materials everyday. They are always around us and the interest in biological systems is still growing. The natural systems inspire the engineering sciences in the design of new materials. One example is the development of different replacement tissues from metal or plastic (Vincent, 1990).

Most natural materials are structured fiber-matrix composites (Wainwright *et al*., 1976; Vincent, 1990). The components in them are quite similar. They consist mainly of natural polymer fibers embedded in a protein matrix. For example, cellulose, pectin and protein build a plant cell wall (Wegst and Ashby, 2004); insect cuticle is the composite of chitin and protein (Neville, 1975; Wainwright *et al*., 1976; Vincent, 1990; Vincent and Wegst, 2004). The biological materials exhibit a hierarchical structure. Natural systems such as skin, bone, cartilage and cuticle are layered composites with different single layer structures.

Despite the limited constituents, the natural systems display a great variety of mechanical properties. Collagen and elastin are the main components in skin, bone and cartilage. However, depending on the amount of the constituents and the fiber orientation, each system has different mechanical properties (Wegst and Ashby, 2004).

The structural and mechanical design of natural systems can be mimicked to provide new so called “intelligent” materials with “smart” structures. Skin, for instance, shows compressive properties useful in the development of tactile sensors (Vincent, 1990). The man-made hydrophobic surfaces have been inspirited from the “lotus effect” of the plant leaf. The technique of the turn around of the beetle arouses the interest of robotics researchers to design a robot being able to cope with any difficulties in movement.

In figures 2.1 and 2.2 (Vincent and Wegst, 2004) the wide spectrum of mechanical properties of natural materials is shown. Figure 2.1 presents Vickers hardness for a range of natural

materials. For example, the arthropod (invertebrates) cuticle displays a great variation of hardness values depending on its function and condition (wet or dry). In the figure 2.2 Young's modulus is plotted versus density for different natural materials. Again arthropod cuticle shows different elastic modulus comparable with human skin, cork, wood and even aluminum.

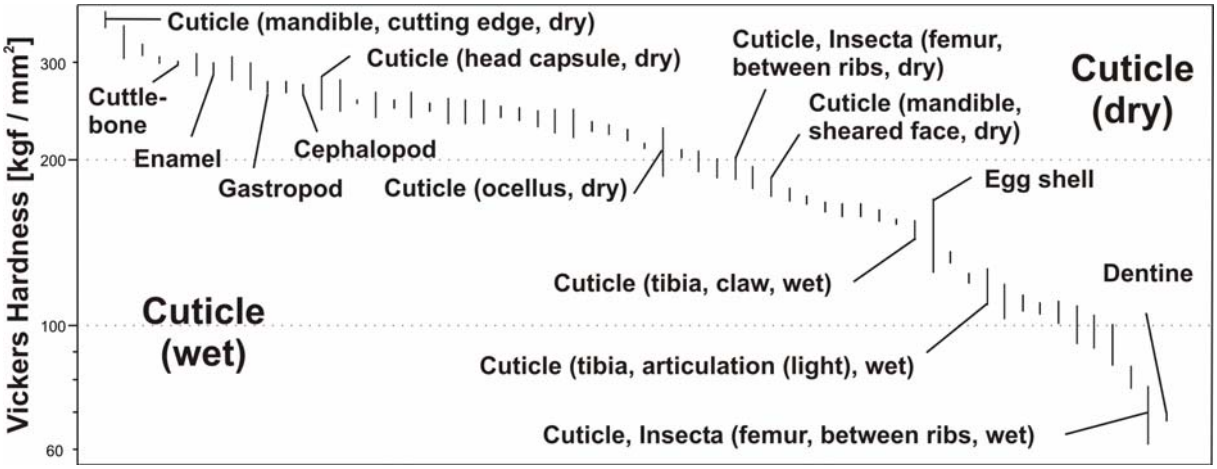

Figure 2.1: A compilation of hardness data for natural materials. (Figure adapted from Vincent and Wegst, 2004, created using the Natural Materials Selector).

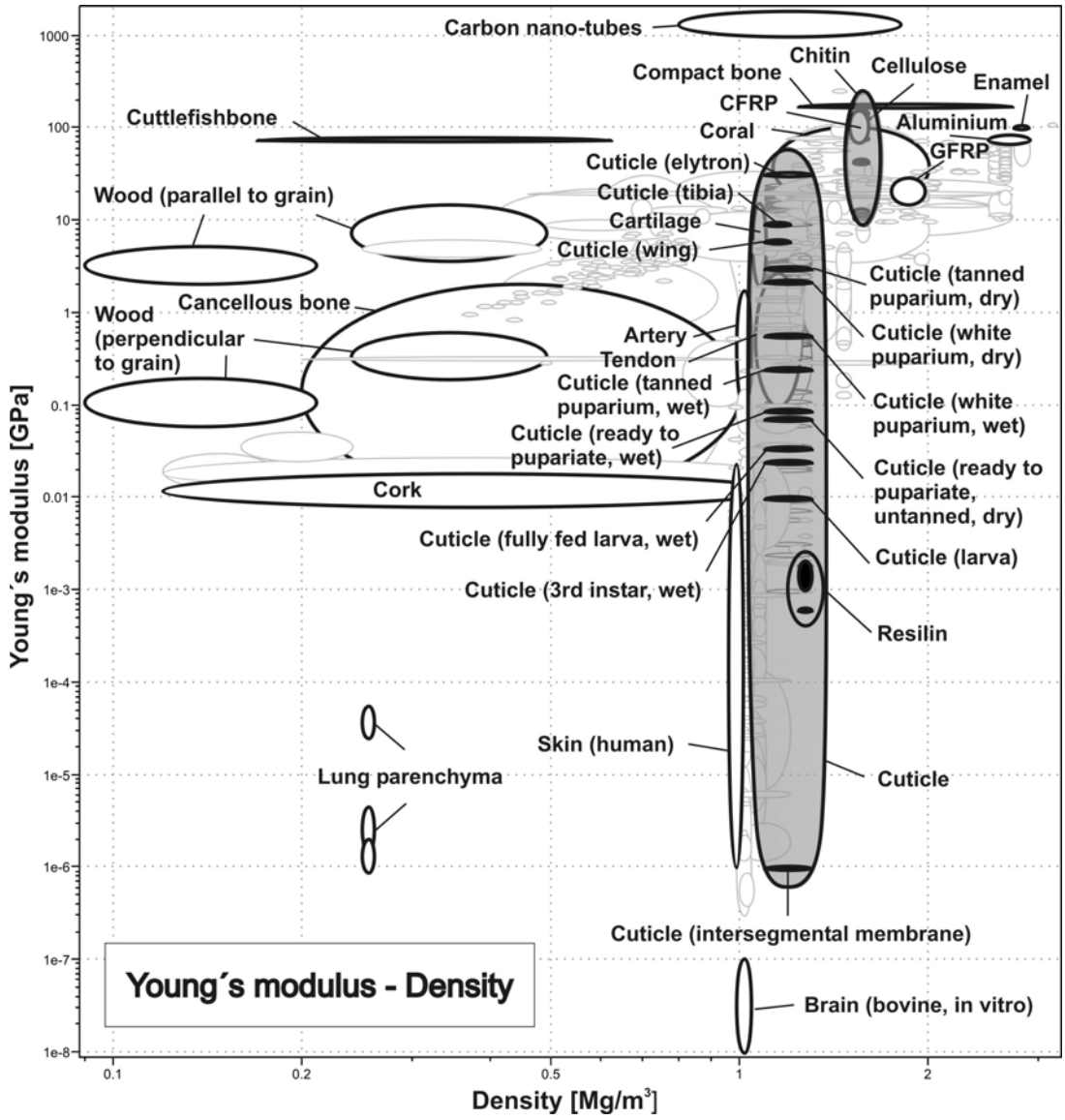

Figure 2.2: Young's modulus versus density chart for natural materials. (Figure adapted from Vincent and Wegst, 2004, created using the Natural Materials Selector).

2.2 Mechanical property measurements by indentation

Mechanical properties of materials have been commonly studied for almost a century using an indentation technique. First tests were done by Brinell with a spherical ball (Tabor 1951; Bhushan, 1999; Li and Bhushan, 2002). The miniaturisation of engineering involving the ultrathin films and the nanocomposits required probing mechanical properties in a small volume of material. The tribological performance of surfaces in micro/nanoelectromechanical systems (MEMS/NEMS) is mainly determined by the mechanical behavior of a few atomic layers of contacting materials. These technical developments created the need to get knowledge of mechanical properties in a small volume. Therefore the Brinell test was rapidly extended down to the micro- and nanometer range (e.g. Tabor 1996; Li and Bhushan, 2002).

An instrumented indentation technique is based on the deformation of the test material using a sharp indenter tip with high hardness and elastic modulus. Smooth surface and well defined geometry are also required for the tip. The most used material here is diamond with an elastic modulus E = 1140 GPa and Poisson's ratio $\nu = 0.07$. A three-sided sharply pointed Berkovich tip is preferred over spherical, conical or pyramidal indenters, especially for nanoindentation testing of thin films (e.g. Li and Bhushan, 2002; Bhushan and Li, 2003).

Mechanical properties such as hardness and elastic modulus are determined from the load-displacement data obtained from the complete loading and unloading cycle (Doerner and Nix, 1986). Modern machines, such as the Nano Indenter XP and Nano Indenter SA2, provide the additional function of continuous stiffness measurement (CSM), developed by Oliver and Pharr (1992). The CSM technique and a method for calculating hardness and elastic modulus values are described in Chapter 3.

Indentation techniques record the elastic-plastic deformation behavior of the material. Depending on the material properties, the solids deform differently. Figure 2.3 shows typical load-displacement curves, surface deformation and residual impression of the indent after indentation test for an ideally elastic, a perfectly plastic and a real elastic-plastic material. The load-displacement curves for the ideally elastic solid coincide with each other (figure 2.3 A). The sample undergoes only elastic deformation, which recovers completely after tip removal

and consequently no impression remains on the surface. The perfectly plastic solid deforms only plastically. Therefore no recovery occurs and the impression of the indent does not change. In the case of the elastic-plastic surface, the sample deforms first elastically and then plastically during the loading process. During the unloading an elastic recovery takes place. The deformation of most materials follows the real elastic-plastic behavior (Bhushan and Li, 2003).

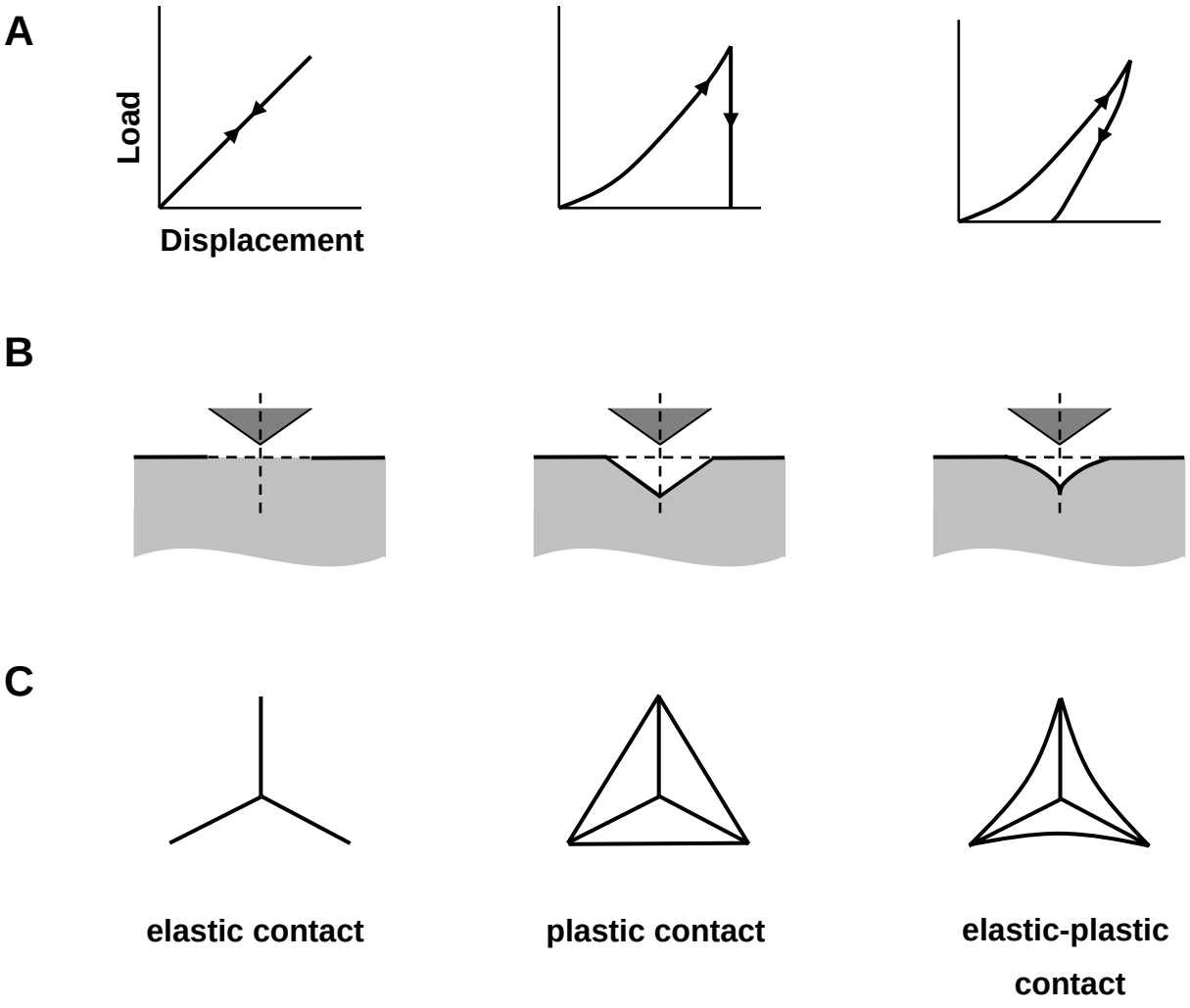

Figure 2.3: Schematics of typical (**A**) load-displacement curves, (**B**) surface deformation after tip removal and (**C**) residual impression of indent on the surface for ideally elastic, perfectly plastic and real elastic-plastic materials (after Li and Bhushan, 2002).

The calculation of mechanical properties is based on the indentation depth (Pethica *et al*., 1983; Doerner *et al*., 1990; Nix *et al*., 1992; Oliver and Pharr, 1992; Hay *et al*., 1999). However depending on the material properties, depth measurements can be subject to some error due to the pile-up and sink-in effect around the indenter (figure 2.4). The results can vary significantly, especially for thin films due to the hardness and elastic modulus differences between the film and the substrate. Pile-up causes the calculation of the contact area smaller than the actual one, while sink-in results in larger calculated contact area. This leads to overestimation or underestimation of the hardness value, respectively (Phillips, 2003; Bhushan and Li, 2003).

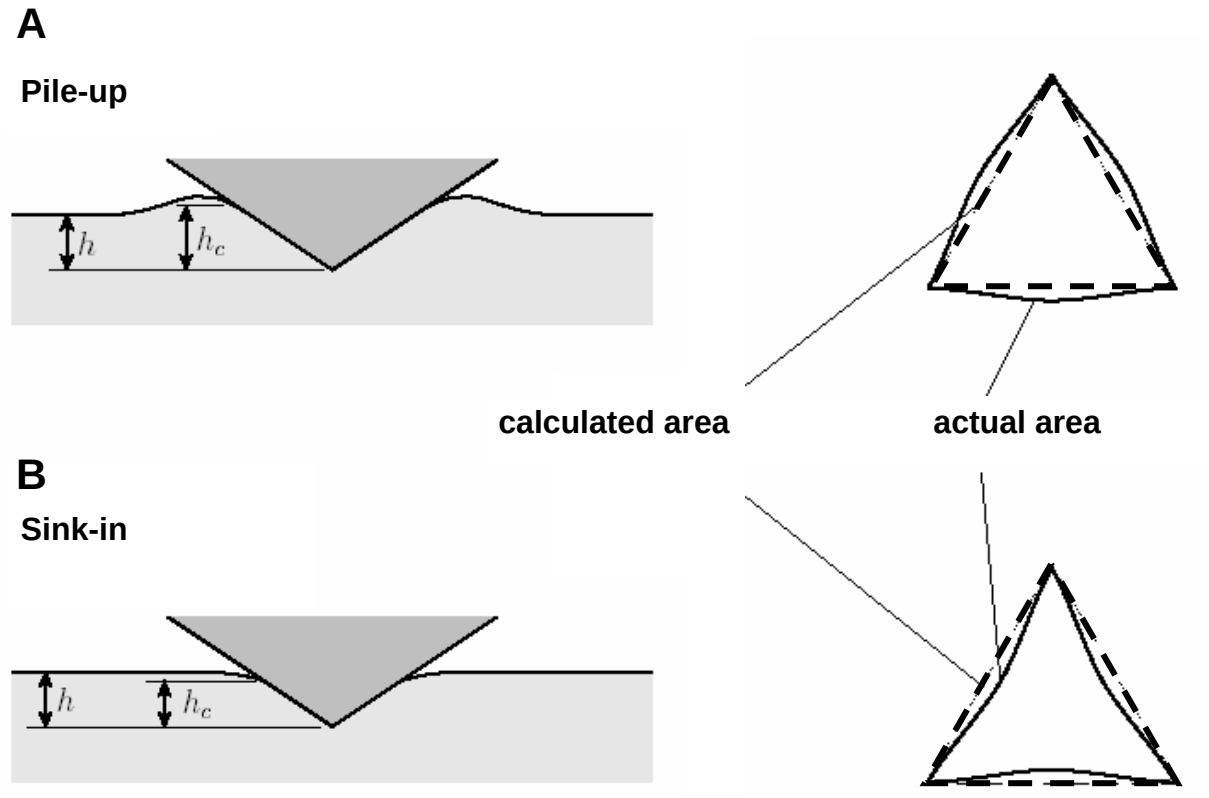

Figure 2.4: Schematic diagrams of (A) pile-up and (B) sink-in around the indenter tip during the indentation. (A) shows that for a pile-up ($h_c > h$) the calculated contact area is smaller than actual contact area; for sink-in (B) ($h_c < h$) the calculated contact area is larger than the actual contact area (taken from Phillips, 2003).

During the past decades, nanoindentation techniques have been commonly used for testing thin metal films. However the separation of mechanical properties of the thin film from the influence of the substrate can become quite difficult. Considerable work has been carried out to determine the hardness of the thin metal film without the substrate effect (Jönsson and Hogmark, 1984; Burnett and Rickerby, 1987; McGurck *et al*., 1994; Korsunsky *et al*., 1998). It is suggested that the hardness of the thin metal film without the substrate influence can be obtained if the indentation depth does not exceed 30% of the film thickness (ASME, 1979). However, after Bueckle (1965), Bhushan (1996) and Bhushan and Li (2003), this value is as low as 10 %. The elasticity and consequently elastic modulus value is believed to be a long-range effect.

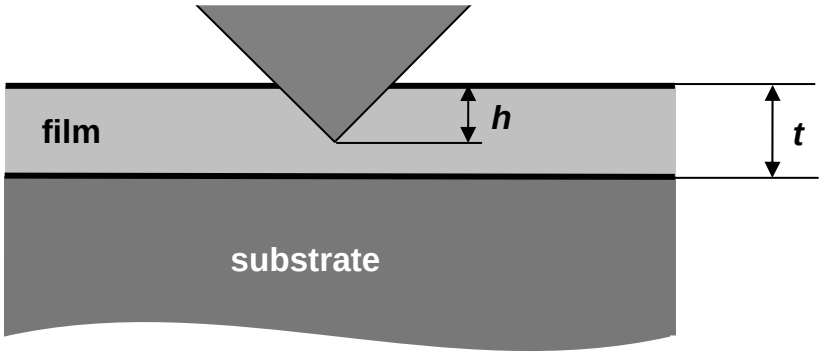

Figure 2.5: Schematic of the film-substrate composite during the indentation. t is the film thickness; h is the indentation depth. The hardness of the film can be obtained when after ASME (1979) $h < 0.3\ t$ and after Bueckle (1965) and Bhushan (1996; 2003) $h < 0.1\ t$.

Only a few studies have been performed to determine the mechanical properties of biological surfaces by indentation. Up to now there are no models describing the deformation behavior of soft materials. Therefore this work attempts, using an experience in the fields of solids and thin metal films, to describe events occurring in various biological materials.

2.3 Tribological properties

Tribology is the science of interacting surfaces in relative motion. The root is the Greek word "tribos", which means rubbing. Tribology combines the fields of friction, wear, lubrication and contact mechanics. It also includes surface topography, lubricant properties (chemical and physical), hydrodynamics, solid mechanics and methods of surface analysis, mechanical dynamics and surface chemistry (Rabinowicz, 1995; Hutchings, 1992; Tichy and Meyer, 2000; Ludema, 2000). The friction related tribological events will be described in Chapter 4.

The contact of dry smooth spheres, when adhesion is neglected, can be described with the model of Heinrich Hertz (Hertz, 1882). His theory considers only elastic deformations of the spherical bodies. The radius of the real area of contact between the surfaces is obtained as

$$a = \left(\frac{3}{4} \cdot \frac{F \cdot R}{E^*} \right)^{1/3} \tag{2.1}$$

where F is the applied normal load, R is the reduced radius and can be calculated with the equation

$$\frac{1}{R} = \frac{1}{R_1} + \frac{1}{R_2} \tag{2.2}$$

where R_1 and R_2 are radii of the contacting spherical bodies respectively.

E^* is the reduced elastic modulus and can be calculated with the equation

$$\frac{1}{E^*} = \frac{\left(1 - \nu^2_1\right)}{E_1} + \frac{\left(1 - \nu_2{}^2\right)}{E_2} \tag{2.3}$$

where E_1 and E_2 are the Young's modulus, ν_1 and ν_2 the Poisson's ratio of the contact spherical bodies respectively.

Johnson, Kendall and Roberts (1971) include adhesive contributions in the contact model. Thus the Hertz equation, modified to take into account the surface energy effect, becomes

$$a^3 = \frac{3}{4}\frac{R}{E^*}\left(F + 3\gamma\pi R + \sqrt{6\gamma\pi R F + (3\gamma\pi R)^2}\right) \tag{2.4}$$

The force required to separate the contacting bodies (called *pull-off* force) is independent of the elastic modulus and is given by

$$F_{pull-off} = -\frac{3}{2}\gamma\pi R \tag{2.5}$$

γ is a work of adhesion and can be obtained as

$$\gamma = \gamma_1 + \gamma_2 - \gamma_{12} \tag{2.6}$$

γ_1 and γ_2 are surface energy of contact bodies respectively. γ_{12} is interfacial energy.

A schematic of the contact radius curves as a function of the applied normal force followed equations (2.1) and (2.4) is given in figure 2.6.

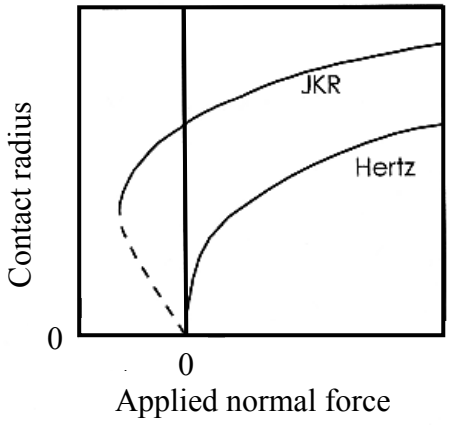

Figure 2.6: Contact radius as a function of the applied normal load calculated without adhesion forces (Hertz theory) and with adhesion forces (JKR theory) (after Persson, 1998).

3 Local mechanical properties of the head articulation cuticle in the beetle *Pachnoda marginata* (Coleoptera, Scarabaeidae)

Abstract

The cuticle (the exoskeleton of an insect) in the head articulation system of the beetle *Pachnoda marginata* is a multilayered fiber-composite material, providing high mechanical stability. We used scanning electron microscopy (SEM) to obtain information about the material structure of the *gula* plate, the head part of the head articulation system. Our results show that the surface of this cuticle is very smooth and that the fibers of the exocuticle (layer of the cuticle) are oriented perpendicular to the surface. Nanoindentation experiments were performed to determine the local mechanical properties such as hardness and elastic modulus. To understand the effect of desiccation and the influence of an outer wax layer on the mechanical behavior, the samples were tested in fresh, dry and chemically treated conditions. Nanoindentation results were found to be strongly influenced by desiccation, but only slightly by chemical treatment. Decreasing water content (about 60 % of the initial mass of the entire head) led to an increase in hardness (from 0.1 GPa to 0.4 GPa) and elastic modulus (from 1.5 GPa to 6.8 GPa). Chemical treatment caused further hardening (0.5 GPa) as well as stiffening (7.0 GPa) of the material.

3.1 Introduction

The body of insects is completely covered by cuticle, which is a multifunctional interface between the animal and the environment (Hepburn and Joffe, 1976; Gorb, 2001). It serves primarily as an exoskeleton that gives the body its shape and stability. The cuticle is also a main barrier against evaporation of water from the body and protects the insects against desiccation (Locke, 1964; Binnington and Retnakaran, 1992).

Like most biological materials, cuticle is a fiber composite (Hepburn and Chandler, 1980). The fibers consist of chitin and the matrix is formed by proteins. Chitin is a natural polymer composed of 300 nm long and 3 nm thick nanofibrils (Vincent, 1980; 2002). Each nanofibril contains about 19 molecular chains (Fraenkel and Rudall, 1940; Vincent, 1980; 2002) running antiparallel to one another (i.e. alpha chitin) (Neville, 1975; Vincent, 1980). Chitin filaments are distributed in the protein matrix (Andersen et al., 1996) which stabilises the chitin. Water contained in the proteins (about 90 % of the protein matrix) presumably functions to separate the two main components of the cuticle from each other (Vincent, 1980).

Arthropod (invertebrates – animals without backbones) cuticle has a multilayer structure (Neville, 1975; Andersen, 1979) (figure 3.1). It typically consists of three main layers: epicuticle, exocuticle and endocuticle. The latter two layers form the procuticle. In some insects there is a mesocuticle between the endocuticle and the exocuticle (Neville, 1975; Andersen, 1979; Binnington and Retnakaran, 1992). The nonchitinous, tanned lipoproteinous epicuticle is the outer layer of the cuticle, which is very thin and has a relatively high tensile strength. The surface of the epicuticle is coated with wax and lipids. The hard and stiff solid part has a dense chitin-protein structure and forms the exocuticle. The endocuticle is the thickest region of the cuticle and has a low chitin content (Locke 1964; Neville 1975, Binnington and Retnakaran 1992).

From a mechanical point of view, there are two main types of insect cuticle: soft and hard. In larvae the cuticle is soft and colorless. A simultaneous hardening and darkening, called sclerotisation (Fraenkel and Rudall, 1940), forms a hard and colored integument in most adults. There is a great variation in kinds of the cuticle depending on the proportions of the

main components and, accordingly, mechanical properties (Hepburn and Chandler, 1976). In various animal groups and on different body parts there are different types of cuticle from very hard and brittle to soft, ductile and also rubber-like (Jensen and Weis-Fogh, 1962).

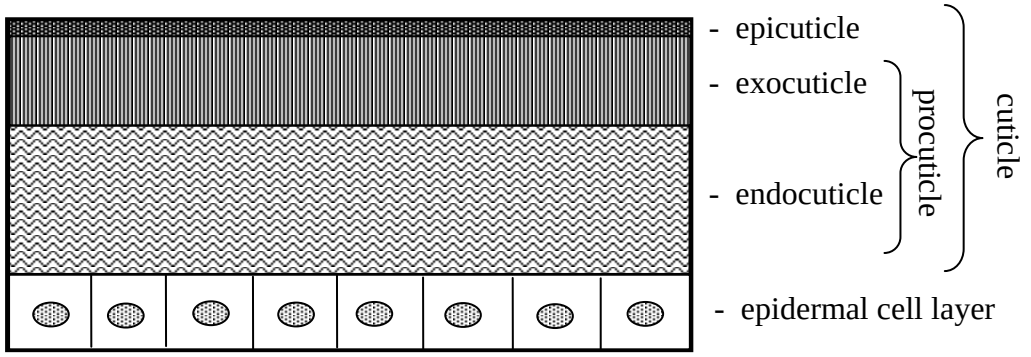

Figure 3.1: Schematic of the multilayered structure in the insect cuticle. The shaded areas represent the single cuticle layers: outer surface layer, epicuticle which does not contain chitin fibers; procuticle with two layers: exocuticle and endocuticle. Last two cuticle layers contain chitin fibers oriented nearly always parallel to the surface. The endocuticle is connected with epidermis cell structure.

The wide spectrum of mechanical properties of the insect cuticle suggests that each body part is optimised to its function. An interesting example is the head articulation system of the beetle *Pachnoda marginata*. The surfaces in this system operate in contact and must be optimised against wear and friction to provide high mobility within the joint. For this study a head part (*gula*) cuticle of the head articulation of the beetle *Pachnoda marginata* was selected. As reported previously for a similar system in the dung beetle *Geotrupes stercorarius* (Arzt *et al*., 2002), the *gula* has a hemispherical shape. Both the structure and the mechanical properties of this material are largely unknown. The first mechanical investigations of the *gula* cuticle were performed on samples prepared from the head-neck articulation of the dung beetle (Arzt *et al*., 2002). In this study, the samples were tested in fresh and dry conditions by a Nanoindenter II (MTS Systems Corporation, Oak Ridge, USA).

As reported, the experiments were carried out without continuous measurement of hardness and elastic modulus. The nanoindentation tests were done not on the whole head but on the cut of the *gula* cuticle (Arzt *et al*., 2002). However desiccation of the *gula* cut differs from that of the whole head (as will be shown below). Consequently, the deformation behavior of the entire head and *gula* cut is expected to be different.

The goal of these investigations was to obtain detailed information about the cuticle structure in the *gula* and to determine its mechanical properties. The surface of the cuticle and its structure were studied by means of scanning electron microscopy (SEM). SEM images were also used for the evaluation of nanoindentation tests. Hardness and elastic modulus were measured using the nanoindentation technique. The samples were mechanically tested in the fresh, the dry and the chemically treated conditions in order to understand the influence of desiccation (fresh versus dry condition) and removal of an outer wax layer (chemically treated condition). Desiccation rate measurements were also performed in order to obtain information about drying dynamics of the cuticle. The questions asked were: What are the structure and the local mechanical properties of the head articulation cuticle? How does the liquid content influence the mechanics of the joint material? How do surface waxes influence hardness and elastic modulus of the *gula*? Since the structure and the mechanical properties of the material are very important for tribological performance, this study aims to make a contribution to exploring the working principle of the *gula* cuticle.

3.2 Experimental

3.2.1 Sample preparation

Samples were prepared from the head articulation system of the beetle *Pachnoda marginata.* The beetles were anesthetized with CO_2. Heads were dissected from the body and freed of soft tissue. To prevent the drying of the specimens, fresh *gula* cuticles were tested immediately (in 3-5 min after dissecting from the body). Dry samples were prepared from fresh cuticles by drying. To obtain the same degree of desiccation, fresh samples were dried in an oven for 24 h at 40°C. Chemically treated samples were prepared from the dry *gula*

cuticles. In order to remove waxes from the surface, dry samples were treated in a solution of chloroform and methanol (2:1) for 50-60 min and air-dried.

3.2.2 Scanning electron microscopy

The samples were fixed in 2.5% glutaraldehyde in a phosphate buffer (pH = 7.3). The specimens were dehydrated in an ascending row of ethanol and then critical-point dried. Pieces of the dried material were fractured using a razor blade. The prepared samples were mounted on holders, sputter-coated with gold-palladium (10 nm thickness) and examined in a Hitachi S-800 scanning electron microscope (SEM) at 20 kV.

3.2.3 Desiccation dynamics measurement

To measure the desiccation rate, the head was cut off the body, freed of soft tissue and put immediately on a Mettler Toledo AG204 DeltaRange® balance, connected to a computer for one mass registration each minute for 12 h. The measurement was performed on the cut of the *gula* cuticle as well. The experiment was repeated for three beetle heads and three *gula* preparations at a room temperature of 23.7-24.4 °C and relative humidity of 41-43 %.

3.2.4 Nanoindentation

Nanoindentation (figure 3.2) provides a fast and reliable technique for evaluating local mechanical properties, such as hardness and elastic modulus, of very small volumes of the material (Oliver and Pharr, 1992; Bhushan and Li, 2003). During the past decade, this method has become an important tool in materials characterization.

During nanoindentation, a precisely defined diamond pyramid is brought into contact with the sample surface. The applied load and the displacement into the specimen are recorded simultaneously. The load-displacement curves obtained during an indentation experiment are essential to calculate the hardness and elastic modulus of the test material.

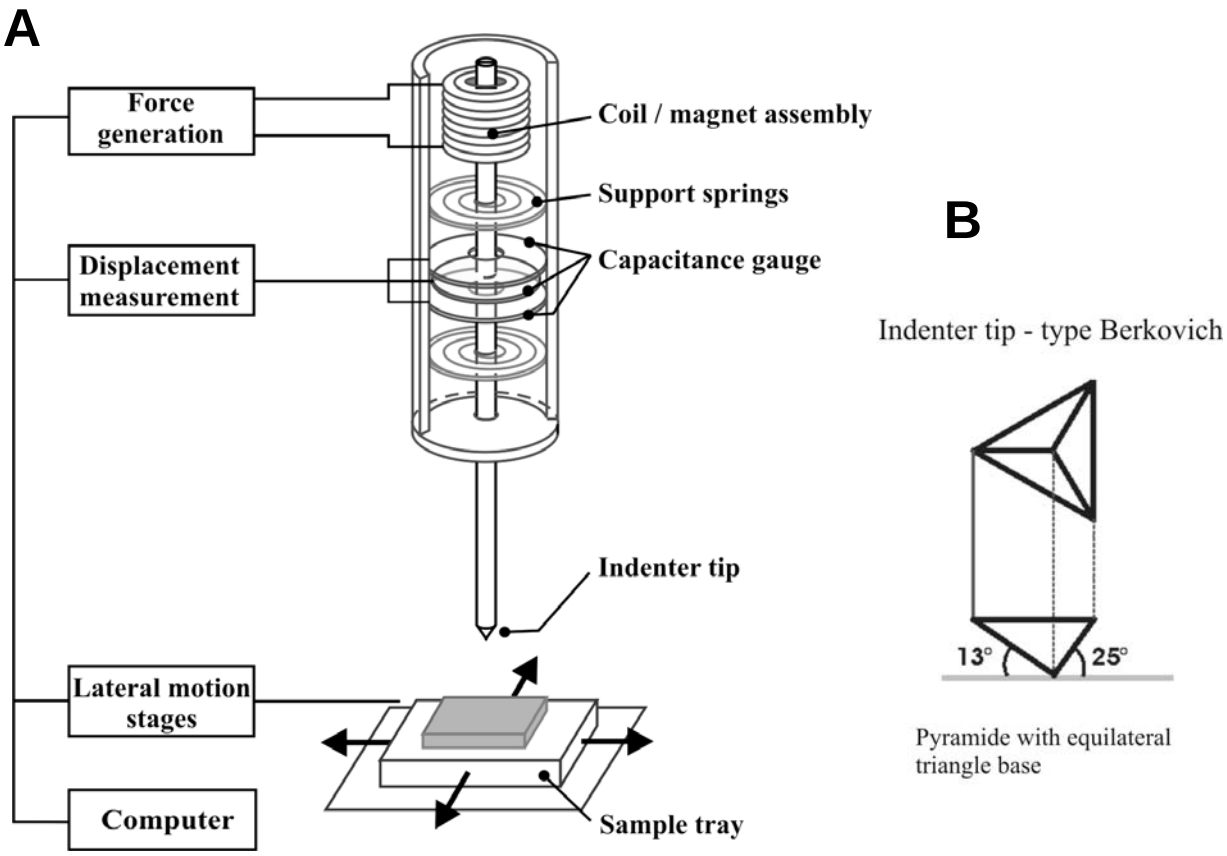

Figure 3.2: **A** Schematic of the nano indenter system used (taken from Enders, 2000). The force imposed on the indenter is generated through a coil that sits within a circular magnet. The displacement sensing system consists of a three-plate (circular disks) capacitor. The two outside plates are fixed to the head and have holes in the center to accommodate the indenter shaft where the center plate is fixed and is free to move vertically between the two outside plates. **B** The Berkovich-tip, an equilateral triangle base pyramid.

The three key experimental parameters of the load-displacement data needed to determine hardness and elastic modulus are the peak load (F_{max}), the depth at peak load (h_{max}) and the initial unloading contact stiffness (S_{max}) (figure 3.3) (Oliver and Pharr, 1992).

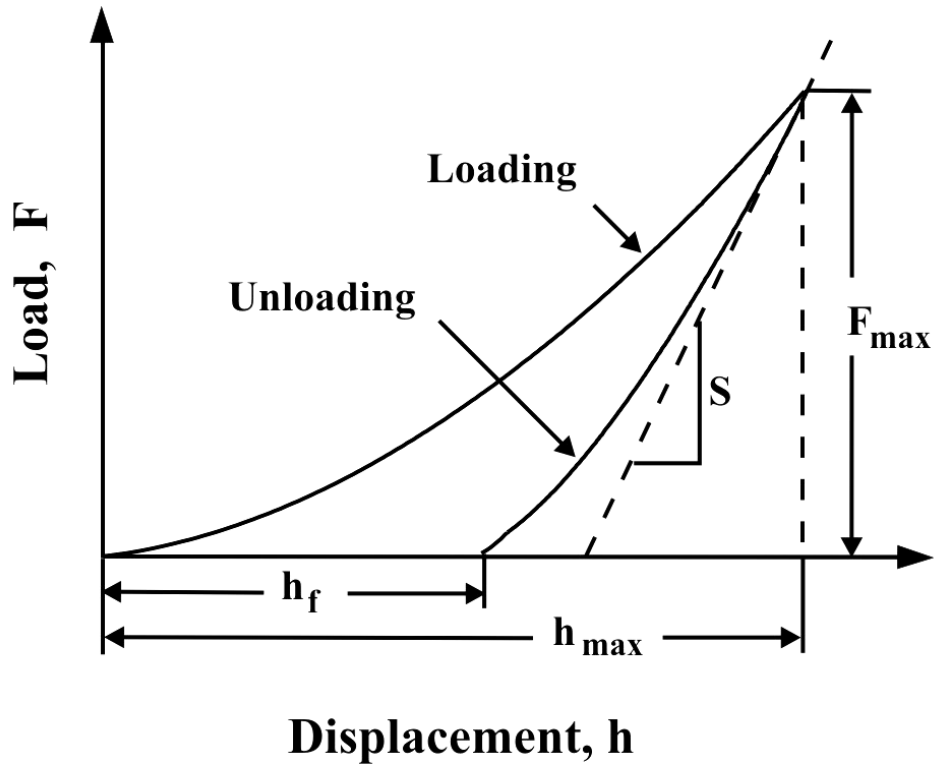

Figure 3.3: Schematic representation of a load-displacement curve with the key experimental parameters. F_{max} peak indentation load; h_{max} indenter displacement at peak load; h_f final depth of the contact impression after unloading; S initial unloading stiffness (After Oliver and Pharr, 1992).

The hardness (H) is defined as the ratio of the maximal load and the contact area produced

$$H = \frac{F_{\max}}{A} \tag{3.1}$$

where F_{max} is the peak load of the indenter and A is the area of contact at peak load given by

$$A = k \cdot h_c \tag{3.2}$$

where k is a geometric constant of the tip (for Berkovich tip k = 24.5) and h_c is the vertical distance along which contact is made, i.e. the contact depth (figure 3.4):

$$h_c = h_{max} - h_s \tag{3.3}$$

where h_{max} is the measured total displacement. The elastic deflection h_s of the surface at the contact perimeter depends on the indenter geometry and is given by

$$h_s = \varepsilon \frac{F_{\max}}{S} \tag{3.4}$$

where ε is a geometric constant of the indenter (Oliver and Pharr, 1992; Hay and Pharr, 2000).

The reduced elastic modulus can be calculated with equation (2.3) applied to the specimen/indenter system:

$$\frac{1}{E_r} = \frac{\left(1-\nu^2{}_s\right)}{E_s} + \frac{\left(1-\nu_i{}^2\right)}{E_i} \tag{3.5}$$

where E_s is the Young's modulus, v_s the Poisson's ratio for the specimen and E_i and v_i are the same parameters for the indenter.

The relationship between the load-displacement behavior and the experimentally measured contact stiffness (S) and the contact area (A) yields

$$E_r = \frac{S \cdot \sqrt{\pi}}{2\beta\sqrt{A}} \tag{3.6}$$

where β is a constant and depends on the geometry of the tip (Oliver and Pharr, 1992; Hay and Pharr, 2000) (β = 1.034 for the Berkovich-indenter).

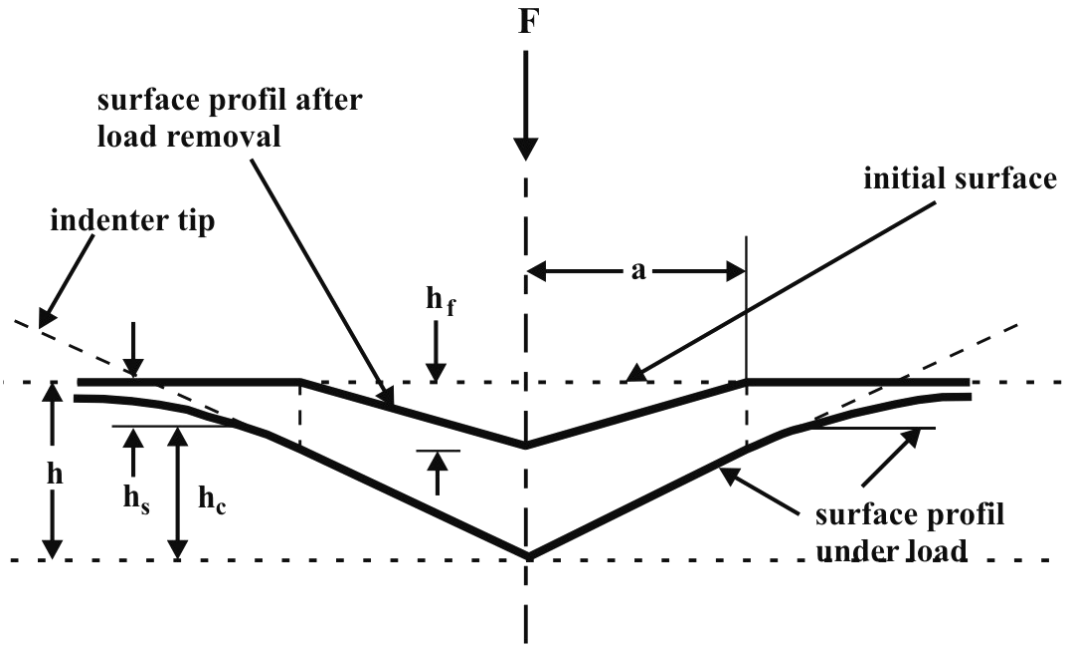

Figure 3.4: Schematic representation of a section through an indentation showing various quantities used in the analysis (After Oliver and Pharr, 1992): F indentation load; h indenter displacement at peak load; h_f final depth of the contact impression after unloading; h_c contact depth; h_S elastic deflection of the surface at the contact perimeter; a radius of the contact circle.

The mechanical properties of most materials and especially biological samples vary with depth. Using a special dynamic technique, the contact stiffness can be measured continuously during indentation. This method, called the Continuous Stiffness Measurement (CSM) (Oliver and Pharr, 1992), aids in obtaining the depth-dependence of the mechanical properties. It also allows control of the test dynamics in a systematic way and the direct measurement of the contact stiffness depending on the depth. The periodic loading/unloading cycles of the indenter give hardness and elastic modulus values at discrete points of the loading curve. This technique may be applied for the characterization of the mechanical properties of soft materials such as biological materials and polymers.

Hardness and elastic modulus of the head cuticle in the beetle were performed using a Nano Indenter® SA2 system (MTS Systems Corporation, Oak Ridge, USA). Indentations were made using a triangular diamond pyramid indenter. The sides of the pyramid form an angle of 65.3° with the normal to the base (Berkovich-type) (figure 3.2). Due to the high damping coefficient and high resonant frequency of the indenter it was possible to perform measurements on materials with low contact stiffness and low damping coefficients.

The beetle head was mounted on a holder so that the ventral surface of the *gula* was facing up. To prevent sample drying, fresh samples were rapidly prepared (the time difference between the sample preparation and the first indent was approximately 10 - 15 min). The indents were located on the top of the hemispherical *gula*. We tested 10 heads with 15 indents each (n=150). The indents were separated from each other by 30 to 50 µm. The nanoindentation experiments were load-controlled. The resonant frequency during the tests was 75 Hz. The maximum displacement was 3000 nm. Since the biological samples bear liquid organic substances on the surface, the indenter tip was contaminated. It was cleaned and then calibrated by means of indentation in Al and SiO_2 (fused silica) samples respectively between the measurements.

3.2.5 Atomic force microscopy

The surface profiles of the samples were investigated by atomic force microscopy (AFM) (DME, DualScope™ C-21 with scanner DS 45-40 BIO). AFM images of the cuticle surface were taken after the indentation tests.

3.3 Results

3.3.1 Structure of the *gula* cuticle

The *gula* surface of the beetle head is rather smooth (figure 3.5A). Island-like places, occurring on the surface, are, presumably, dried secretory substances, delivered to the surface by well-defined pores, which run deep into the material and apparently are connected with epidermal cells (figure 3.5C and 3.5D). Cracks found on the surface are probably caused by material desiccation (figure 3.5D). The cross-section of the cuticle shows the layered structure of the fiber composite (figure 3.5B). The thickness of the *gula* cuticle is about 80 µm. A very thin (7-8 µm) and dense epicuticle can be distinguished. Procuticle is present with two layers: dense exocuticle, which is about 22 µm thick and the endocuticle, which is very thick (about 50 µm) and less dense compared to the exocuticle layer. As can be distinguished in figure 5 B, chitin fibres are oriented nearly perpendicular to the surface in the exocuticle layer and parallel to the surface in the endocuticle.

3.3.2 Desiccation

In figure 3.6 mass (in %) of sample is plotted versus drying time (min). Each curve shows an average value of the drying measurements of three entire head and three cuts of the *gula* cuticle respectively. The loss of water in an entire head sample was very high and the mass of the beetle head initially decreased rather rapidly. After six hours, the rate of mass loss was slower. After 10 h, the samples were completely dry (they had lost about 60 % of their initial mass). The *gula* preparations were dry in approximately 40 min and the mass loss was about 18 %. Water loss leads to changes in the structure of the cuticle and, as a result, in the mechanics of the material as will be shown below.

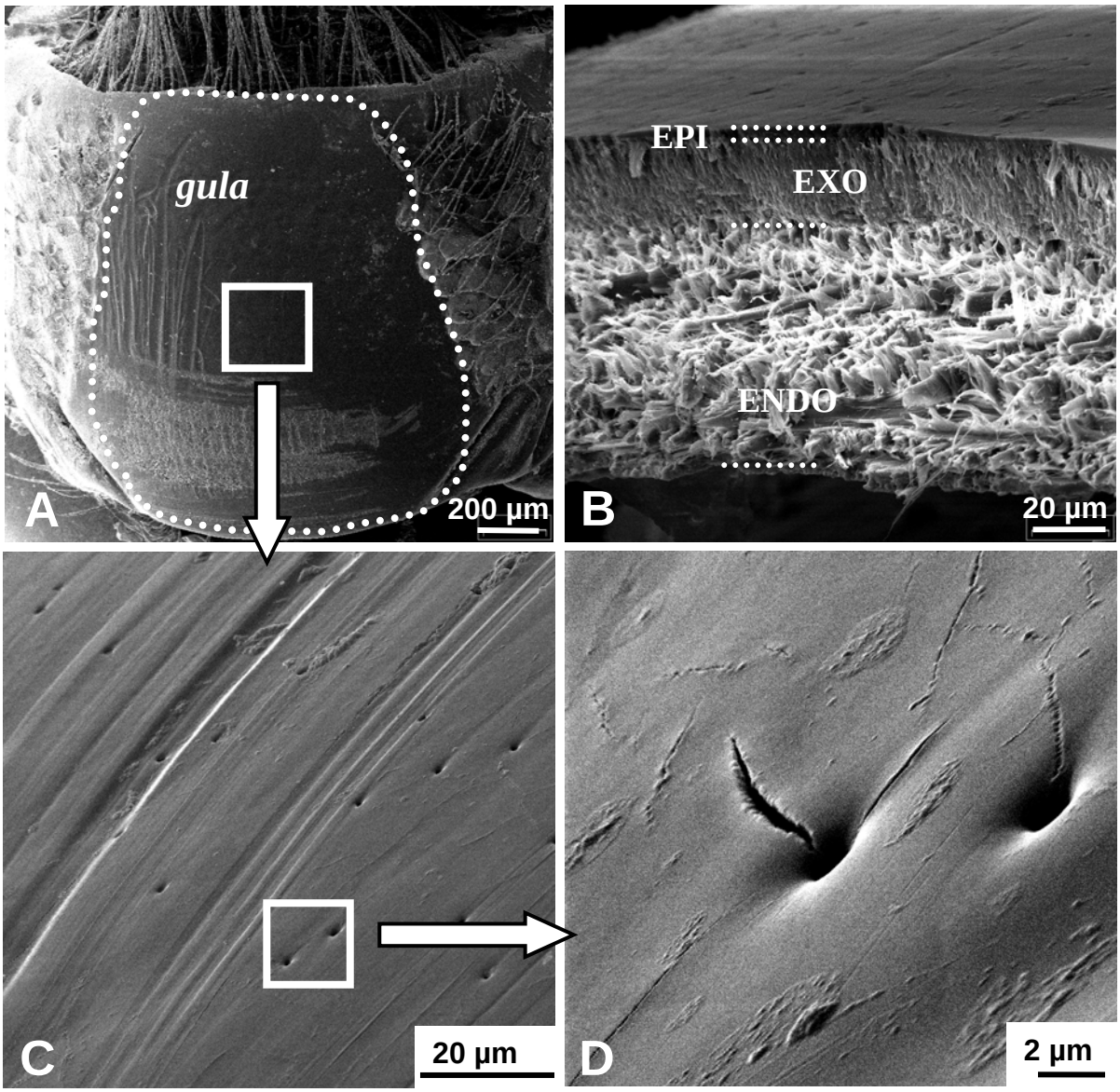

Figure 3.5: SEM images of the *gula* surfaces. A: shows entire surface of the *gule*. B: cross section of the *gula* cuticle showing the single cuticle layer: EPI – epicuticle, EXO – exocuticle and ENDO – endocuticle. Perpendicular orientation of the chitin fibers can be distinguished in the exocuticle layer. The well-defined pores, dried organic substances and cracks can be seen on the cuticle surface (C and D).

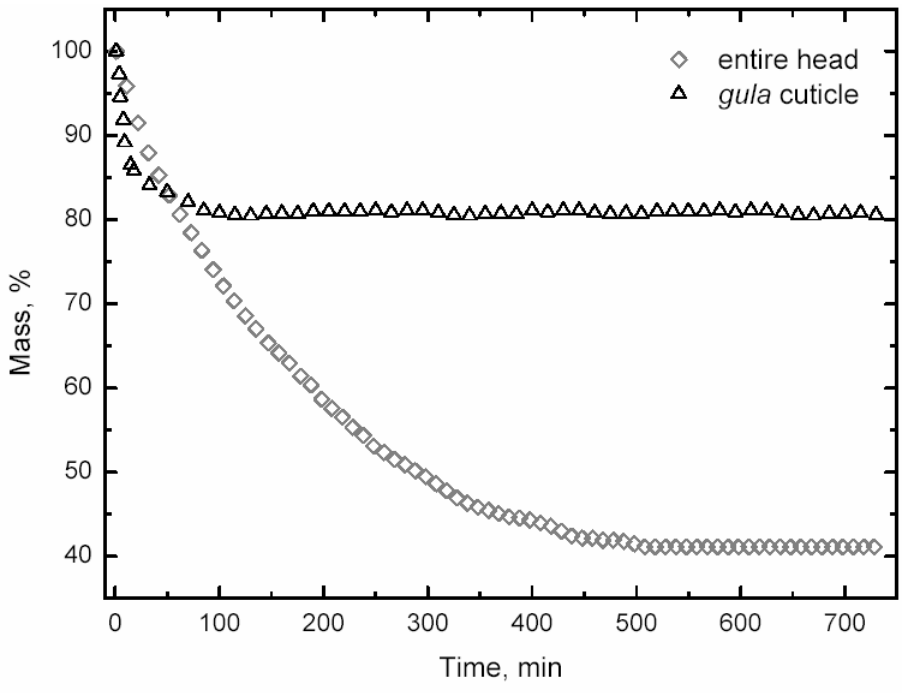

Figure 3.6: Desiccation curves of the entire head in comparison with the *gula* cuticle. Mean values of three drying measurements for entire head and three measurements for *gula* cuticle are shown. The gula cuticles were dry in approximately 40 min and water loss was about 18 % of the initial mass of the sample. The drying time of the entire head was about 10 h with water loss of 60 % of the initial mass of whole head. The initial mass of each head preparation was of about 25 to 30 mg.

3.3.3 Mechanical properties

Figure 3.7 presents load-displacement curves from indentation tests on the fresh, dry and chemically treated samples. They show that the deformation behavior depends on the sample conditions. In figures 3.8 A and 3.8 B hardness and elastic modulus results are plotted vs. displacement (indentation depth into the sample surface). Each data point is the average value of approximately 150 indents (10 beetle heads with 15 indents on each, 150 indents in all).

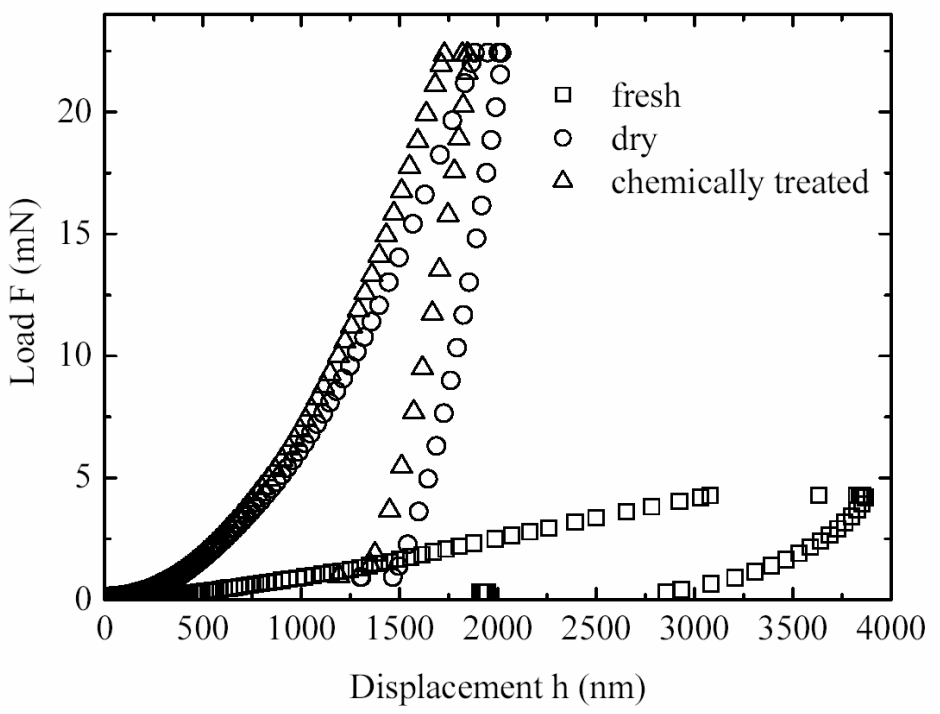

Figure 3.7: An example of load-displacement curves for one sample in the fresh, dry and chemically treated condition.

The measurements revealed a strong dependence of the mechanical behavior on the preparation conditions of biological samples. The significance of the differences due to the conditions was checked by means of statistical calculations. The experimental data were compared with a one-way ANOVA and a Tukey post tests (Origin 7 SR2). Hardness and elastic modulus values of the fresh, the dry and the chemically treated samples were compared with each other by different displacements of 250, 500, 1000 and 1500 nm. The results of the statistical calculations are summarised in table 3.1. Hardness and elastic modulus differ significantly for the fresh, dry and chemically treated conditions. Exceptions are the elastic modulus values of the dry and chemically treated samples at indentation depths of 1000 and 1500 nm. The effect of the chemical treatment on the sample stiffness at these depths can hardly be observed. Statistical calculations show no significant difference between elastic moduli of the dry and chemically treated samples at indentation depths higher than 1000 nm.

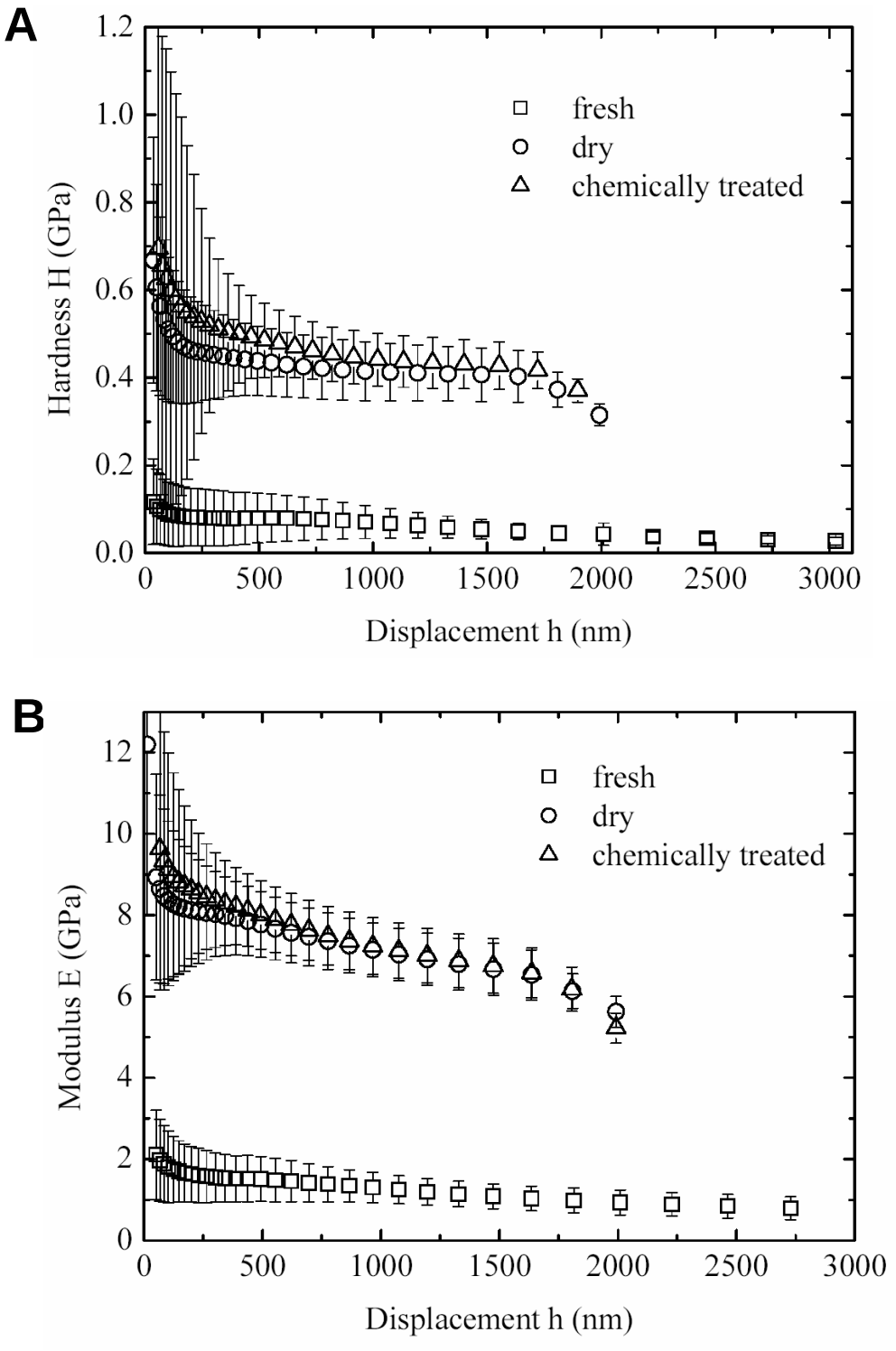

Figure 3.8: The results of hardness and elastic modulus from indentation tests on the *gula*-cuticle: hardness (**A**) and elastic modulus (**B**) are plotted versus displacement for fresh, dry and chemically treated samples. Hardness and elastic modulus were calculated by using the CSM technique from the projected contact area during indentation. Each data point corresponds to the mean value of approximately 150 measurements.

The average hardness value (H=0.10±0.07 GPa) of the fresh samples is significantly lower than that of the dry (H=0.49±0.14 GPa) and the chemically treated (H=0.52±0.15 GPa) ones (figure 3.8 B) (ANOVA $p<0.0005$, Tukey post test $p<0.0005$). The difference between the hardness results of the dry (H=0.49±0.14 GPa) and chemically treated samples (H=0.52±0.15 GPa) is lower but also significant (statistic: ANOVA $p<0.0005$), especially in the displacement range of 200-1000 nm.

The same tendency was observed for the elastic modulus (figure 3.8C). The dry (E=7.50±1.80 GPa) and chemically treated (E=7.70±1.90 GPa) samples are significantly stiffer than fresh ones (E=1.50±0.80 GPa) (statistic: ANOVA $p<0.0005$, Tukey post test $p<0.0005$). In this case the chemical treatment causes a slight increase of the elastic modulus below 1000 nm indentation depth into the sample surface. At a depth higher than 1000 nm, the elastic modulus values of the dry and chemically treated samples are not significantly different.

The maximum displacement for the fresh samples was 3000 nm, but for the dry and chemically treated samples only 2000 nm, because the maximum load of the instrument had been reached. High values of the hardness and elastic modulus in the first 50 nm of indentation are erroneous data caused by contact building between the indenter tip and sample due to the roughness and contamination of the sample's surface. The hardness and elastic modulus for all samples slowly decreases with indentation depth. However, after 1700 nm, both parameters drop rapidly for the dry and chemically treated specimens.

3.3.4 Atomic force microscopy

Figure 3.9 shows the surface profile of the *gula* cuticle after an indentation test. Residual deformation of the cuticle surface after indentation seems similar to elastic-plastic contact, which is typical of most engineering materials (see chapter 2). An elastic recovery on the indent-image can be distinguished. This is due to a visco-elastic relaxation expected for soft biological materials (Wainright *et al*., 1976; Vincent, 1990; Kohane *et al*., 2003).

	Hardness / Elastic modulus				
Fresh		+ / +	+ / +	250	Depth, nm
Dry	+ / +		+ / +		
Chem. treated	+ / +	+ / +			
Fresh		+ / +	+ / +	500	
Dry	+ / +		+ / +		
Chem. treated	+ / +	+ / +			
Fresh		+ / +	+ / +	1000	
dry	+ / +		+ / —		
Chem. treated	+ / +	+ / —			
Fresh		+ / +	+ / +	1500	
Dry	+ / +		+ / —		
Chem. treated	+ / +	+			
Condition	Fresh	Dry	Chem. treated		

Table 3.1: Results of statistical calculations of the significance (One-Way-ANOVA and Tukey post tests) of differences between the hardness and elastic modulus for various indentation depths (250 nm, 500 nm, 1000 nm and 1500 nm) in fresh, dry and chemically treated conditions. + means that there is a significant difference between the values compared; - means that there is no significant difference between the values compared. There is no significant difference in the elastic modulus values between the dry and chemically treated samples an indentation depth of 1000 nm and 1500 nm.

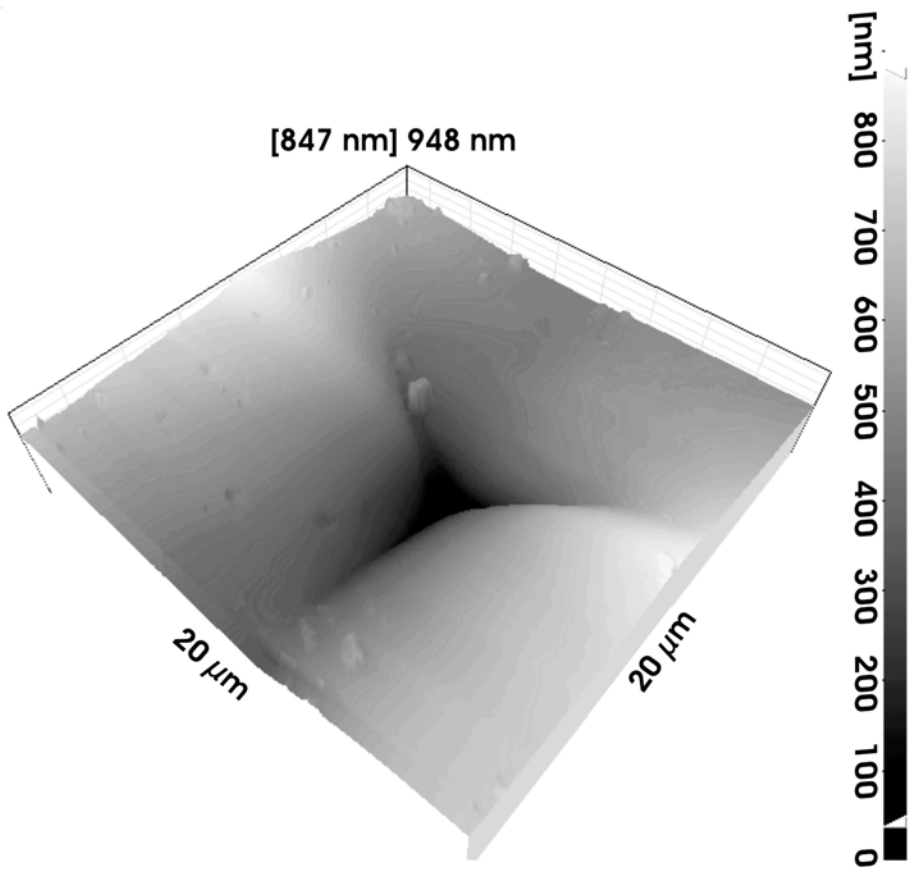

Figure 3.9: AFM images of the cuticle surface after indentation test showing the residual deformation. The image of the indent shows elastic recovery, which is characteristic for the elastic-plastic contact in most engineering materials. However such shape of the indent here is thought to be caused by visco-elastic relaxation expected for biological materials.

3.4 Discussion

3.4.1 Structure of the *gula* cuticle

SEM images (figure 3.5) provide information on the shape of the *gula* cuticle and the ultrastructural architecture within a single cuticle layer. The *gula* of the beetle *Pachnoda marginata* has an ultrastructure similar to that in *Geotrupes stercorarius* (Arzt *et al*., 2002). The exocuticle structure of the *gula* differs from the layered pattern of regular cuticle, where the orientation of the chitin fibers is parallel to the surface (Neville, 1975; Wainwright *et al*., 1976; Vincent, 1990). The fibers in the exocuticle are oriented perpendicular or at some angles to the surface. A similar fiber orientation has previously been found in attachment pads of grasshopper (Gorb and Scherge, 2000). However, the advantage of such structures is not understood at present. Further investigations are required to clarify the reason for this perpendicular fiber orientation.

3.4.2 Desiccation

As expected, the cut of the *gula* cuticle dried faster (40 min) than the entire head (10 h). Indentations were performed on the *gula* cuticle of the entire head. The samples were ready for testing in 3 – 5 min. The time elapsed between the head has been removed from the body and the end of the experiment was less than 1.5 h. Thus, indentations were carried out in the native (fresh) condition.

Desiccation measurements show that the water content of the cut of *gula* cuticle was about 18 mass % (mean value of three measurements). This value is comparable with the literature data of approximately 12 % for hard and brown type of cuticle (Vincent and Wegst, 2004).

3.4.3 Condition dependence of the mechanical behavior

In general, soft and compliant cuticle contains more water than hard and stiff (Vincent and Wegst, 2004). Since the *gula* cuticle belongs to the hard and brown type of cuticle, it has a low content of water. But even so, the results show that desiccation has a great influence on the mechanical behavior of the cuticle tested. After drying, the *gula* cuticle becomes about 5 times harder and stiffer (H = 0.49 ± 0.14 GPa, E = 7.50 ± 1.80 GPa) than in the fresh state (H = 0.10 ± 0.07 GPa, E = 1.50 ± 0.80 GPa). Water content seems to be the crucial factor, which influences the mechanical properties such as hardness and elastic modulus. According literature data, humidity loss changes the mechanical behavior of biological materials significantly (Andersen *et al*., 1996; Arzt *et al*., 2002; Enders *et al*., 2004; Vincent and Wegst, 2004). In the fresh cuticle, chitin filaments are spaced within a protein-matrix containing about 90 % water (Andersen *et al*., 1996; Vincent, 1980). Therefore absence of water, one of the main components of the cuticle, is expected to lead to some changes of the structure. There are literature data on the structural changes depending on water reduction in the cuticle during sclerotisation (Andersen *et al.*, 1996), but nothing is known about how drying alter the cuticle structure. However it is obvious that the water content makes cuticle soft and compliant. The increase in hardness and elastic modulus, especially of the cuticle layer near the surface up to 1700 nm, is thought to be caused by structural changes due to water loss. Indentation tests on various biological surfaces (insects and plants) display a considerable difference in the mechanical behavior between fresh/hydrated and dehydrated materials (Hillerton *et al*., 1982; Arzt *et al*., 2002; Enders *et al*., 2004; Vincent and Wegst, 2004).

Removal of surface waxes and lipids causes only small changes in the indentation results (slight increase in hardness and stiffness), especially at a depth below 1000 nm. Without water, the mechanical behavior of the *gula* cuticle is influenced only a little by the outer wax/lipid layer and is presumably determined mainly by proteins and chitin, which could not be removed by the chemical treatment used in this study. In order to understand how the two main components (proteins and chitin) contribute to the mechanical properties of the cuticle, further studies are necessary.

3.4.4 Hardness and elastic modulus

SEM images were helpful to evaluate indentation data. The maximum indentation depth in our experiments was 3 µm. Therefore, measurements of the mechanical properties were done in the epicuticle (figure 3.5 B), which is about 7 µm thick. According to several models (Jönsson and Hogmark, 1984; Burnett and Rickerby, 1987; McGurck *et al*., 1994; Rother and Jehn, 1996; Korsunsky *et al*., 1998) concerning the hardness determination for thin metal films, the results obtained could also be influenced by layers of the exocuticle. After Bueckle (1965) and Bhushan (1996), hardness measured up to an indentation depth of 0.7 µm (displacement < 1/10 of the layer thickness) can be assumed to characterize the epicuticle. With larger displacements the hardness will be characteristic of the whole composite of the epicuticle/exocuticle layers. This suggestion is true only for hardness measurement. The elastic modulus measurements will be influenced by the whole composite since it is a long-range effect.

The mechanical behavior of the *gula* cuticle can be regarded as that of a soft substrate coated by a hard film. A decrease in hardness and elastic modulus with increasing indentation depth is caused by the underlying layers. As already mentioned, deeper layers in cuticle are softer and more compliant than the outer ones. The influence of the underlying layers on the mechanical properties is stronger on dry and chemically treated samples than on fresh ones. Without water, surface layers appear to become harder and stiffer than the deeper layers showing a lower density and higher protein content (Locke 1964; Neville 1975, Binnington and Retnakaran 1992).

Several studies of elastic modulus and hardness of insect cuticle using different methods can be found in the literature. Almost all experiments were performed on dry or rehydrated samples. There are only a few measurements of the mechanical properties of cuticle made by indentation. The average hardness (0.10 - 0.52 GPa) and elastic modulus (1.50 - 7.70 GPa) values obtained in this study are similar to those of various sclerotised cuticles (Vickers hardness 0.2-0.5 GPa and Young's modulus 1 - 10 GPa (Vincent and Wegst, 2004)). However the hardness (0.10 GPa) of the fresh samples is below this range (0.2 - 0.5 GPa). It is believed

that these are possibly the first measurements of hardness and elastic modulus on the insect cuticle in native condition.

Comparable hardness values were obtained on other cuticle elements. For example, the dry wing membrane cuticle of the dragonfly *Aeshna cyanea* tested with a nanohardness-test-machine (Hysitron TriboScope) exhibited a hardness of 0.2 GPa (Kreuz *et al*., 1999). The different parts of the dehydrated locust cuticle measured by means of a Leitz Miniload hardness tester (using a Vickers diamond) (Hillerton *et al*., 1982) revealed H = 0.24-0.33 GPa. However the dry samples of the beetle head tested in this study (H = 0.49 GPa) were still harder than the cuticles mentioned above.

The elastic modulus values (E = 7.50 ± 1.80 GPa) obtained for the dry beetle cuticle is very high when compared to the elastic modulus from tensile test of the dry wing membrane of the dragonfly *Aeshna cyanea*, where E = 1.5 ± 0.5 GPa (Kreuz *et al*., 1999). The reduced modulus for different body parts of the dehydrated dragonfly (*Odonata, Anisoptera*) were calculated from quasistatic nanoindentation experiments (Hysitron Inc., Minneapolis, MN) (Kempf, 2000). The mean values were lower (1.5 – 4.7 GPa) as well than elastic modulus obtained for dry samples in this study. Recent nanoscale study (quasistatic nanoindentation testing instrument, Hysitron Inc., Minneapolis, MN) of *Drosophila melanogaster* integument during development (Kohane *et al*., 2003) shows that the thickness and the development stage of the cuticle was very important for stiffness measurements. The average reduced elastic modulus (E_r) of 0.41 MPa, 15.43 MPa and 4.37 MPa were determined by *in vivo* experiments for the cuticles of the larval, puparial and adult insects respectively. Thickness of the cuticles of *Drosophila melanogaster* was very low (2.3-17.7 µm) when compared to that of *gula* cuticle (about 80 µm). However, the mechanical properties of the cuticle are strongly influenced also by proportions of the main components (chitin and proteins) (Fraenkel and Rudal, 1940; Locke, 1964; Neville, 1975; Hepburn and Chandler, 1976; Binnington and Retnakaran, 1992).

The nanoindentation experiments in this study were carried out in the epicuticle, which is a nonchitinous layer. It contains proteins and is covered with lipids and surface waxes (Neville, 1975; Binnington and Retnakaran, 1992). Surprisingly the elastic modulus of the fresh *gula* cuticle (E = 1.50 ± 0.80 GPa) is comparable to that of the chitin filament (1.97 ± 0.07 GPa) (Joffe and Hepburn, 1973). There are contradictory data in the literature about which

component (chitin or protein) is responsible for the elastic modulus of the cuticle. According to Fraenkel and Rudall (1940), the mechanical properties of the cuticle are determined by chitin, whereas Vincent (1980; 2002) suggests that the protein matrix is decisive for its mechanical behavior. Elasticity which is expected to be a long-range effect is influenced by the underlying exocuticle layer consisting of a high amount of chitin in a protein matrix (Neville, 1975; Binnington and Retnakaran, 1992). Nevertheless, according to our experimental results, it can be concluded that the elastic modulus in fresh cuticle is not only influenced by only chitin or only the protein-matrix, but by both components.

3.5 Summary and conclusion

This section has focused on the structure and the local mechanical properties of the head articulation cuticle of the beetle *Pachnoda marginata*. The surface structure of the samples was explored by scanning electron microscopy (SEM). Nanoindentation experiments were carried out on the fresh, dry and chemically treated samples. The structural and mechanical properties of the material which presumably serves to reduce friction and wear in the head articulation system of the beetle can be summarized as follows:

- The head part of the head articulation in the beetle *Pachnoda marginata* has a hemispherical convex shape. The surface of the *gula* cuticle appears to be very smooth.

- The structure of the *gula* cuticle was found to differ from that of most cuticles ever tested. The exocuticle contains fibers oriented perpendicular to the surface rather than parallel. However the advantage of such a structure is unclear at present.

- The desiccation dynamics measurements have shown that the loss of the aqueous fluids is very high – 60 % of the whole mass of the fresh head of the beetle. The water loss in the cut of the *gula* is 18 %, which is expected to be equivalent to the water content in the sclerotised cuticle.

- The preparation conditions of the samples were found to be crucial to the mechanical behavior. Nanoindentation results revealed that dry samples were significantly harder and stiffer than fresh ones. However removal of wax/lipid layer from the surface caused only a small change (little increase in hardness and stiffness) in cuticle properties.

- The mechanical behavior of the *gula* cuticle can be regarded as that of the composite consisting of a hard film on a soft substrate. Due to the influence of the underlying layers, values of the hardness and the elastic modulus were found to decrease with increasing indentation depth.

- According to the experience in the field of thin metal films, the hardness value obtained up to an indentation depth of 0.7 µm were assumed to be typical of the epicuticle, the thickness of which was about 7 µm. At displacements greater than 0.7 µm, the hardness will be influenced by underlying layers.

- Nanoindentation can successfully be applied to study hardness and elastic modulus of biological materials. The structural studies (SEM) and the mechanical properties determined by nanoindentation can contribute to an understanding tribological behavior of the *gula* cuticle.

4 Friction measurements on a biological micro-tribo system: the head articulation of the beetle *Pachnoda marginata* (Coleoptera, Scarabaeidae)

Abstract

The head articulation of the beetle *Pachnoda marginata* is a micro-tribological system which consists of the *gula* and the *prothorax*. The surfaces of both parts are in contact and are expected to be optimised for friction reduction. The relationship between structure, material properties and functional properties of this system is investigated for the first time. The material structure of the *gula* plate and the *prothoraxic* counterpart were studied using scanning electron microscopy (SEM). Friction and contact area measurements between the *gula* and a glass plate were carried out for different normal loads (100-10000 µN) using a microtribometer and a micro-tester. The tribological behavior of the *gula* cuticle was studied in the fresh, dry and chloroform-methanol treated conditions. The fresh *gula* cuticle, the surface of which was very smooth, showed the largest contact area and the highest friction coefficient. The drying of the cuticle led to a decrease in the friction coefficient and the contact area. The dry samples exhibited a rough surface. The chemical treatment led to a decrease in surface roughness. The friction coefficient was lowest in chemically treated cuticles, although the contact area was larger than in the dry condition.

4.1 Introduction

Any movement involving contact between two surfaces or between a surface and a medium has to deal with the resistance of the surfaces or medium. This resistance is a friction phenomenon, believed to have a great influence on the design of biological structures (Gorb, 2001). Living microsystems have developed different ways to save muscular energy by the use of friction-optimised systems. Surface pairs in biological objects are designed to maximise or to minimise contact forces within joints. In biology they are defined as friction and anti-friction systems respectively. Working principles of friction and anti-friction systems are based on mechanical interlocking and a maximisation or a minimisation of the contact area (Gorb, 2001). Frictional systems require high friction to fixate body parts to one another (Gorb, 2001). The surface pair can be predefined as in the wing-locking mechanisms of beetles (Hammond, 1989; Gorb, 1997; Gorb, 1999b) and the head-arresting system of dragonflies (Gorb, 1999a; Gorb, 2001). Attachment pads of insects (Gorb, 2001) are friction systems where one surface is predefined and the other is unpredictable. Among various cases of contact pairs in biology, anti-friction systems always have a predefined pair of surfaces like the head articulation system in beetles (Arzt *et al*., 2002; Enders *et al*., 2004) or the hemelytra-hindwing locking mechanism in bugs (Perez Goodwyn and Gorb, 2004).

The head articulation of the beetle *Pachnoda marginata* is an anti-friction system. A predefined, functionally corresponding pair of the contacting surfaces forms a tribological system with specific ultrastructural architecture and properties. However, each contacting piece has a different structure. The rather smooth surface of the hemispherical head-part or *gula* is believed to contribute to the friction minimisation in contact with its counterpart in the ventral part of the *prothorax*, covered by asymmetric outgrowths (Enders *et al*., 2004). In living conditions the organic substances on the cuticle surface, such as lipids and waxes are expected to serve as lubrication materials to reduce the friction in this biological microsystem.

The tribological properties of one part of the head articulation (*gula* cuticle) of the beetle *Pachnoda marginata* were investigated. In this section, the relationship between frictional behavior, structure, contact area, surface properties such as roughness and hydrophobicity, and mechanical properties such as hardness and elastic modulus will be discussed. Assembly

of the head articulation and structure of both contacting surfaces were studied by means of computer tomography and scanning electron microscopy. The samples prepared from *gula* cuticle were tested in the fresh condition to evaluate its working principle in nature. Tribo-mechanical experiments were performed in dry and chemically treated conditions to understand the influence of desiccation (dry condition) and removal of the outer wax layer (chemically treated condition) on the surface properties of the *gula* cuticle. Friction and contact area measurements were carried out by a microtribometer and a micro-tester respectively for different normal loads (100 - 10000 µN). This section characterises the surface structure by means of structural and tribo-mechanical tests. It aims to discuss how this type of surface reduces friction in a microbiological insect device and which material properties are crucial for low friction. It is believed that this is the first study which describes the relation between the structure, material properties and frictional function of the *gula* cuticle.

4.2 Experimental

4.2.1 Materials and sample preparation

The samples for the tribological investigations were prepared from the head articulation system of the beetle *Pachnoda marginata*. The process of sample preparation was the same as for the nanoindentation experiments. (For details see section 3.2.1. Materials and sample preparation in chapter 3).

4.2.2 Computer tomography

To observe the working position and the shape of the contacting surfaces, the anatomy of the head articulation system of the beetle *Pachnoda marginata* was explored with high resolution computer tomography (X-Ray µ-CT system, model 1072 tomograph by Sky Scan at the Institute für Kunststoffprüfung (IKP) at the University of Stuttgart, Germany). This method allows non-invasive imaging of the internal structure. The measurements were performed on dry samples. The images of the head articulation of the beetle were taken in two directions: transversal and sagittal (magnification × 30).

4.2.3 Scanning electron microscopy

The surface structure of *gula* and *prothorax* cuticles (the counter part of the *gula* cuticle) in the head articulation system of the beetle *Pachnoda marginata* was studied in scanning electron microscopy (SEM). (For detailed information see section 3.2.2. Scanning electron microscopy in chapter 3).

4.2.4 Friction measurements

Friction measurements were performed using the microtribometer Basalt-BT01, which was developed for microtribological studies on biological materials (figure 4.1). This instrument contains a computer-controlled seven-axis high-precision positioning system. The main lever can be extended by 15 mm and tilted to the horizontal position in both directions. The glass plate is attached to the glass double-leaf spring which forms part of the piezo-electric precision drive with nanometer resolution. A biological specimen is fixed on the sample holder containing a rotating and a tilting mechanism. The system can be used for microindentation and microtribological measurements.

For friction measurements, the biological specimen was brought into contact with a glass plate. A normal force (F_N) was applied perpendicular to the bottom of the sample holder. The sliding of the plate was parallel to the sample holder and perpendicular to the applied force direction. The tangential force (F_T) was measured from the deflection of the spring. The experiments were done for 7 different normal loads: 30, 100, 300, 1000, 3000, 5000 and 10000 μN. Friction properties of 10 heads were measured for fresh, dry and chemically treated conditions. The microtribometer was calibrated using a sapphire ball (1.5 mm in radius). The glass plate was cleaned with alcohol after each experiment.

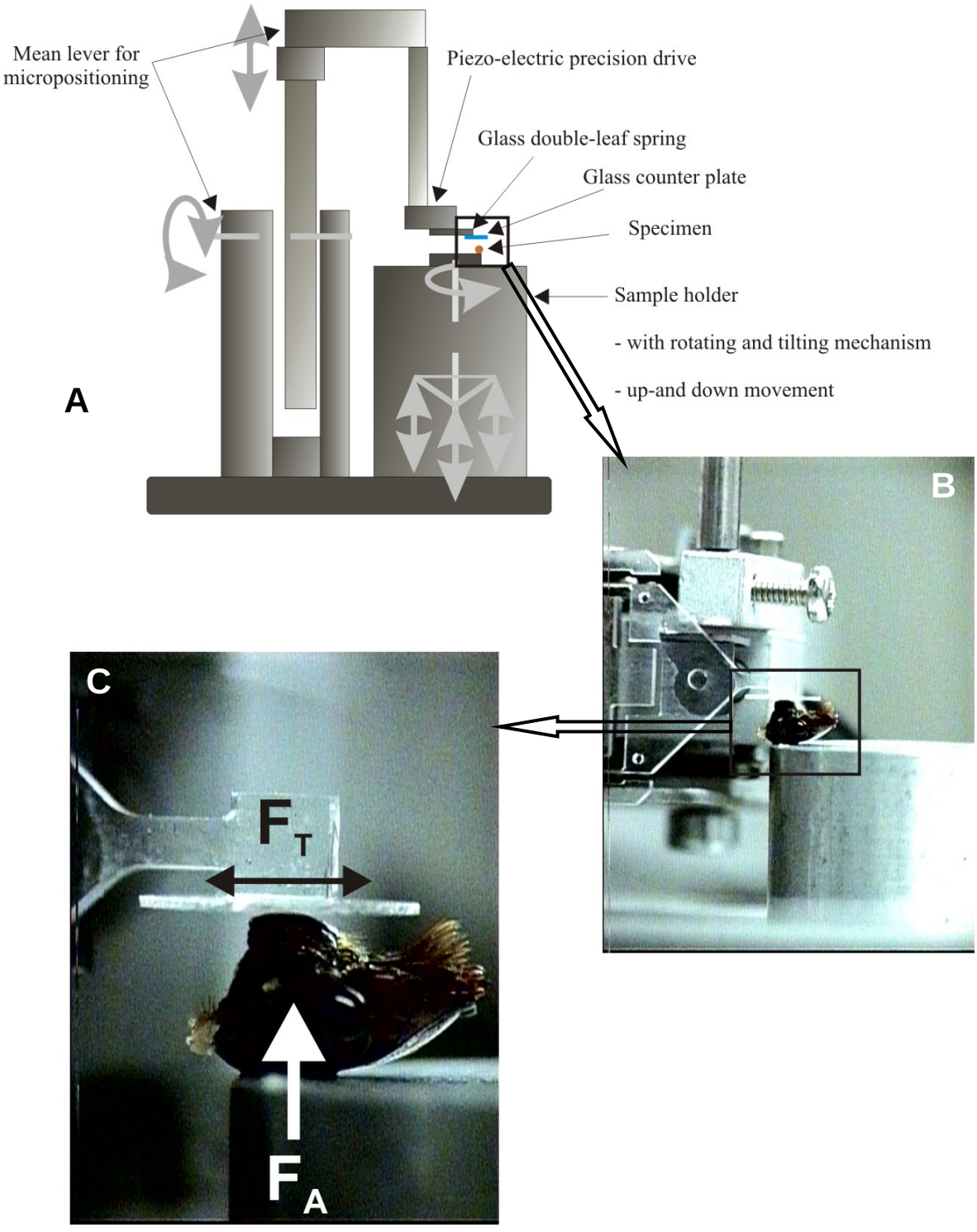

Figure 4.1: Schematic of the microtribometer Basalt BT01 (Tetra GmbH, Ilmenau, Germany) for tribological applications (friction measurement) (**A**) and photographs of the friction measurement (**B** and **C**) showing the whole head of the beetle *Pachnoda marginata* in contact with the glass plate. F_A and F_T are applied and tangential forces respectively.

4.2.5 Surface roughness measurement

The sample surface was studied using a white-light interferometer **(**Zygo New View 500, Zygo Corporation, USA). The shape of the surface was measured by an optical interference method, based on the information how much the interference fringes depart from being straight and equally spaced (Bhushan, 2001). This technique can be used to obtain the average surface roughness (*Ra*), the average absolute value of ten-point height (*Rz*) or root mean square (rms) representing the height profile's roughness. Three heads were tested for each condition.

4.2.6 Measurement of apparent contact area

The size of the apparent contact area of the *gula* on the glass plate could not be obtained during the friction experiment. Therefore, a separate measurement of the contact area was necessary. The experiments were performed using the Micro-Tester, a motorized micromanipulator (DC3001R with controller MS314, World Precision Instruments, Sarasota, FL, USA) combined with a force monitor via a load cell force transducer (100 g capacity, Biopac Systems Ltd, Santa Barbara, CA, USA). For these tests, the same applied loads as for the friction measurements were used. It was difficult to obtain precise values because of the very small size of the contact area, especially at low normal loads.

The sample was fixed on the sensor connected to the force transducer mounted on the micromanipulator. The applied force was monitored by the force transducer once the specimen was brought into contact and pressed onto the glass plate, which was attached to the immobile stage. Another glass plate, arranged at 45° to the first glass plate, was lit by a fiber optic light and the picture of the contact area was recorded through a microscope. The contact area was measured for 7 different normal loads: 30, 100, 300, 1000, 3000, 5000 and 10000 µN. For each load and condition 10 *gula* cuticles were tested. Sapphire balls with a radius of 1.5 mm and 0.5 mm were used for calibration of the Micro-Tester. The glass plate was cleaned with alcohol after each experiment.

4.2.7 Contact angle measurement

Contact angle measurements on the head articulation of the beetle were performed by contact angle measurement device OCA 20 (Data Physics Instruments GmbH, Filderstadt, Germany). In this sessile drop method, a microdrop of water is applied to the biological specimen surface. The contact angle is measured through a tangent to the contours of the drop. The experiments were performed on three heads for the fresh, dry and chemically treated conditions.

4.3 Results

4.3.1 Micro-tomography

Images showing cross sections of the contact parts (*gula* and *prothorax*) of the head articulation were taken in dry insects in two directions: transversal (figure 4.2 A) and sagittal (figure 4.2 B). The hemispherical convex shape of the *gula* cuticle can be seen in the cross section image in both transversal and sagittal direction. As can be distinguished in the figures, the head articulation system is an open joint. In the transversal image, the head articulation of the beetle is reminiscent of a technical ball bearing system.

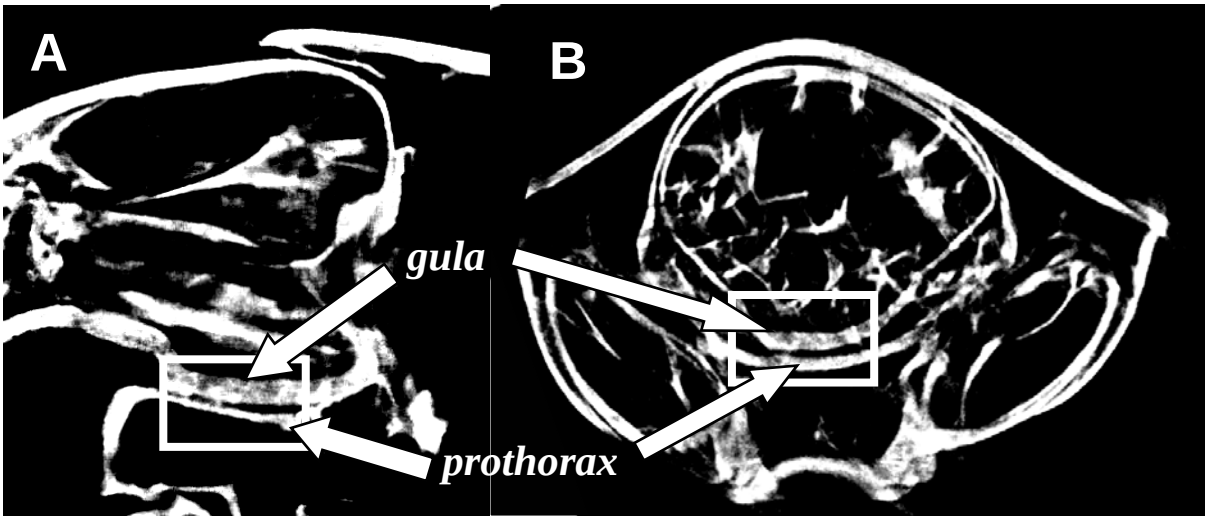

Figure 4.2: X-Ray tomography (µ-CT system) images in sagittal (A) and transversal (B) planes of the head articulation of the beetle *Pachnoda marginata*.

4.3.2 Structure of the cuticle

The surfaces of the contacting pair of the head articulation system were studied in the scanning electron microscopy (SEM). Figures 4.3 A and 4.3 C show the surface of the *gula* plate. The cuticle pores and dried organic substances can be seen on the smooth surface of the *gula*. A description of the surface structure and cross section of the *gula* cuticle is given in chapter 3 (section 3.3.1. Structure of the *gula* cuticle). Figures 4.3 B and 4.3 D show surface structures of the counterpart (*prothorax*) of the *gula*. Its surface is covered by cuticular outgrowths. A hierarchical surface structure of the *prothorax* cuticle can be distinguished. The arrows in the figures 4.3 A and 4.3 B show that these surfaces contact each other in the head articulation of the beetle.

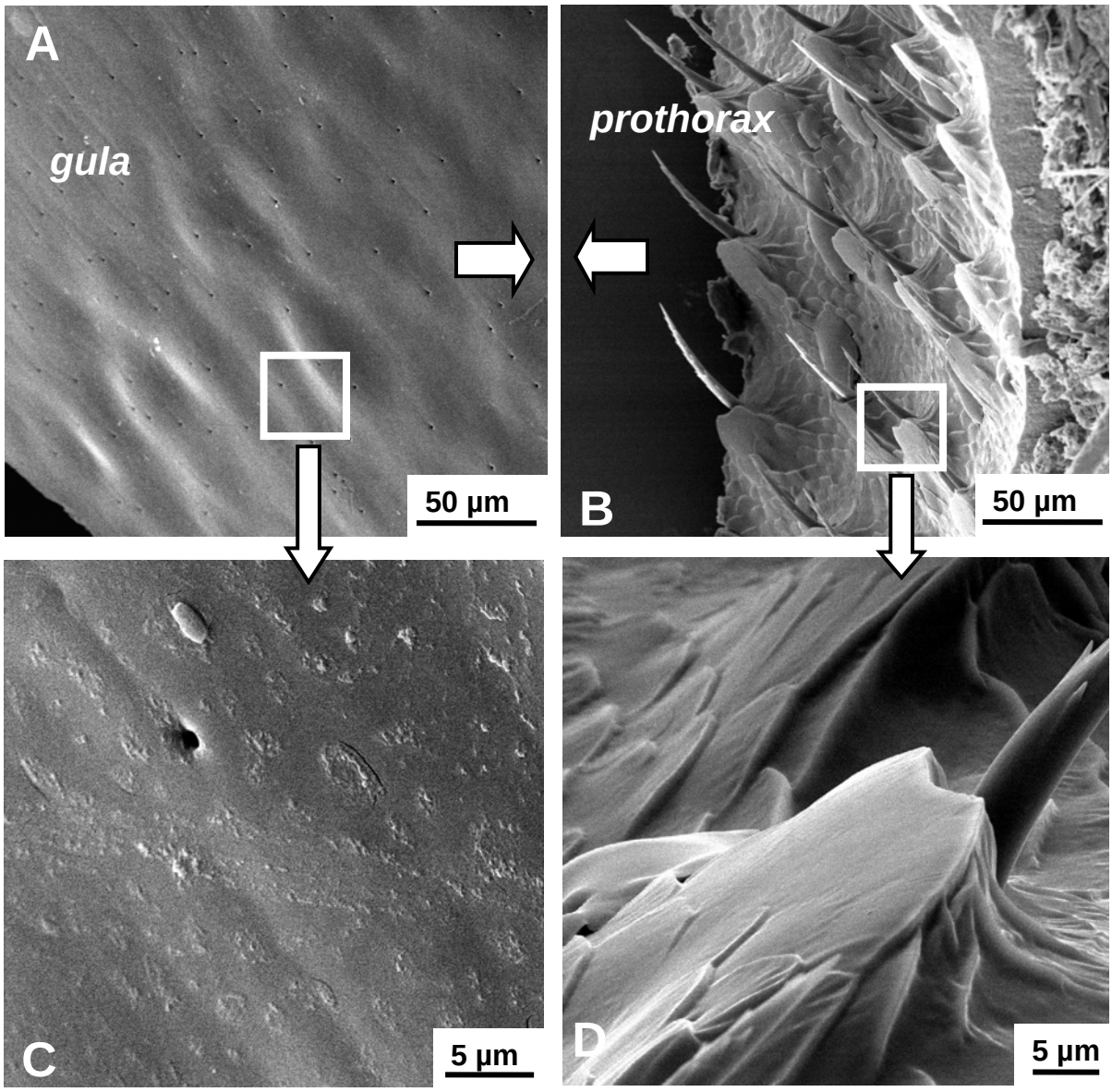

Figure 4.3: SEM images of the *gula* (A, C) and *prothorax* (B, D) surfaces. On the *gula* surface pores (A, C) and dried organic substances (C) can be distinguished. The figures B and D show cuticlar outgrowths on the *prothorax* surfaces. The *gula* and the *prothorax* surfaces operate in contact (shown with arrows on the figures A and B) in the head articulation system of the beetle *Pachnoda marginata*.

4.3.3 Friction properties

The frictional behavior of the *gula* cuticle was tested in five cycles of sliding a glass plate onto the sample surface over a distance of 100 µm. Figure 4.4 shows the friction forces as a function of time (A) and sliding distance (B). Normal loads (30-10000 µN) were applied and tangential forces were measured while sliding the sample along the x-axis in both directions (distal-proximal). In figure 4.4 B, the tangential force is plotted versus the sliding distance for one sample in the fresh, dry and chemically treated conditions for one cycle and at an applied normal force of 5000 µN.

The relation between tangential and normal force is shown for 7 different applied forces (F_{AN}=30; 100; 300; 1000; 3000; 5000; 10000 µN) and for the fresh, dry and chemically treated conditions (figure 4.5). The tangential force increases with increasing applied normal load. The friction coefficient was calculated from the applied normal load F_{AN} and the measured tangential force F_T (F_T/F_{AN}). It varies depending on the sample condition. Figure 4.6 presents average values of approximately 10 measurements for each condition and at each applied load. Fresh cuticle exhibits the highest friction coefficient, that of dry cuticle is lower. Chemically treated samples display the lowest friction coefficient. The results show a dependence of the friction behavior on the applied load. At small applied loads, the friction coefficient is high. It decreases with an increase in applied load.

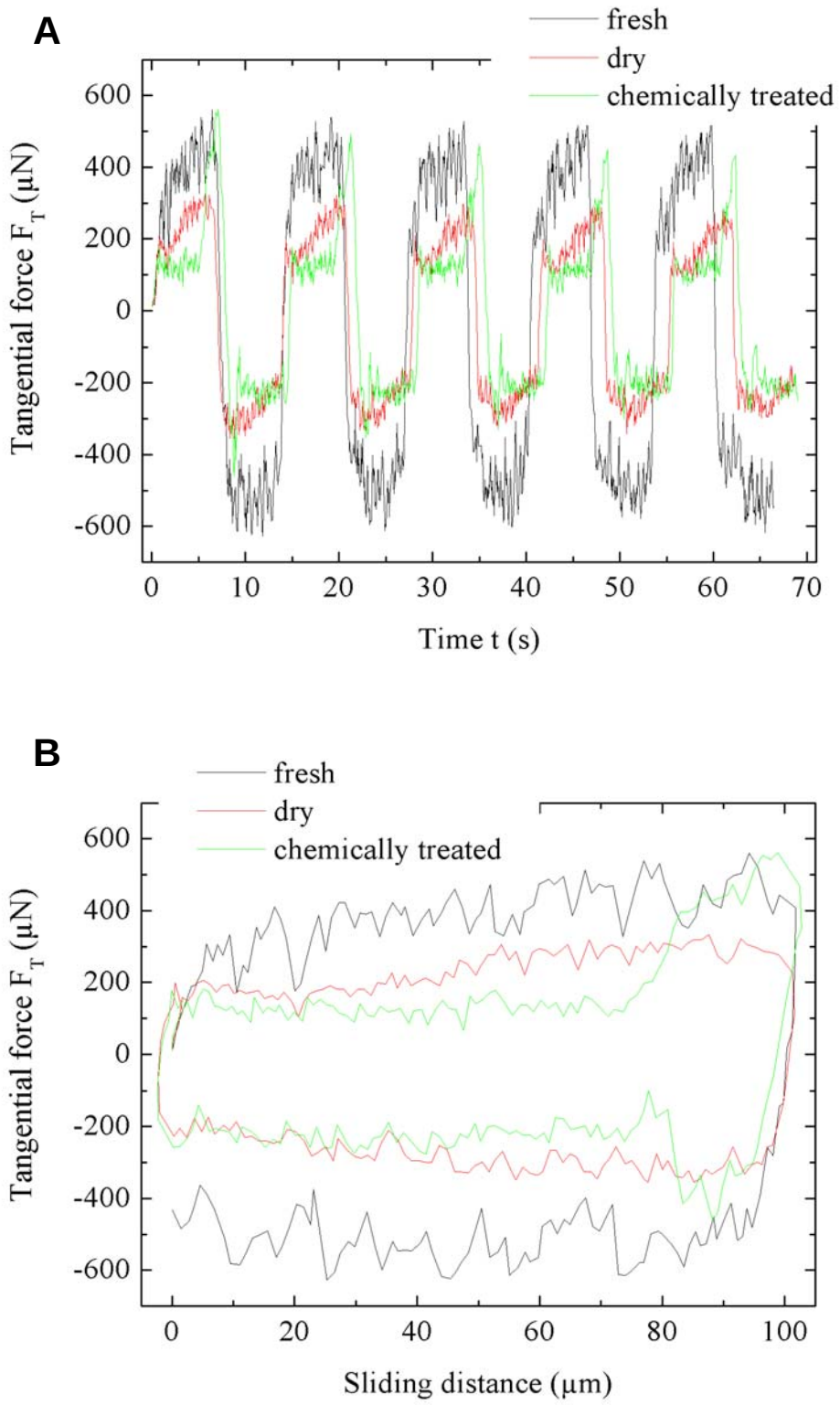

Figure 4.4: Tangential force versus time (A) and tangential force versus sliding distance (B). The results for fresh, dry and chemically treated cuticles are shown.

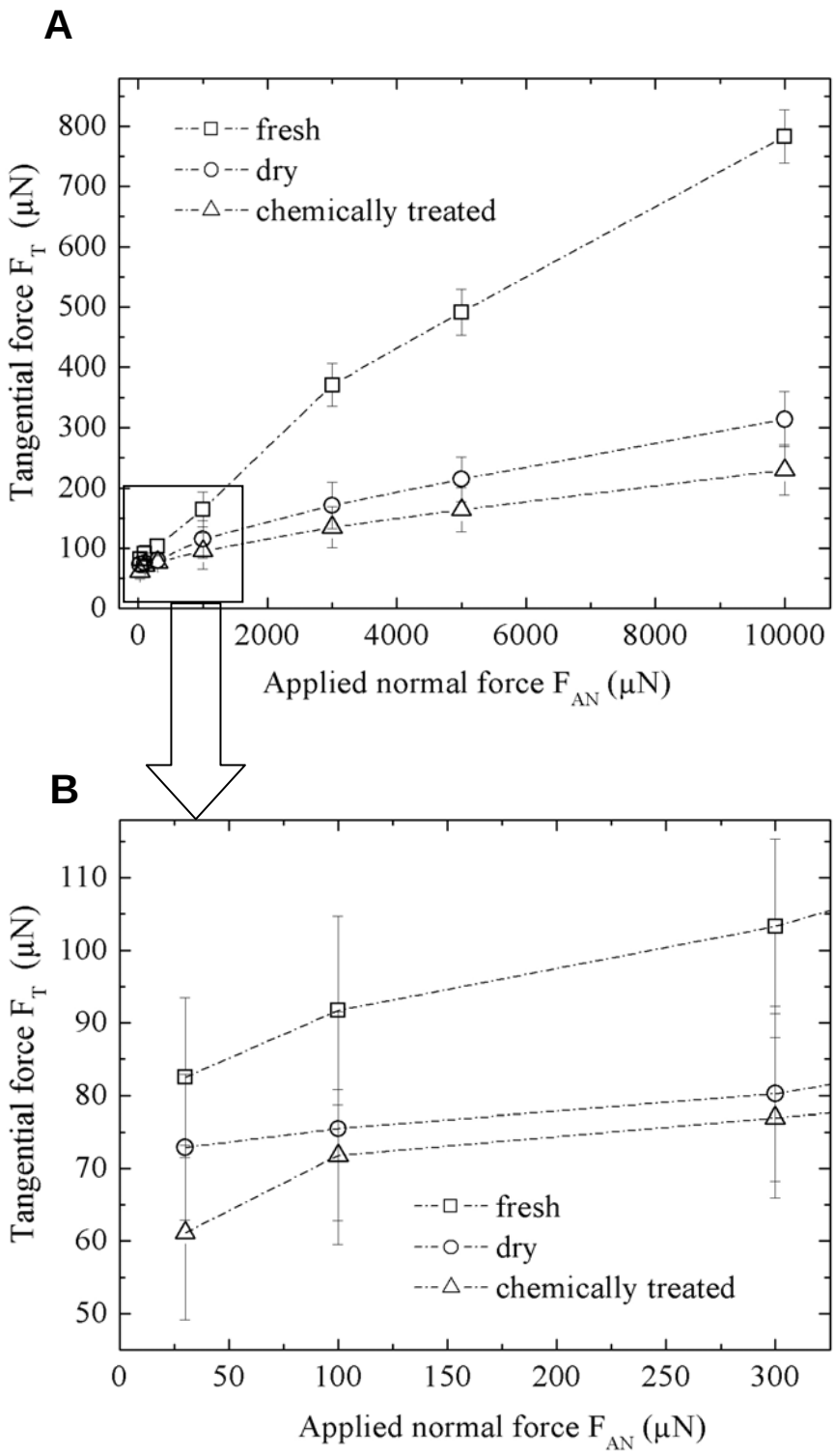

Figure 4.5: Tangential forces plotted versus applied normal forces for fresh, dry and chemically treated cuticles. A: relationship at all applied loads (30, 100 and 300 µN and 1, 3, 5, and 10 mN) used in friction experiments; B: relationship at low applied loads (30, 100 and 300 µN). Each data point corresponds to the mean value of 10 measurements.

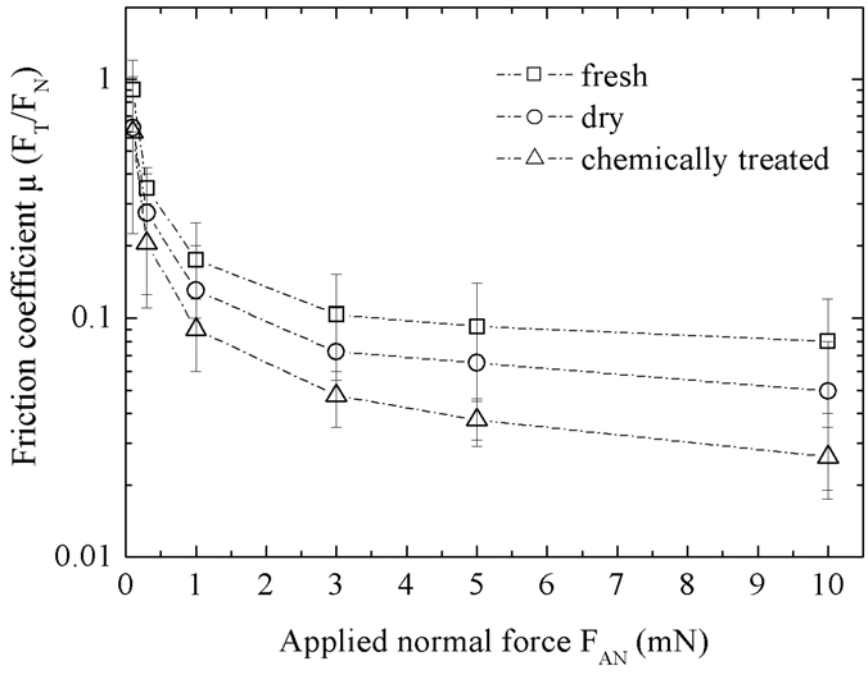

Figure 4.6: Friction coefficients for fresh, dry and chemically treated cuticles plotted versus applied normal force. Mean values for with the standard deviations of 10 measurements for each applied normal load in each condition are shown.

4.3.4 Surface roughness

The results of surface roughness measurements using white-light interference microscopy are summarized in table 4.1. The average values of the surface roughness parameter *Ra* and *rms* with standard deviations are presented. Figure 4.7 shows the surface profiles of the top of the *gula*. The hemispherical convex shape of the *gula* top can be seen. Surface profiles in fresh, dry and chemically treated condition are different. Fresh samples are very smooth (*Ra* = 33 ± 5 nm, *rms* = 38 ± 7 nm) (figure 4.7 A). Drying causes an increase in roughness (*Ra* = 161 ± 11 nm, *rms* = 197 ± 15 nm) of the *gula*-cuticle (figure 4.7 B), which is reduced (*Ra* = 103 ± 8 nm, *rms* = 117 ± 11 nm) after chemical treatment (figure 4.7 C).

Table 4.1: Summary of surface roughness parameters, *Ra* and *rms*, obtained by white-light interference microscopy for fresh, dry and chemically treated *gula* cuticles. The surface roughness measurements were carried out on three samples for each condition (SD = standard deviation).

Surface roughness parameter / Sample condition	***Ra*** **(nm)**	SD	***rms*** **(nm)**	SD
fresh	33	± 5	38	± 7
dry	161	± 11	197	± 15
chemically treated	103	± 8	117	± 11

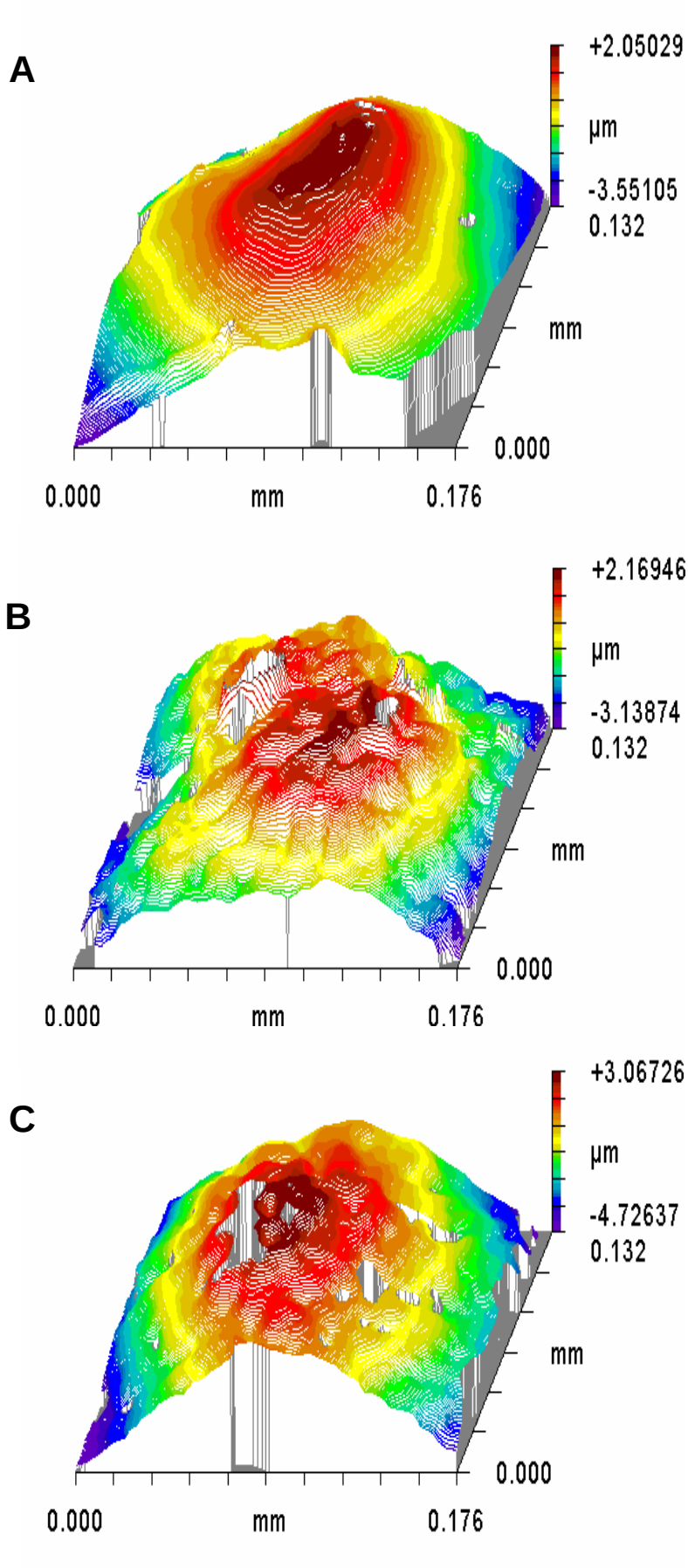

Figure 4.7: Surface profiles of fresh (A), dry (B) and chemically treated (C) cuticles. The images were obtained by white light interference microscopy.

4.3.5 Contact area

In figure 4.8, all results of the contact area measurements are summarized. Each data point is the average value of 10 tests for each condition and at each normal load. For all specimens, the expected increase of the area of contact with increasing normal load could be obtained. There is a strong dependence on sample condition. The values of the contact area are higher for the fresh samples than for dry and chemically treated ones. After chemical treatment, the contact area becomes larger than that of the dry samples.

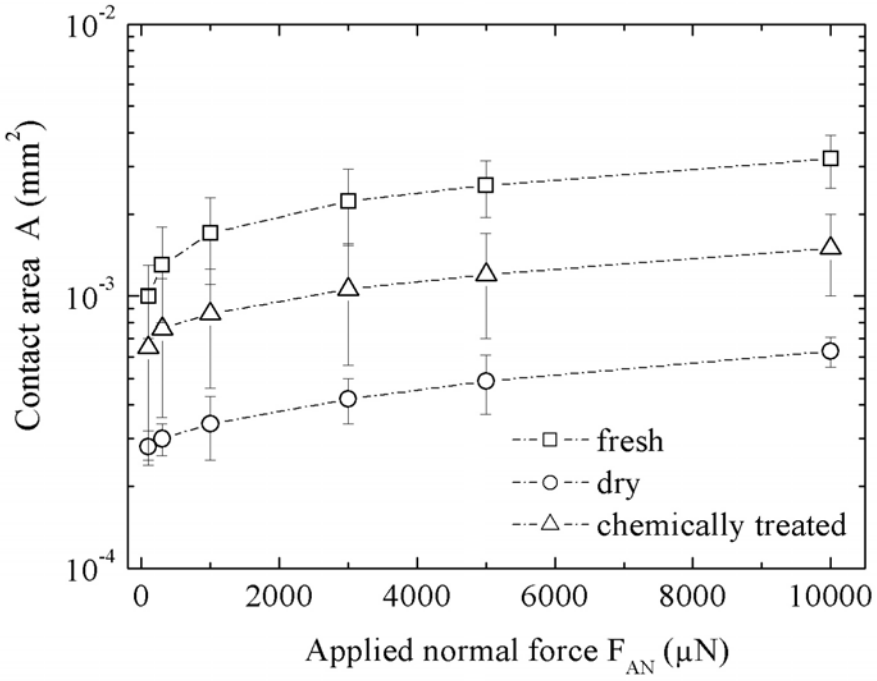

Figure 4.8: Contact area in dependence on the applied force for fresh, dry and chemically treated cuticles. The contact area was measured at different applied loads. 10 measurements for each applied load in each condition were performed.

4.3.6 Contact angle

Figure 4.9 presents the results of all *gula* cuticles tested (3 samples in the fresh, 3 in the dry and 3 in the chemically treated condition). Within the large variations, no significant difference between the sample conditions could be detected (see also appendix 7.1).

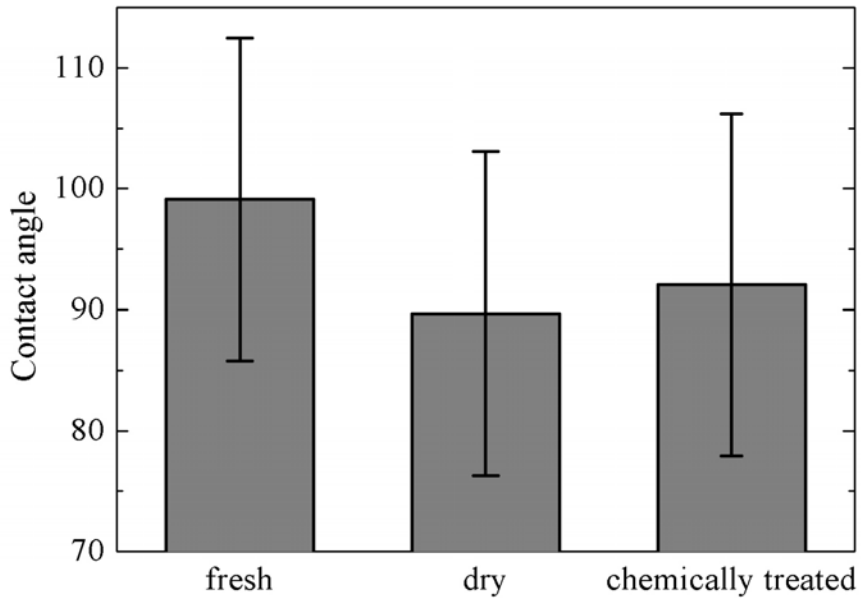

Figure 4.9: Contact angle of fresh, dry and chemically treated cuticles are shown. The experiments were performed on 3 samples in each condition. 3 measurements on each sample were carried out. Error bars mark the variation of the results in the same condition.

4.4 Discussion

To evaluate the working principle of *gula* cuticle in nature, an understanding of the relationship between surface properties and tribological behavior of the material is necessary. The first subsection focuses on how the material properties and the tribo-mechanical behavior of the cuticle are influenced by the sample condition. To understand which properties are relevant for friction minimisation in this biological system, the experimental results will be discussed in the light of the tribological events on the micrometer level in the second subsection.

4.4.1 The influence of the condition on the properties of the *gula* cuticle

The influence of water loss

The results show that desiccation has a great influence on the tribo-mechanical behavior of the cuticle tested. As the integument of the adult insect, *gula* cuticle is of the hard and stiff type and contains less water than the soft and compliant one. However, water is one of the essential components of the cuticle (Vincent and Wegst, 2004) and together with chitin, proteins and lipids, it is responsible for the cuticle properties.

In the fresh condition, the surface of the *gula* cuticle is extraordinarily smooth for a biological material (Ra = 0.033 ± 0.005 µm, rms = 0.038 ± 0.007 µm). After desiccation, the outer layer of the cuticle builds up high roughness. The water loss is thought to cause the constriction of the structure in inner layers and folding of the outer layer. These structural changes could be the reason why dry samples exhibit a rougher surfaces (Ra = 0.161 ± 0.011 µm, rms = 0.197 ± 0.015 µm).

Desiccation changes the apparent contact area during normal loading. Soft and compliant fresh *gula* cuticle has a smooth surface and displays a larger contact area than the dry one.

The changes in the mechanical properties appear to be the cause of the different contact area. Due to hardening and stiffening of the samples, the contact area becomes smaller.

The water content in the cuticle, as already shown, greatly influences the material properties. It results in changes in the friction behavior of the cuticle tested. According to Rabinowicz (1995), hard and stiff materials are better than soft and compliant for friction minimization in sliding applications.The mechanical properties such as the hardness and the elastic modulus with low surface roughness are believed to be the reason for the higher friction coefficient of the soft and compliant fresh cuticles than that of the dry ones, which showing the high surface roughness, are hard and stiff.

The influence of the wax/lipid layer

Washing of the dry samples in chloroform-methanol solution causes only small changes in the indentation results (see chapter 3). After chemical treatment sample surface becomes harder ($H = 0.52 \pm 0.15$ GPa). A slight increase in stiffness ($E = 7.70 \pm 1.90$ GPa) only in first 1 µm of the indentation depth could also be observed. Further hardening and stiffening of the cuticle after chemical treatment is thought to be caused by the removal of the dry organic substances (waxes and lipids) from the sample surface.

As already shown, the mechanical properties of the dry and chemically treated cuticles differ only a little from each other. After the chemical treatment, the surface roughness becomes lower ($Ra = 0.103 \pm 0.008$ µm, $rms = 0.117 \pm 0.011$ µm). It could be caused by dissolving the dry organic substances or structure on cuticle surface. However, the roughness of the fresh samples remains lower than that of dry and chemically treated ones. The contact area becomes larger after the chemical treatment when compared to the contact area of dry samples.

The organic substances such as lipids and waxes on the cuticle surface were believed to serve as lubrication to reduce the frictional forces. Therefore, the friction coefficient of the fresh samples was expected to be lower than that of the dry ones. A chemical treatment, performed in order to remove lipids and waxes from the sample surface, were thought to remove the lubrication effect and the samples in the chemically treated condition were expected to show

the highest friction coefficient. However, the effect of the organic substances as the lubricants could not be confirmed. Frictional forces were lowest in the chemically treated samples. The highest friction coefficient was measured for fresh samples with a wax/lipid layer as lubricants on the surface. Friction properties are, thus, not influenced only by lubrication, but also by other factors such as surface geometry, hydrophobicity or mechanical properties.

4.4.2 Friction behavior

The friction behavior of the *gula* cuticle was studied in relation to its surface properties. The friction depends on a variety of complex phenomena of the contacting surfaces. The literature states that there is no strong correlation between only one material property and friction parameter (Rabinowicz, 1995). The frictional forces are determined by several different factors (Klein, 2001) such as contact area, hydrophobicity and/or roughness of the surface. To understand the friction behavior of the *gula* cuticle, tribological events in general and the differences between macroscopic and microscopic tribology are briefly reviewed.

Background

When two solids touch each other, forces of action and reaction exist. This event is influenced by several factors including surface topography, lubricant properties, hydrodynamics, solid mechanics, surface chemistry (Hutchings, 1992; Rabinowicz, 1995; Ludema, 2000; Tichy and Meyer, 2000). Friction is the resistance to relative motion of contacting surfaces. First investigations on friction were carried out by Leonardo da Vinci (1452-1519), later by Amontons (1699) and Coulomb (1785). They discovered that the friction force is proportional to the applied normal load and independent of the contact area. These are the fundamental laws of macroscopic friction that is mainly due to the mechanical interlocking of asperities on the surfaces of the contacting materials (Rabinowicz, 1995; Scherge and Gorb, 2001).

According to Amontons, the friction force is directly proportional to the applied load so that the friction coefficient is

$$\mu = \frac{F_T}{F_N} \tag{4.1}$$

where F_T and F_N are the measured tangential force and the applied normal load, respectively. According to this law, the friction coefficient μ remains constant.

According to equation (4.1), the friction force is independent of the apparent area of contact and the surface roughness (Bowden and Tabor, 1950; Rabinowicz, 1995; Persson, 1997). The area independence means that the coefficients of friction of large and small bodies are the same (Rabinowicz, 1995).

These classical laws of friction fail, however, for the description of tribology at the micro- or nanometer scale. In contrast to macroscopic friction, recent microscopic tribological studies indicate that friction forces do depend on the apparent contact area and also on the microroughness of the contacting surfaces (Rabinowicz, 1995; Scherge and Schaefer, 1998; Enachescu *et al*., 1999; Ciulli, 2001). In regard to the contact area dependence, friction is thought to be caused by adhesive forces arising between the contacting surfaces (Rabinowicz, 1995).

Microfriction is influenced by surface interaction phenomena. When two bodies form a contact, adhesion occurs, the strength of which depends on the surface energy (Johnson *et al*., 1971). Van-der-Waals forces, capillarity, hydration or electrostatic forces influence the tribological behavior under low applied forces in the range of mN down to nN. An important factor is whether the contacting surface is wettable (hydrophilic) or non-wettable (hydrophobic). The formation of a water film on hydrophilic surfaces and capillarity have a great effect on the friction behavior in the micronewton range. With an increase in thickness of the water film on the surface, a meniscus is formed that bridges single asperities and increases shear forces (Bhushan, 1999). On hydrophobic surfaces, the formation of a water film is prevented. Under increasing applied loads the surfaces come closer together and the frictional forces increase due to adhesion caused by Van-der-Waals forces. For large contact radii, the forces mentioned above are no longer relevant and surface energy effects can be neglected in macrofriction (Rabinowicz, 1995; Scherge and Schaefer, 1998; Bhushan, 1999; Scherge and Gorb, 2001; Hild *et al*, 2002).

With regard to the attraction forces mentioned above the normal load is not the same as the applied load, but

$$F_N = F_L + F_A \tag{4.2}$$

where F_L is the contribution of attraction forces and F_A applied load.

Now Amontons equation (4.1) can be rewritten as

$$\mu = \frac{F_T}{F_L + F_A} \tag{4.3}$$

Depending on the amount of attractive forces, the friction between two ideal (molecularly smooth) surfaces can be “adhesion-controlled” (high attraction) or “load-controlled” (low attraction). “Adhesion-controlled” friction is proportional to the area of the real (molecular) contact. “Load-controlled” friction is proportional to the applied load.

Since it is difficult to prepare molecularly smooth surfaces, roughness plays an important role in the tribological performance. Even a few nanometers of roughness can change the tribological behavior of the contacting surfaces as deformation of the surface asperities becomes important. Therefore the contact area as well as the mechanical properties of the material such as hardness and stiffness determine the tribological performance. The contact behavior of the material depends on the surface roughness in combination with the mechanical properties. With an increase in roughness of one of the contacting surfaces, the contact area and, consequently, the adhesion between two hard solids can be reduced resulting in low frictional forces. However, roughness can cause high frictional forces due to an increase in contact area and therefore in adhesion in soft viscoelastic surfaces (Israelachvili, 2001).

Friction behavior of the gula cuticle

The frictional behavior of the *gula* cuticle was found to be influenced not only by the mechanical but also by the surface properties of the specimens, which is in good agreement with literature (Rabinowicz, 1995; Scherge and Schaefer, 1998; Enachescu *et al*., 1999; Ciulli, 2001; Israelachvili, 2001). The cuticles tested behaved differently depending on their condition. Fresh ones were soft and compliant with low surface roughness. Desiccation significantly increased their hardness, stiffness and roughness. After chemical treatment the samples became harder and stiffer. The roughness of the chemically treated samples was lower than in the dry ones. There was, however, no significant difference in hydrophobicity of fresh, dry and chemically treated surfaces. All samples tended to be hydrophobic. Therefore, an influence of this factor on tribological behavior can be neglected.

In spite of the differences in surface properties, all results showed a strong dependence on the applied load: the higher the normal load the higher was the tangential force. In all experiments, the friction coefficient, however, was not constant. It was found to decrease with increasing applied load. An influence of contact area was also observed. The higher the applied force, the larger was the contact area (figure 4.8). Correspondingly the attractive forces between the contacting surfaces were expected to increase (Scherge and Schaefer, 1998). Thus the necessary tangential force to break a mechanical interlocking between the contacting surfaces was low at low applied forces and increased with increasing applied load (figure 4.5).

According to these considerations, the friction coefficient would be expected to increase with increasing applied normal load. Surprisingly, the opposite has been measured (figure 4.6). The friction experiments were carried out with applied loads increasing from 30 µN to 10 mN. It is possible that the cuticle surface is damaged during sliding. When applying the next higher load the adhesion is thought to act not on whole contact area but only on the new contact area created under the increased load (J. Israelachvili, personal communication). In general the adhesion is believed to influence strongly the micro friction at the low applied loads. Therefore friction coefficient decreases with increasing the applied load due to the reduced effect of adhesion.

According to Israelachvili (2001), friction of the ideal (molecularly smooth) surface depends either on the normal load or on the contact area. But the surfaces in nature are rough. Even if the fresh cuticles were extraordinary smooth for biological surfaces, they would not be ideally (molecularly) smooth. Surface roughness in connection with hardness and stiffness could be one of the reasons that the friction experiments show both contact area and load dependence of the friction at the same time.

In order to understand the relationship between friction behavior and contact area, frictional force is plotted versus contact area in figure 4.10 using the data of figures 4.5 and 4.8. The relation between the friction behavior and the mechanical properties is shown in figures 4.11 A (hardness versus friction coefficient) and 4.11 B (elastic modulus versus friction coefficient). The dependence of the frictional force on the contact area is nearly linear. Two completely different relationships between friction behavior and contact area can be detected. They depend on the sample condition. Comparing fresh and dry samples, friction force are found to decrease with decreasing contact area. This is attributed to surface hardening and stiffening (Israelachvili, 2001) caused by drying of the specimens. The same behavior can be observed comparing fresh and chemically treated samples. The smooth surface of fresh cuticle has larger contact area and frictional forces than the rough surface of the cuticle after chemical treatment. It is not surprising that the hard, stiff and rough chemically treated surfaces display lower friction coefficients than soft, compliant and smooth fresh cuticles. A comparison between the dry and chemically treated samples reveals another trend. Chemically treated samples show only a small increase in hardness and stiffness, but a decrease in surface roughness. The contact area after chemical treatment is larger than that of the dry ones. However, the frictional force is found to be lowest in chemically treated samples. After chemical treatment the samples display a smaller surface roughness, but a higher hardness and stiffness than dry ones. The mechanical properties of the material are believed to be the relevant factor influencing the friction behavior in this case as well.

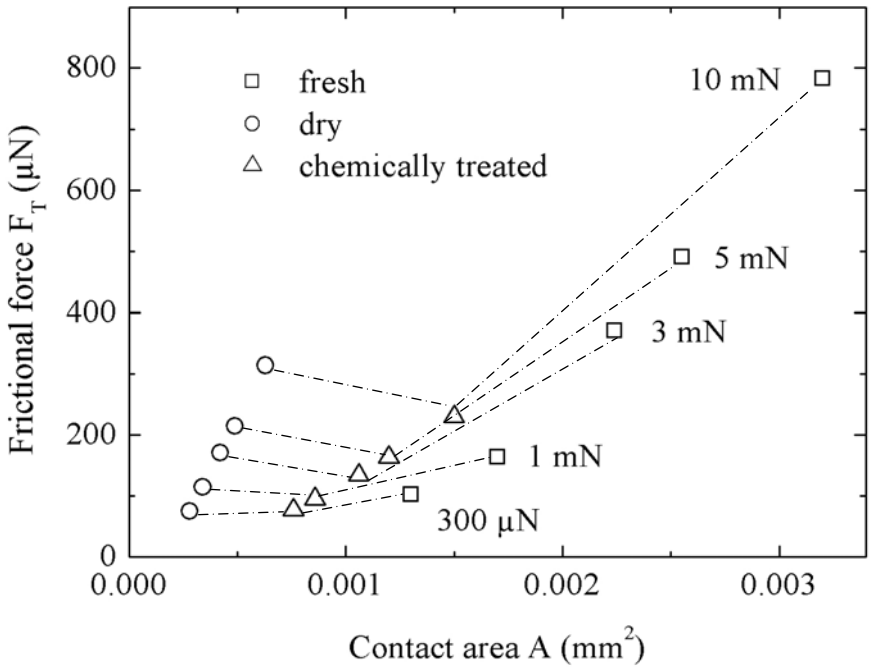

Figure 4.10: Friction force versus contact area obtained at different applied loads (300 µN and 1, 3, 5 and 10 mN) for fresh, dry and chemically treated cuticles. Results corresponding to 30 and 100 µN are not shown.

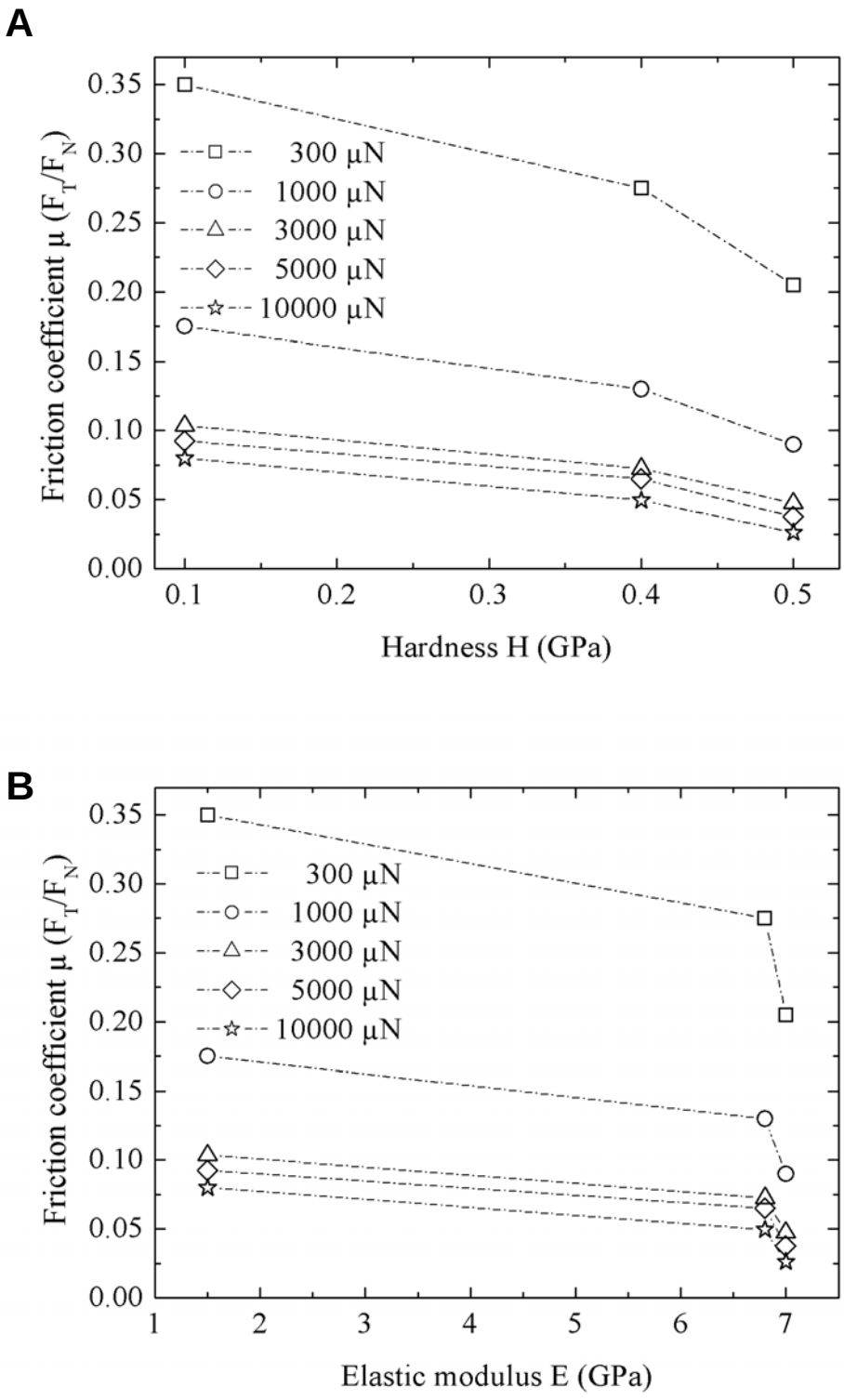

Figure 4.11: The friction coefficient is plotted versus hardness (A) and elastic modulus (B). The hardness and the elastic modulus values determined by nanoindentation (see Chapter 3) are shown for fresh, dry and chemically treated cuticles. The friction coefficient is shown for different applied loads (300 μN and 1, 3, 5 and 10 mN) and for fresh, dry and chemically treated cuticles.

Contact behavior

In order to show a correlation between mechanical properties and contact behavior the hardness (determined by nanoindentation, see chapter 3) (figure 4.12 A) and the elastic modulus (determined by nanoindentation, see chapter 3 (figure 4.12 B) versus contact area for applied loads of 300 µN and 1, 3, 5 and 10 mN have been plotted. In general, independent of the hardness and elastic modulus values, the contact area increases with increasing applied force. However, the applied force greatly influences the contact area of the fresh samples, which are soft and compliant. As expected with hardening and stiffening of the cuticle, after drying the contact area decreases. The applied load has only a small influence on the contact area in this case. After Rabinowicz (1995), the contact area is primarily determined by the mechanical properties of the material. Comparing dry and chemically treated samples reveals a different behavior. Hardness and elastic modulus increase after chemical treatment and surprisingly, so does the contact area.

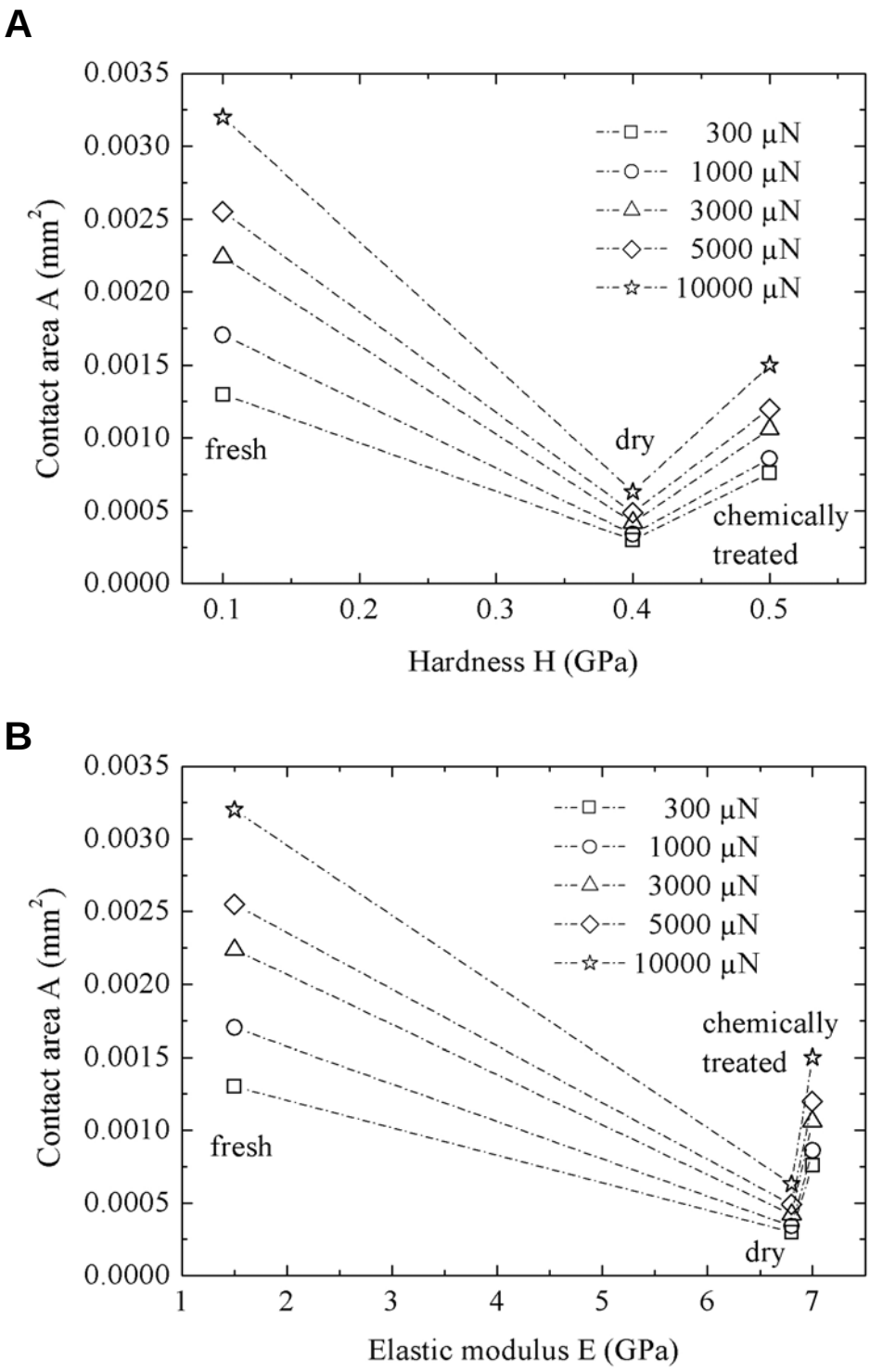

Figure 4.12: The contact area is plotted versus hardness (A) and elastic modulus (B). The mean values of the hardness and the elastic modulus determined by nanoindentation (see Chapter 3) are shown for fresh, dry and chemically treated cuticles. The contact area is shown for different applied loads (300 µN and 1, 3, 5 and 10 mN) and for fresh, dry and chemically treated cuticles.

In an attempt to learn more about the contact behavior between the fresh *gula* and the glass plate under the applied normal load, the radius of the circle of contact was calculated from experimentally measured contact area and plotted versus applied normal load in figure 4.13. The experimental data have been fitted by the Hertz (1882) as well as JKR (1971) models. For fitting the experimental values of applied normal load, contact area and the radius of the *gula* (1.3 mm) (see appendix 7.2) have been used. Both Hertz and JKR fits are presented in figure 4.13 as well.

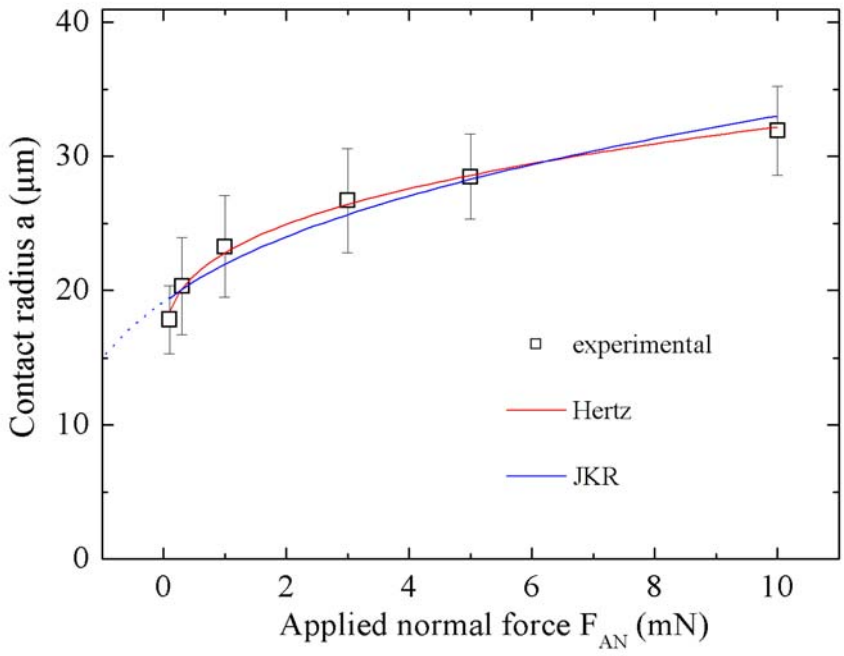

Figure 4.13: The contact radius between the fresh *gula* and glass plate determined from the experimentally measured contact area (figure 4.8) versus applied normal load. The experimental data are fitted by Hertz and JKR models. Taking into account that the $a_0 \neq 0$ but a_0 = 14.68 µm by $F_0 = 0$, the Hertz fit is better than JKR fit.

The reduced elastic modulus predicted by the Hertz fit (1.8 GPa) is in excellent agreement with the elastic modulus value measured experimentally by nanoindentation for fresh *gula* (1.5 ± 0.8 GPa) (see chapter 3). However the Hertz fit gives the contact radius, a_0 corresponding to F_0 (applied normal force) not 0 as described by Hertz theory but 14.68 µm.

This difference is thought to be caused by several factors. Hertz theory describes contact behavior between two spherical bodies. A non-ideal spherical shape and a microroughness of the *gula* are believed to exhibit even flat surface in micrometer range. This non-ideal geometric condition compared to Hertz model is expected to lead to an increase in the experimentally obtained contact area just by applied normal load $F_0 = 0$. Consequently, the contact radius calculated from the contact area data is not 0 as expected by Hertz model but 14.68 µm. Also meniscus forming on the surface asperities due to the intrinsic water layer cannot be excluded.

The JKR fit results in a reduced elastic modulus of 0.48 GPa which is very small compared to the experimentally measured data (1.5 ± 0.8 GPa). A work of adhesion estimated with the JKR fit is very high (γ = 140 mJ/m^2). Correspondingly the equation (2.5) gives high pull-off force value (~ 0.9 mN) which could not be seen during the experiments. This is clearly incompatible with the experimental data.

Based on these estimations can be concluded that the contact radius versus applied normal load data can be fitted very well by the Hertz model. However important condition is to take into account that when applied normal load $F_0 = 0$, the contact radius $a_0 \neq 0$ but a_0 = 14.68 µm, which is due to non-ideal spherical shape of *gula* and also possible meniscus building on the surface asperities.

4.4.3 How does the *gula* cuticle reduce the friction?

Since the *gula* cuticle is part of a biological system and as it operates in the head-articulation system of the living beetle, the properties of the fresh samples are important to understand its working principle. Frictional properties of the *gula* cuticle were studied in contact with glass plate. It was shown that the surface of the hemispherical *gula* is very smooth in the fresh condition. Friction between the fresh sample and glass plate can be considered as a sliding of two smooth surfaces against one another. One of them, described above, the fresh cuticle is hydrophobic, the other, the glass plate, is hydrophilic. Due to the factors mentioned above, this combination exhibits a large contact area and consequently a large shear force (Scherge and Schaefer, 1998). However in the native condition, the *gula* slides on the *prothorax*

surface, which is covered by cuticular outgrowths. This is a very different combination: a smooth surface with a rough one. During the relative motion, the two parts in this system will, because of their different structure not form an intimate contact of the whole surfaces with one other, but form contact points in the micrometer range. Since the surface of the *gula* cuticle is hydrophobic, the surface of the *prothorax* cuticle (same type of cuticle) is assumed to be hydrophobic as well, thus the formation of a water film is inhibited. With decreasing contact area friction forces will be reduced. This is the better combination of the surfaces to minimize the frictional forces as a result of decreasing the contact area. According to the experiments, this suggestion seems to be correct. However as already shown, friction behavior cannot be determined only by a few factors such as surface roughness and area of contact. Material properties such as hardness and elastic modulus are very important and cannot be neglected. Since *prothorax* belongs to the same type of sclerotized cuticle as *gula* and is a part of the same system, it can be supposed that the mechanical properties of the material are nearly the same. However, the *prothorax* is covered with cuticular outgrowths which can change the mechanical behavior significantly. The structuring of the *prothorax* can lead to the softening of its surface. According to the literature concerning bearing systems (Barwell, 1979) materials for contacting surfaces should be selected with different hardnesses so that the shape of the bearing will be determined by the harder surface.

The results obtained describe the material properties optimized to hold and to move the head of the beetle *Pachnoda marginata*. It is reasonable to assume that the head articulation system requires low friction for movement of the head, but high friction for fixation the head, for instance, during digging. Low friction can be reached with decreasing in contact area between the smooth and structured surfaces under low load. An increase in contact forces between the *gula* and the *prothorax* will increase the contact area and, consequently, the friction.

To understand how friction influences the head articulation of the beetle, further investigations on this system, including studies of the counter-part of the *gula*, are necessary. In addition, the suggestions mentioned above can be probed using the contacting pair of the same polymer but with different surface roughness.

4.5 Summary and conclusion

The tribo-mechanical behavior of the head articulation cuticle of the beetle *Pachnoda marginata* was studied in order to understand the working principle of a materials system designed for friction minimization in biology. To investigate the effect of desiccation and removal of an outer wax/lipid layer, the samples were tested in three conditions: fresh, dry and chemically treated. The results obtained can be summarized as follows:

- The tribo-mechanical behavior of the *gula* cuticle depends on the sample condition. Surface properties are greatly influenced by moisture content. The removal of the outer wax/lipid layer also changes the mechanical behavior of the samples.

- The frictional behavior of the *gula* cuticle was found to depend on the applied load and the contact area at the same time. The fundamental laws describing the friction coefficient to be independent of load and contact area at the macroscopic scale do not seem to hold at the microscopic scale.

- The friction at the micrometer range was found to be influenced by several properties of the contacting surfaces. A strong correlation between only one fundamental property and the frictional performance could not be found. The frictional forces were influenced by the material's mechanical properties as well as by the contact area or roughness of the surface.

- Two different types of correlation between friction and contact area could be detected. Friction decreases with decreasing contact area after drying. Subsequent chemical treatment increased the contact area, but decreased the friction slightly. The friction coefficient decreased with increasing applied load. All samples revealed a good correlation with the mechanical properties: an increase in hardness and stiffness caused a decrease in friction.

- The contact behavior of the cuticle tested is found to be fitted very well by the Hertz model with taking into account that when applied normal load $F_0 = 0$, the contact radius $a_0 \neq 0$ but $a_0 = 14.68$ µm. The increased experimental value of the contact radius is thought to be caused by non-ideal spherical shape of *gula* and also possible meniscus building on the surface asperities.

- Fresh *gula* cuticle showed the highest friction coefficient in contact with a glass plate when compared to the dry and chemically treated samples. In nature it forms a contact with the *prothorax* surface covered with cuticular outgrowths. A friction reduction could be expected as a result of the contact area minimization. However, a description of the working principle of a tribological system is only possible if the material properties of both contacting surfaces are known. Therefore investigations on the counter-part of the *gula* are necessary.

5 Mechanical behavior of wax coated plant surfaces

Abstract

The cuticle of plants is usually covered by a wax layer, which is essential for functional and ecological reasons in the interaction between the plant and its environment. An epicuticular wax layer is present primarily on the surface of leaves, stems and fruits. The layer is a mixture of different chemical compounds and varies in thickness from 1 to 20 µm. On the amorphous wax layer of several plants emerges a crystalline wax structure. Insects cannot attach to the plant surfaces covered with wax crystals. In this project, the leaves of two pea (*Pisum sativum*) mutants (wild type with normal wax layer and glossy type with reduced waxy bloom) in fresh and dry conditions were tested by using Nano indenter® SA2. The mechanical measurements on the plant surfaces show a dependence of the mechanical properties (hardness and elastic modulus) on the condition (fresh or dry). Desiccation makes plants soft and compliant. No difference in the deformation behavior between the fresh samples with normal and with reduced wax layer can be seen. The cell structure and especially the pressure of the cell fluid appear to determine the mechanical behavior of the fresh samples. This makes it impossible to obtain hardness and elastic modulus values of the wax layer on the fresh leaf. The dry plant surfaces with wax layer are softer and more compliant than the sample with reduced waxy bloom.

5.1 Introduction

The cuticle is an essential element of a plant. Being the outer surface layer, it is of fundamental functional and ecological importance for the interaction between plants and their environment (Barthlott, 1990; Bianchi, 1995; Gorb, 2001). The plant cuticles display different surfaces. They may be pigmented or colorless, smooth, textured or hairy, dry or covered with epicuticular secretions (Jeffree, 1986; Gorb, 2001). The extraordinary diversity of the plant surface structure is a reflection of their different environment (Jeffree, 1986). Preventing desiccation and allowing controlled exchange of gases are the important functions of epicuticular components (Baker, 1982; Jeffree, 1986; Barthlott, 1990).

The plant cuticle is a multilayered composite consisting of a polymeric cutin matrix and the cuticular waxes (Eigenbrode, 2002). Figure 5.1 shows the generalized structure of the plant cuticle (Gorb, 2001). An outer wall of epidermal cells is covered by a pectinaceous cuticle membrane, which is protected by a layer made up of cellulose microfibrils. On the cuticle proper consisting of a lamellate layer, cutin and the epicuticular waxes are deposited (Bianchi, 1995; Gorb, 2001). Cutin is a high molecular weight lipid polyester (Bianchi, 1995).

The epicuticle waxes are surface lipids (Bianchi, 1995). They display considerable ultrastructural and chemical diversity. The plant waxes are a complex mixture of very long-chain aliphatics including different chemical compounds, such as hydro-carbons, wax esters, primary and secondary alcohols, fatty acids, aldehydes, ketones, ß-diketones, triterpenoids and flavonoids (Walton, 1990; Eigenbrode, 2002). A current classification of plant epicuticular waxes, based on the studies of 13 000 plant species using high resolution scanning electron microscopy (SEM), distinguishes 23 types of wax crystals (Barthlott, 1990; Barthlott *et al*., 1998). The most common types of crystal shapes are tubes, solid rodlets, filaments, plates, ribbons and granules (Baker, 1982; Jeffree, 1986; Bianchi, 1995; Barthlott *et al*., 1998). The wax crystalloid structure correlates with its chemical composition (Barthlott, 1990; Bianchi, 1995; Barthlott *et al*., 1998). For example, aldehydes are very important for the formation of wax filaments, which is characteristic of the pea *Pisum sativum* leave surface (Gorb, 2001). The eucalyptus epicuticular wax, containing ß-diketones and

primary alcohols, exhibits mixed tubes and plates structure (Hallam and Chambers, 1976; Jeffree, 1986).

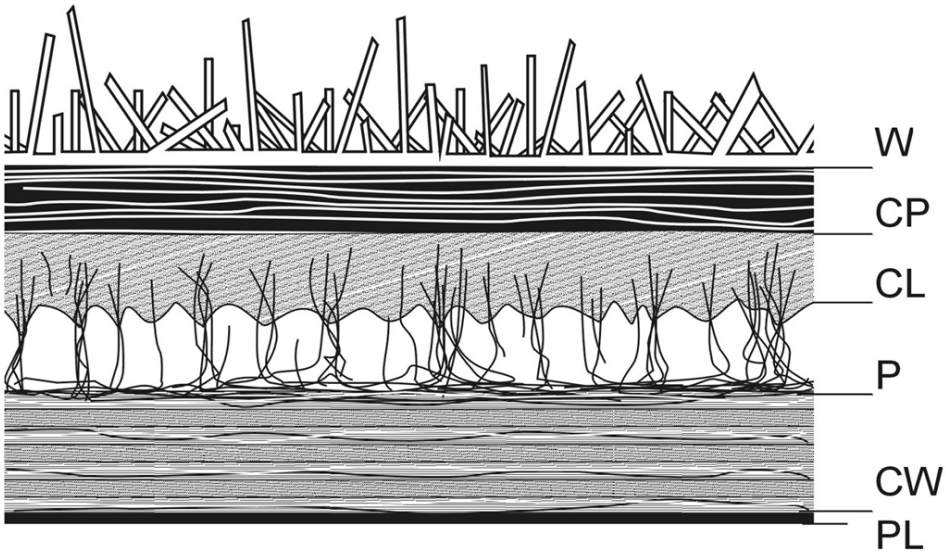

Figure 5.1: The generalised structure of a plant cuticle: W - epicuticular wax; CP - cuticle proper; CL - cuticular layer of reticulate region traversed by cellulose micro fibrils; P - pectinaceous cuticle membrane and middle lamella; CW - cell wall; PL - plasma lemma (taken from Gorb, 2001).

All plant surfaces carry a partial or a continuous layer of the amorphous wax as the obligatory final layer of the cuticle (Baker, 1982, Barthlott *et al*., 1998). However some plants consist of even two amorphous wax layers. Upon the amorphous layer, wax crystals of different shapes emerge and grow. The wax crystal layer varies widely in thickness from 1 to 20 µm. The thickness of the wax crystalloids lies in the nanometer range (Gorb, 2001; Enders *et al*., 2004). Wax morphology varies with the environmental conditions. The thickness of the layer, the size, the orientation and the density of wax crystals can be significantly modified by temperature and humidity (Baker, 1982). The epicuticular waxes occur in plants primarily on the surface of leaves, stems and fruits (Bianchi *et al*., 1978; Avato *et al*., 1984; Baker and Gaskin, 1987; Barthlott, 1990; Bianchi, 1995; Barthlott *et al*., 1998; Gorb, 2001). On the surfaces of many plant species, such as *Eucalyptus* leaves, the wax is continuously regenerated. In this way the surface is protected and kept in a fully functional state. However,

the epicuticular wax cannot be replaced after having been removed by abrasion from some plant surfaces (Bianchi, 1995).

Although no study on mechanical properties of the wax layer has been carried out, it is believed in biology that the plant wax and the underlying layers display different mechanical properties. A cuticularisation of the thick outer epidermal walls contributes to mechanical stability of the surface. The wax covering is mechanically very unstable and in biology known as “soft film” (Barthlott, 1990, Barthlott *et al*., 1998). Being fragile, the waxes are easily removed by rubbing (Barber, 1955; Jeffree, 1986). The wax crystalloids increase the roughness. Together with the wax chemistry, the roughness makes the plant surface hydrophobic and decreases its wettability. The hydrophobic constituents of the wax and surface microroughness reduce the adhesion of the dust and other particles on the outer cell wall. This “anticontamination function” called “lotus effect” is thought to be the most important ecological function of the water-repellent plants (Baker, 1982; Barthlott, 1990; Barthlott and Neinhuis, 1997).

An interaction between the plant surfaces and their environment also involves the complex and very important relation between plants and insects (Juniper and Southwood, 1986). Insects possess the attachment devices allowing the hold and the movement anywhere and on nearly any kind of surfaces (Gorb, 2001). The structures of attachment pads adapted for the natural, mainly plant surfaces enable the insects to move freely on any technical surfaces as well. However, some surfaces even in nature raise difficulties for their visitors. The wax layer on the plant is a barrier for the attachment systems of insects. Walking on the plant surface structured with the wax crystals was found to be impossible for insects (Eigenbrode, 1996; Gaume *et al*., 2002; Gorb and Gorb, 2002). Even though the interaction between the wax crystalloid layer and the insect has been of great interest to researchers for about a century (Kerner von Marilaun, 1898; Haberlandt, 1909; Knoll, 1914), the function of such epicuticular layer preventing adhesion remains largely unknown. There are only a few experimental studies reporting some hypotheses, why the insects cannot attach on the wax coated plant surfaces (Eigenbrode, 1996; Gorb and Gorb, 2002; Gaume *et al*., 2002): (1) the location of wax crystals on the plant cuticle may be responsible for an increase in the surface microroughness; this can be the reason for reduced real contact area between the plant surface and the attachment system of insects (Stork, 1980); (2) the wax crystals are mechanically unstable and fragile; attachment can be prevented by the contamination of the attachment

system of insects by the adhesion of the wax crystals to its pads (Juniper and Burras, 1962); (3) the possible reaction between the wax layer and the secretion liquid of the attachment system of insects (Gaume *et al*., 2002).

The interaction between the insect attachment systems and the plant anti-attachment surfaces motivated this work. The goal was to study the mechanical behavior of plant surfaces coated with wax crystals to understand the anti-attachment mechanism of the wax and to clarify the first two hypotheses. The leaves of two pea (*Pisum sativum*) mutants were selected for this study. The wild type pea leaves are strongly covered with wax crystals (filaments). In "glossy" mutation, the amount of waxy bloom is greatly reduced (Eigenbrode and Espelie, 1995; Eigenbrode and Jetter, 2002). The samples in fresh and dry conditions were mechanically tested using the Nano indenter® SA2. The structure of plant surfaces was explored by means of scanning electron microscopy (SEM). This study is believed to be the first attempt to characterize the mechanical properties of the wax crystals of plant surfaces.

5.2 Experimental

5.2.1 Materials and sample preparation

The experiments were performed with the pea *Pisum sativum*. The wild and glossy mutants of the pea plant were planted and grown in the laboratory. The samples were prepared from the pea leaves of both mutants: the wild type with normal wax layer and the glossy type with reduced waxy bloom. The top and bottom sides of the leaves were tested in the untreated condition. The nanoindentations were performed on the specimens in the fresh and dry conditions. To prepare dry samples, the fresh cuts of leaves were air dried at room temperature for 48 h.

5.2.2 Scanning electron microscopy

The surfaces of the pea leaves were observed using scanning electron microscopy (SEM). The samples, 7×7 mm in size, were cut from the leaves and mounted on an aluminum holder. The surface structure of the wild and the glossy plants were tested at 5 kV. The observations of top and bottom surfaces of both pea mutants were performed in the untreated, fresh condition.

5.2.3 Nanoindentation

The measurements of the mechanical properties of the pea plant were performed using the Nano Indenter® SA2 (MTS Systems Corporation, Oak Ridge, USA). Due to the Continuous Stiffness Measurement (CSM) technique, stiffness data were recorded dynamically along with load and displacement data, allowing hardness and elastic modulus to be calculated at every data point acquired during the indentation. Indentations were made using a triangular diamond pyramid indenter (Berkovich-type). (For detailed information about this method see nanointentation in chapter 3). All nanoindentation experiments were load-controlled. The resonant frequency during the tests was 75 Hz. During the experiments, a constant strain rate of 0.05 s^{-1} was measured. The samples (7×7 mm in size) were cut from the leaves of pea and mounted on an aluminum holder. To prevent desiccation of plants, fresh samples were rapidly prepared in about 2 to 5 min and tested immediately. The time between the first and last indent was approximately 1 h. The fresh samples were in fully native state during the whole experiment. The measurements on the pea samples were carried out up to a displacement of 3 µm. 10 top and 10 bottom sides of each mutant (wild and glossy) pea leaves were tested in the fresh and the dry conditions. During the tests, 10 indents on each sample were realized. In total, 100 measurements were performed on the samples of the top side of the leaf and 100 on the samples of the bottom side of the leaf for each pea mutant (wild and glossy) and each condition (fresh and dry). Inspection of the indenter tip in optical microscopy showed that the wax coverings on the plant surfaces contaminated the indenter tip. Therefore, it was necessary to clean and recalibrate the indenter tip after each experiment by indentation on aluminum and fused silica, respectively.

5.3 Results

5.3.1 Structure of wax layer

Figures 5.2 and 5.3 show the surface structure of the wild and glossy pea leaves respectively. The images are taken on the top and the bottom side of the leaf for each plant type. The cell structure of the plant surfaces can be distinguished in figures 5.2 A, B and 5.3 A, B. The wax crystals cannot be seen in these images and the surfaces of the top and bottom side of the wild and glossy pea leaves appear to be similar. The openings on the figures 5.2 A, B and 5.3 A, B are stomata for gaseous exchange. The wax crystals are shown in figures 5.2 C, D and 5.3 C, D. There is a great difference in the leaf surface between the wild and glossy pea. The wild pea samples are completely covered with wax crystals (figures 5.2 C, D, E, F), while the glossy pea surface only shows single wax crystals (figures 5.3 C, D, E, F). The comparison of SEM images of the two plant mutants (figures 5.2 C, D and 5.3 C, D) leads to the estimate that the surface of the glossy pea leaf bears only about one third of wax crystals. There is a small difference in the wax covering of the top and bottom side of the same plant species as well. The bottom side of the wild pea sample shows a denser wax crystal structure than the top side (figure 5.2 C, D). The single wax crystals appear to be larger on the top surface of the glossy pea leaf than on the bottom side (figure 5.3 C, D). The single wax crystals can be estimated to be 1 – 2 µm long with a diameter of 100 - 200 nm (figures 5.2 E, F and 5.3 E, F). As can be seen in the figures 5.2 E, F and 5.3 E, F, the wax crystals are oriented at different angles to the surface.

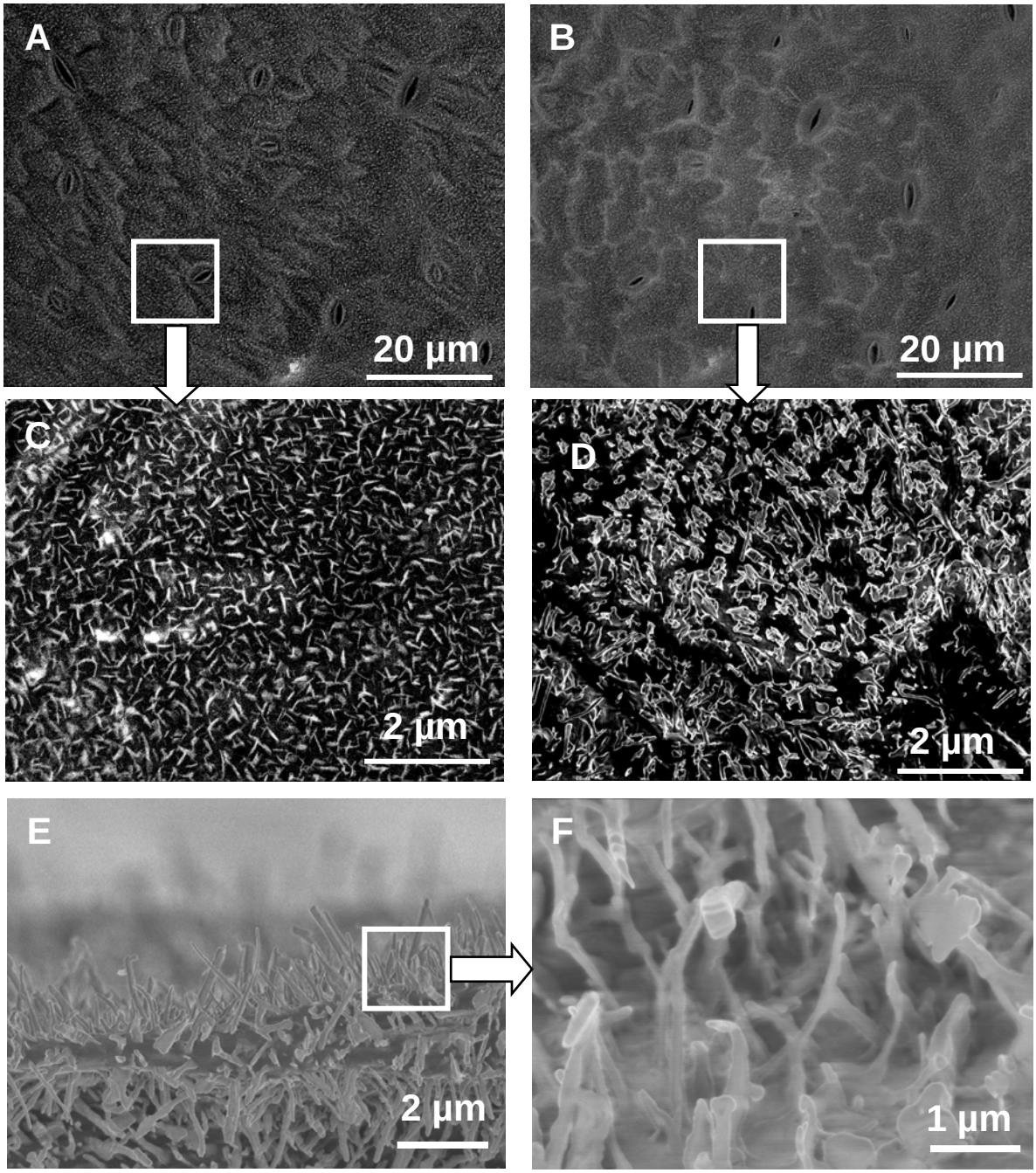

Figure 5.2: SEM images of the wax crystalloid layer on the wild pea leaf surface. A and C show the surface of the top side; B and D show the surface of the bottom side. Images A and B show cell structure of the plant leaf. On the C and D images wax crystal covering the leaf can be distinguished. The bottom side (D) of the pea leaf appears to have more dense waxy bloom than the top side (C). E and F show the top side of the wild pea leaf.

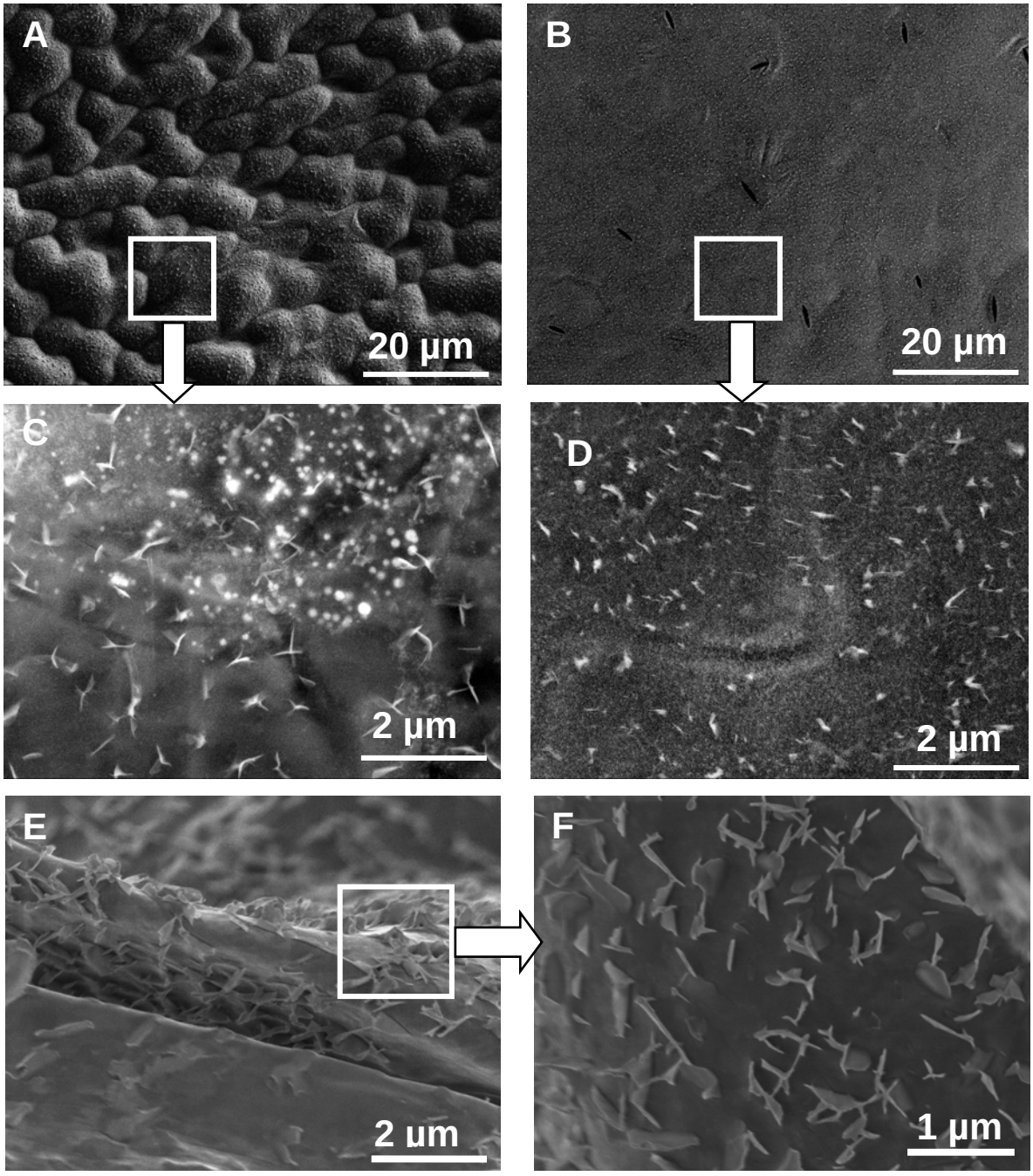

Figure 5.3: SEM images of the wax crystalloid layer on the glossy pea leaf surface. A and C show the surface of the top side; B and D show the surface of the bottom side. Images A and B show cell structure of the plant leaf. On the C and D images single wax crystals on the leaf can be distinguished. The top side (C) of the glossy pea leaf appears to have more wax crystals than the bottom side (D). E and F show the top side of the glossy pea leaf.

5.3.2 Mechanical properties

Figures 5.4 and 5.5 present the load-displacement curves obtained for the tested pea samples. Figure 5.4 shows the deformation behavior of the fresh and dry samples of the wild pea leaves. In figure 5.5 the results for the glossy pea leaves are shown. The load-displacement curves are similar for the top and the bottom surface of fresh pea leaves. However, a little difference could be observed at displacements up to 500 nm (figure 5.4 B and 5.5 B). The deformation behavior of the bottom side of the fresh wild leaves tends to be more compliant than that of the top surface (figure 5.4 B). The opposite show the fresh samples of the glossy pea leaves. The top side of the glossy leaves exhibit more compliant deformation behavior than the bottom surface (figure 5.5 B).

In general, all dry samples are more compliant than the fresh ones. The difference in the deformation behavior between the dry samples is obvious. All dry specimens with reduced wax layer display nearly the same deformation behavior as those with normal waxy bloom. The loading curves corresponding to the dry samples with normal wax layer are more scattered than the loading curves of the dry plants with reduced wax layer. There is more difference in the load-displacement relation between the top and the bottom surface of wild leaves than between the top and the bottom surface of glossy leaves.

In the figures 5.6 – 5.9 hardness and elastic modulus are plotted versus displacement for the wild (figures 5.6 and 5.8) and glossy (figures 5.7 and 5.9) pea leaves. The mean values of approximately 100 indents (10 samples with 10 indents on each) for each pea type (wild and glossy) and each condition (fresh and dry) are shown. There are no or very small differences in the mechanical properties between the fresh samples with normal and with reduced waxy bloom. The fresh specimens are harder and stiffer than the dry ones. The dry samples with reduced waxy bloom are harder and stiffer than dry samples with normal wax layer. At depths of 2 – 3 μm, all hardness curves, corresponding to fresh samples, drop rapidly.

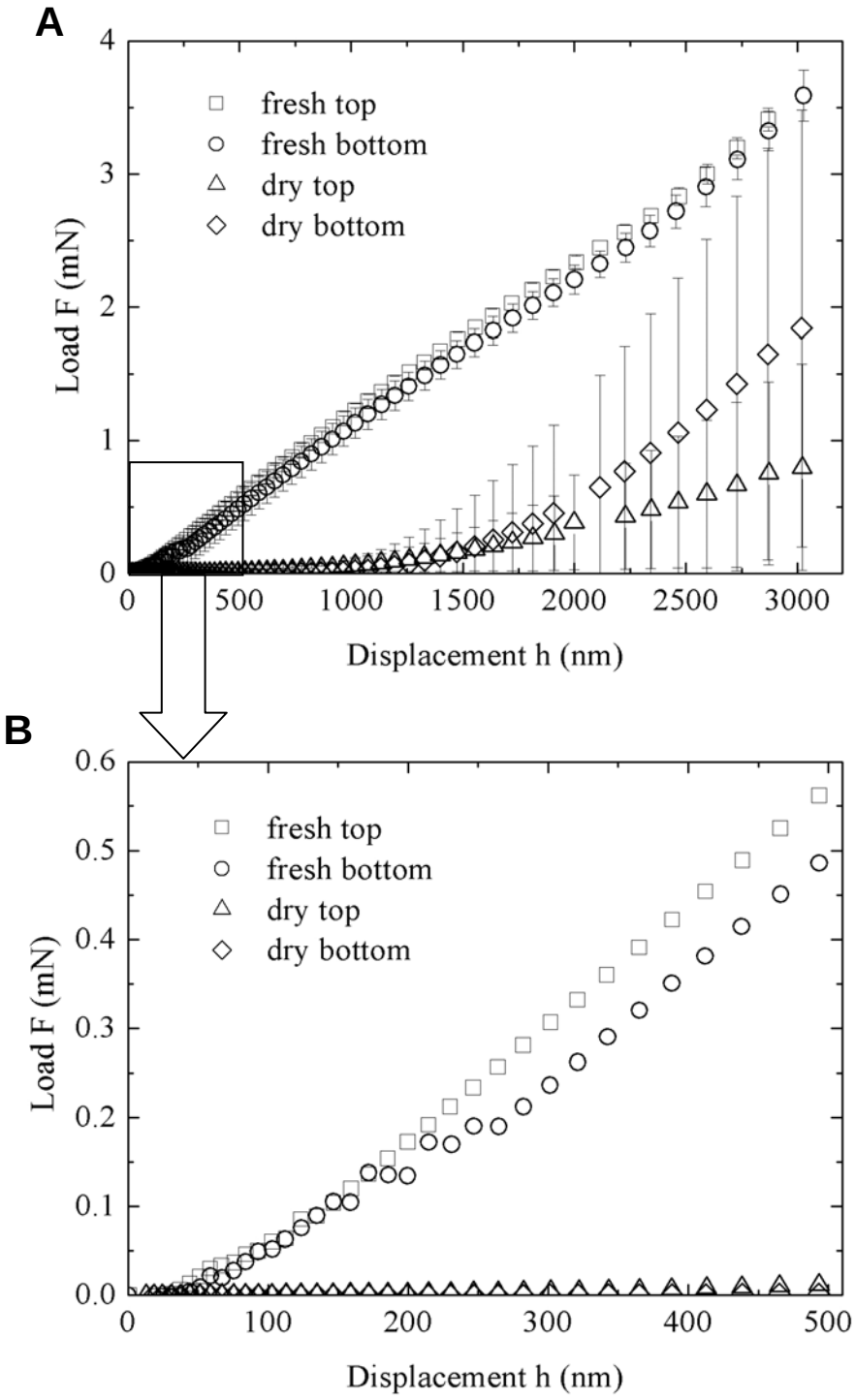

Figure 5.4: Load - displacement curves of the fresh and dry samples of the wild pea. A: shows the deformation behavior in the displacement range until 3 µm (mean values with the standard deviations of approximately 100 measurements); B: shows the deformation behavior until 500 nm (mean values of approximately 100 measurements).

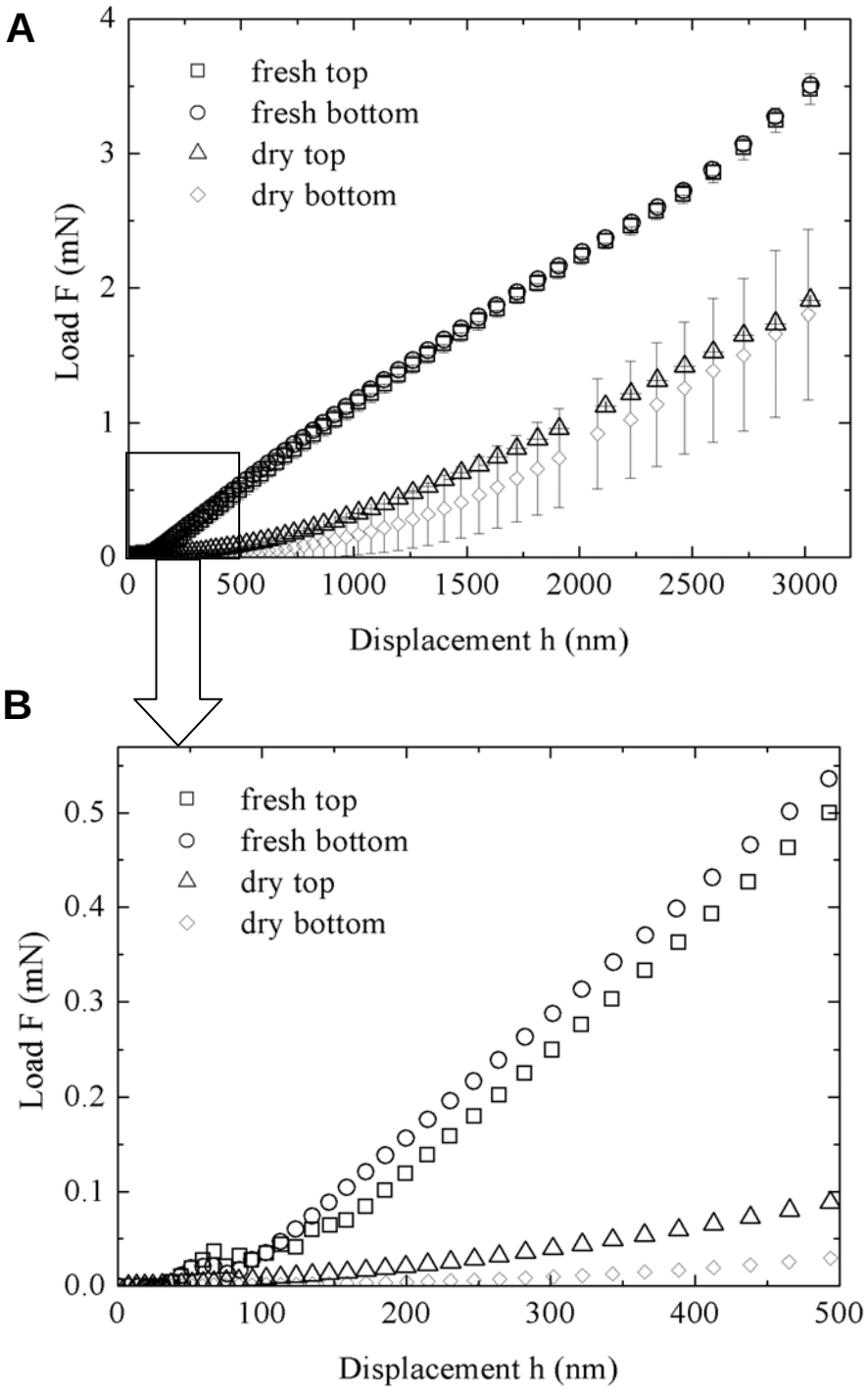

Figure 5.5: Load - displacement curves of the fresh and dry samples of the glossy pea. A: shows the deformation behavior in the displacement range until 3 µm (mean values with the standard deviations of approximately 100 measurements); B: shows the deformation behavior until 500 nm (mean values of approximately 100 measurements).

The hardness values for all fresh plants were measured to lie in the range of 100 - 800 MPa. The top surface of the dry wild type pea leaves with normal wax layer exhibit hardness values in the range of 2 – 10 MPa. The hardness for the bottom side of the wild pea leaf is 0.3 – 10 MPa. For the dry glossy pea leaves with reduced waxy bloom H = 8 - 100 MPa for the top surface and H = 5 - 50 MPa for the bottom surface.

All fresh plant samples have elastic modulus values of 2 - 5 GPa. The elastic modulus for dry wild pea leaves with normal wax layer was 200 - 600 MPa for the top side and 100 - 500 MPa for the bottom side. The elastic modulus of dry glossy pea leaves with reduced waxy bloom ranges from 300 to 2000 MPa for the top and from 300 to 1500 MPa for the bottom side. Table 5.1 summarise the results of mechanical properties, hardness and elastic modulus.

Table 5.1: Summary of mechanical properties obtained at the displacement of 100 and 500 nm for fresh plant samples.

Plant species	Hardness (GPa) by indentation depth of		Elastic modulus (GPa) by indentation depth of	
	100 nm	500 nm	100 nm	500 nm
wild top	0.7 ± 0.5	0.7 ± 0.2	3.2 ± 0.8	1.1 ± 0.2
wild bottom	0.7 ± 0.4	0.6 ± 0.4	2.7 ± 0.3	1.0 ± 0.3
glossy top	0.5 ± 0.5	0.5 ± 0.3	2.2 ± 0.5	1.0 ± 0.2
glossy bottom	0.4 ± 0.5	0.6 ± 0.2	2.6 ± 0.7	1.1 ± 0.1

Table 5.2: Summary of mechanical properties obtained at the displacement of 100 and 500 nm for dry plant samples.

Plant species	Hardness (MPa) by indentation depth of		Elastic modulus (MPa) by indentation depth of	
	100 nm	500 nm	100 nm	500 nm
wild top	5.2 ± 2.8	2.3 ± 0.9	285.2 ± 153.1	238.3 ± 194.2
wild bottom	1.2 ± 0.8	0.3 ± 0.1	168.2 ± 90.1	96.4 ± 59.3
glossy top	50.7 ± 41.1	23.7 ± 19.3	799.3 ± 569.1	570.4 ± 381.2
glossy bottom	7.5 ± 6.1	5.7 ± 3.9	526.8 ± 382.7	403.1 ± 291.1

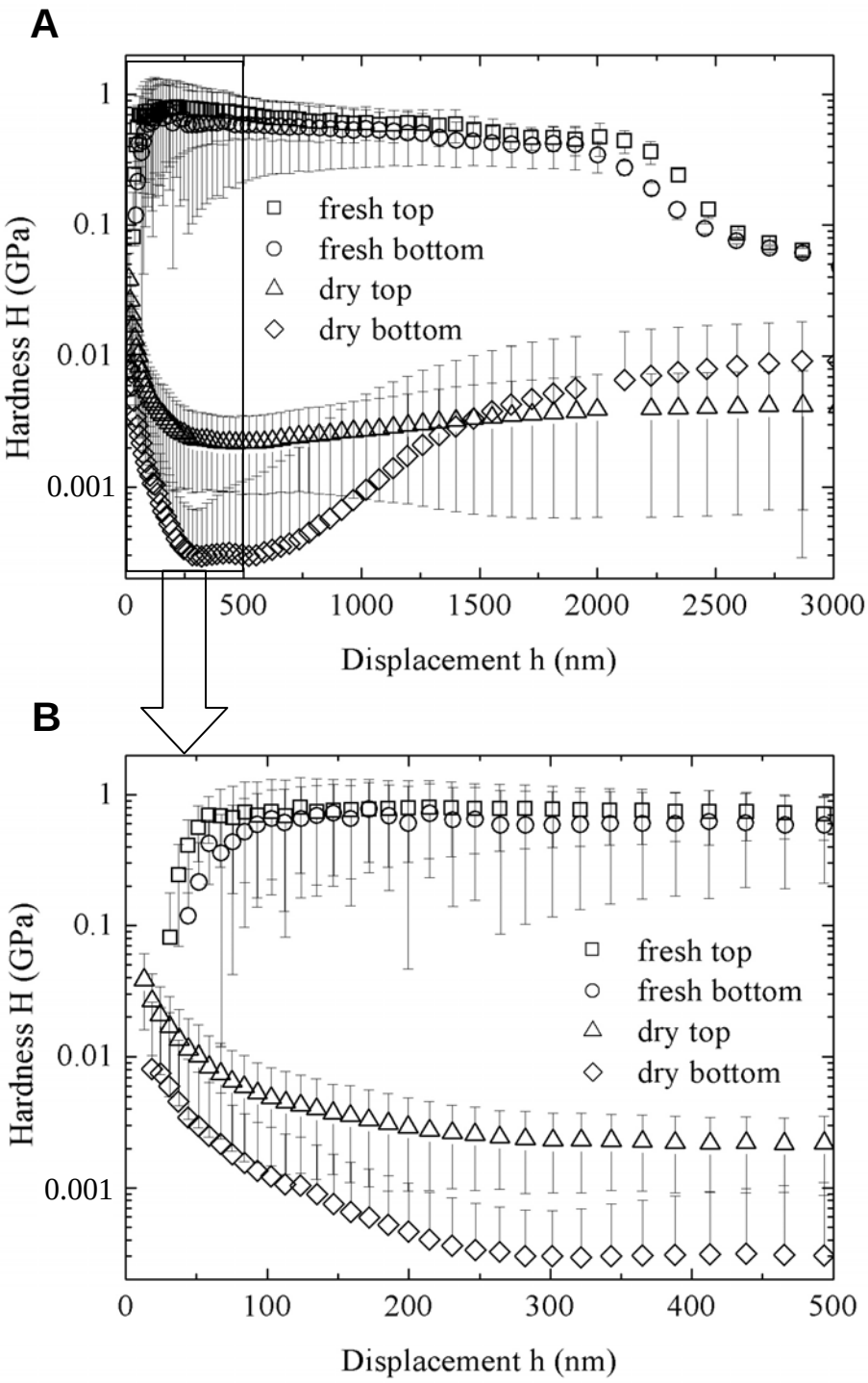

Figure 5.6: Hardness versus displacement curves of the fresh and dry wild pea leaves (top and bottom surfaces). A: shows the results at displacements up to 3 µm; B: shows the results at displacements up to 500 nm. Each data point corresponds to the mean value (with the standard deviations) of approximately 100 measurements.

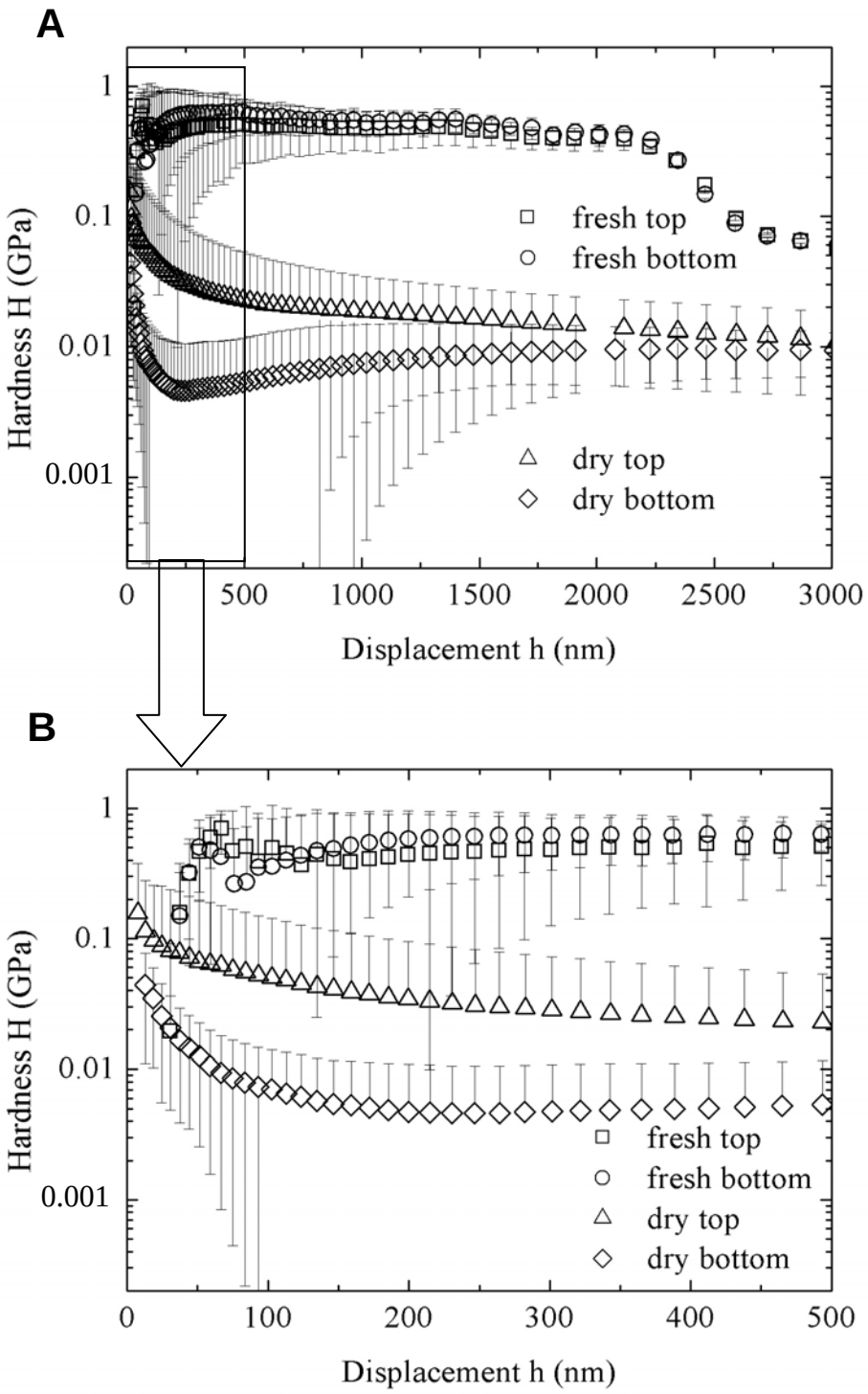

Figure 5.7: Hardness versus displacement curves of the fresh and dry glossy pea leaves (top and bottom surfaces). A: shows the results at displacements up to 3 µm; B: shows the results at displacements up to 500 nm. Each data point corresponds to the mean value (with the standard deviations) of approximately 100 measurements.

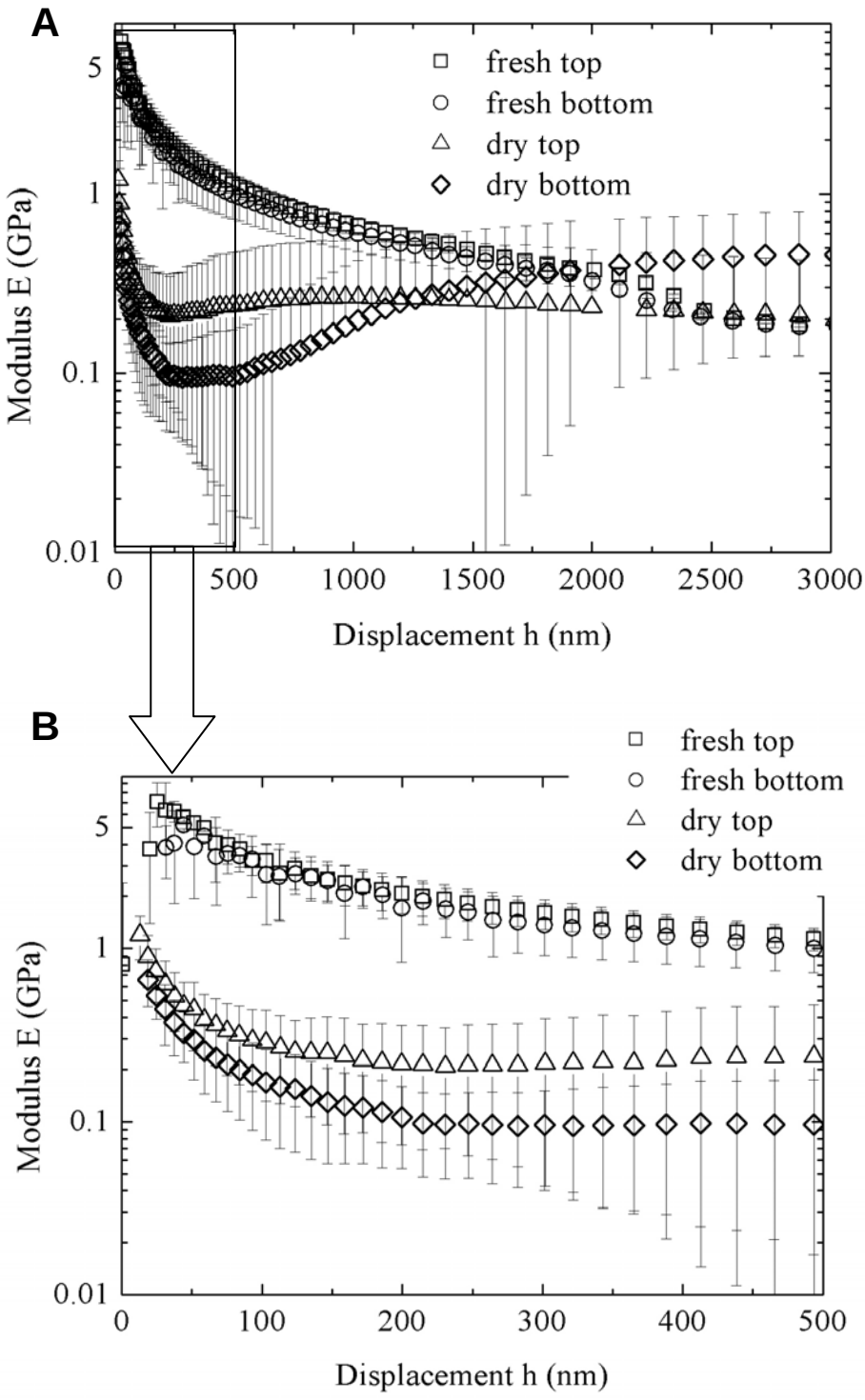

Figure 5.8: Elastic modulus versus displacement curves of the fresh and dry wild pea leaves (top and bottom surfaces). A: shows the results at displacements up to 3 µm; B: shows the results at displacements up to 500 nm. Each data point corresponds to the mean value (with the standard deviations) of approximately 100 measurements.

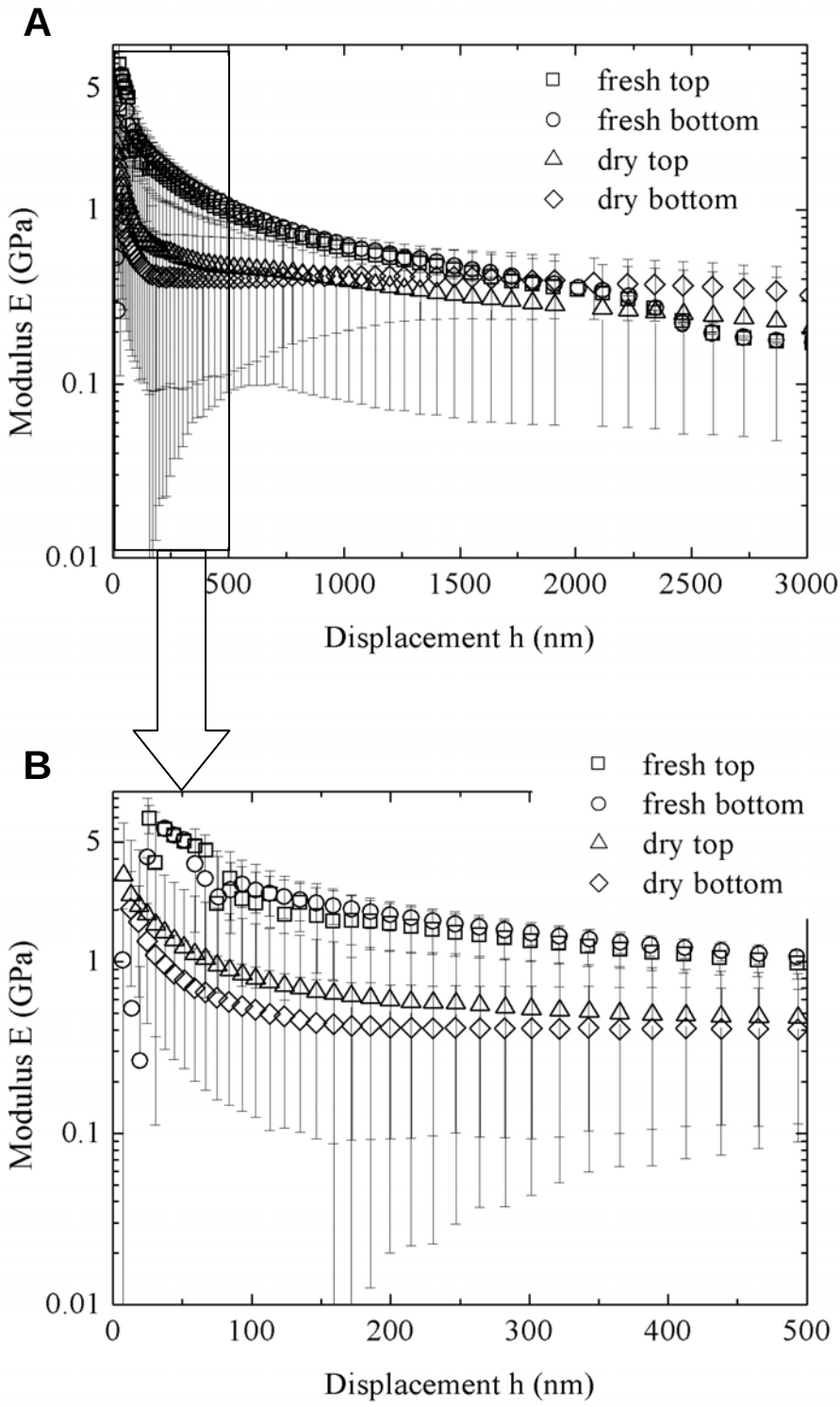

Figure 5.9: Elastic modulus versus displacement curves of the fresh and dry wild pea leaves (top and bottom surfaces). A: shows the results at displacements up to 3 µm; B: shows the results at displacements up to 500 nm. Each data point corresponds to the mean value (with the standard deviations) of approximately 100 measurements.

5.4 Discussion

5.4.1 Mechanical behavior

The mechanical behaviors of the sample surfaces differ presumably depending on the amount of wax crystalloids in the dry, but not in the fresh condition. It is surprising that there is no difference in the mechanical properties (hardness and elastic modulus) between the fresh samples with normal and with reduced wax layer. The maximum load corresponding to the maximum displacement (3 µm) is about 3.5 mN for all fresh samples (figures 5.4 A and 5.5 A).

The wax layer appears to have an influence on the mechanical behavior of the dry plants. The top and bottom surface of the same plant differ due to the different density and amount of the wax crystals as well. In general, the surface with more wax shows lower hardness and elastic modulus values (figure 5.10 and 5.11). The wax layer is believed to make the plant cuticle surface soft and compliant.

In the figure 5.10 and 5.11, hardness and elastic modulus (mean values of approximately 100 measurements are shown) are plotted versus displacement for all fresh (figure 5.10 A and 5.11 A) and all dry (figure 5.10 B and 5.11 B) samples. By looking at the curves showing hardness values at the beginning of the indentation, a little influence of the wax layer could be observed only at the first 200 nm of indentation depth. In this range the fresh samples display a slightly different behavior depending on the presence of the wax layer. Fresh plant samples with normal wax layer tend to be harder only at the first 200 nm of indentation depth than those with reduced wax. In the first 200 nm the indenter tip obviously contacts single wax crystals. This is thought to be caused by high mechanical stability of single wax crystalloids that build a very unstable and soft wax layer (Barthlott, 1990). However, a difference in the elastic modulus values between the fresh samples is not noticeable.

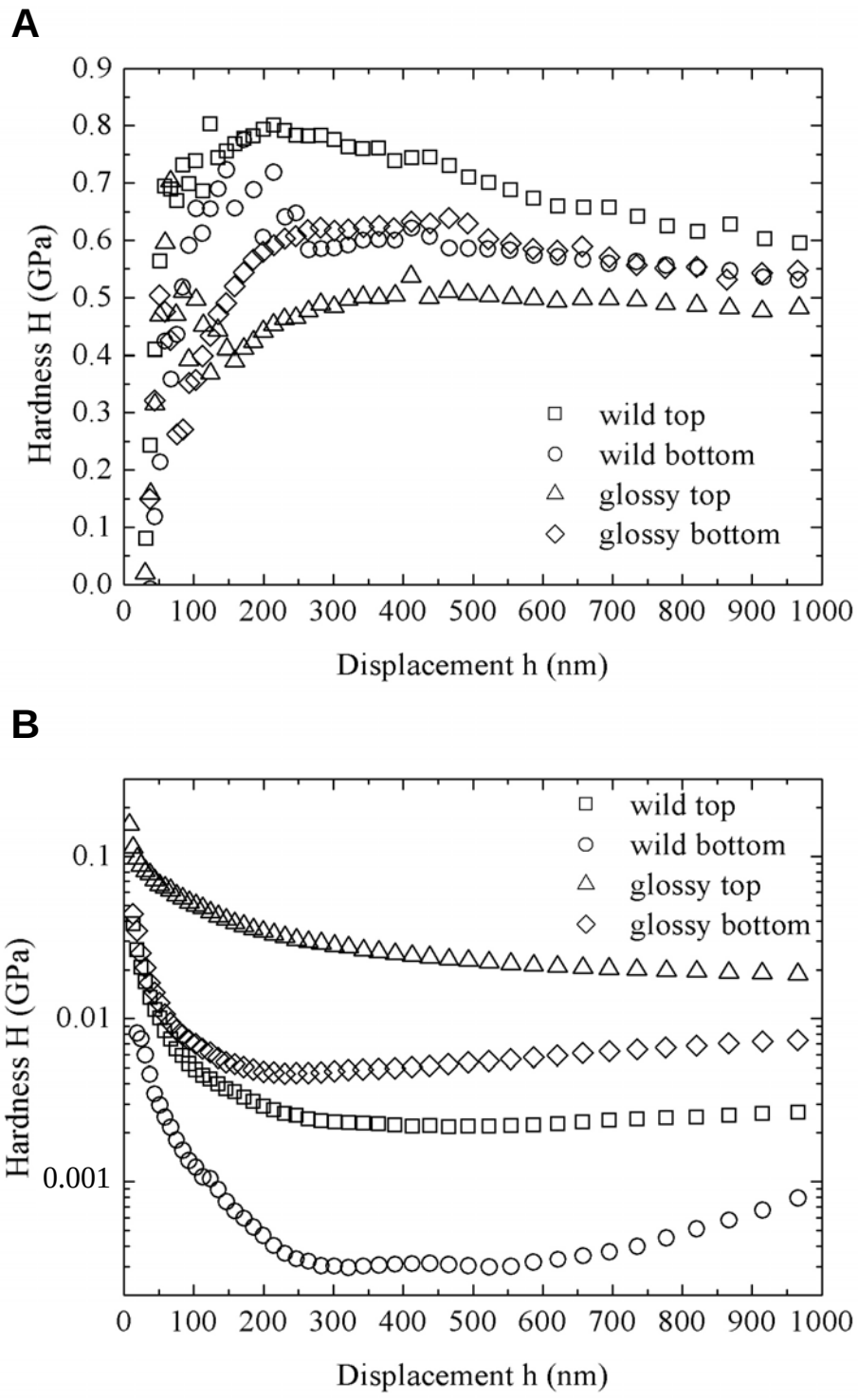

Figure 5.10: Hardness versus displacement curves of all fresh (A) and all dry (B) pea leaves. The mean results of approximately 100 measurements are shown up to 1 µm.

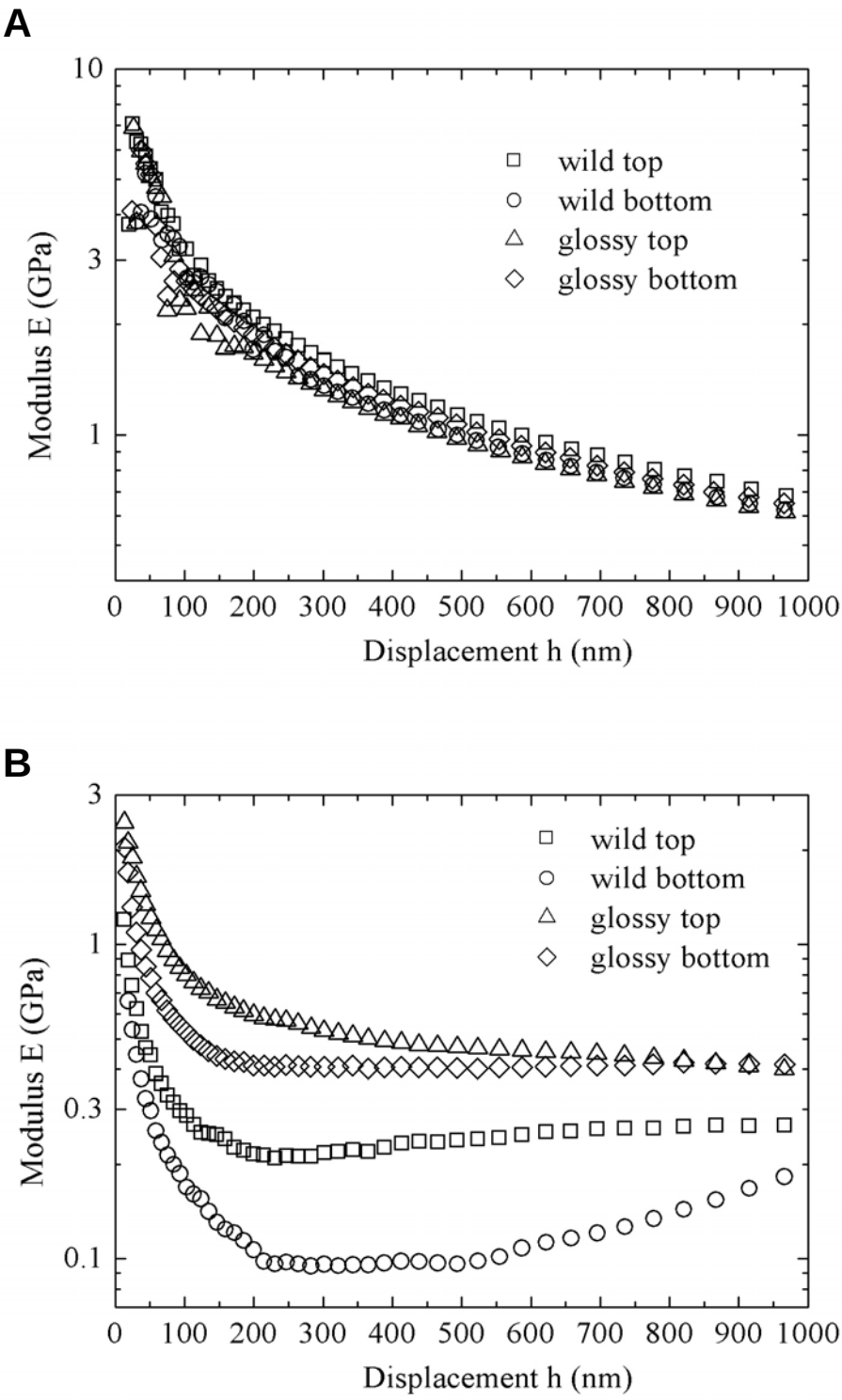

Figure 5.11: Elastic modulus versus displacement curves of all fresh (A) and all dry (B) pea leaves. The mean results of approximately 100 measurements are shown up to 1 µm.

All fresh samples exhibit the same mechanical behavior at larger displacements apparently due to the influence of the underlying layers. The plant cuticle has a multilayered structure (Eigenbrode and Jetter, 2002), which consists of the mechanically stable cuticularised epidermis covered by unstable and soft wax layer (Barthlott, 1990; Barthlott *et al*., 1998). The hardness and the elastic modulus values corresponding to the fresh samples are expected to be strongly influenced by cell walls and pressure of the cell fluid. However, the cell wall itself appears to be soft and compliant (dry samples are softer and more compliant than fresh ones). The cell structure, filled by fluid, appears to be influenced by internal pressure of the cell fluid and therefore, is hard and stiff. This is why the effect of the wax layer cannot be detected. A schematic of the cross section of the plant sample during the indentation is shown in figure 5.12.

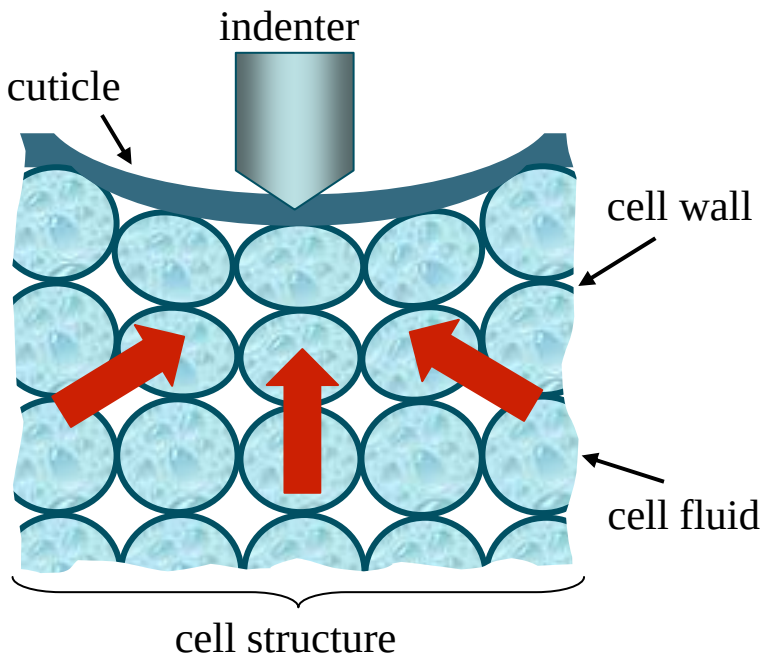

Figure 5.12: Schematic of the cross section of the plant during indentation experiment. The arrows show pressure of the cell fluid under the indenter.

In the dry condition, the influence of the cell fluid is minimized or removed and there is a great difference in the mechanical behavior between the plant surfaces with normal and with reduced wax layer. The dry samples with normal wax layer are softer and more compliant than the dry ones with reduced wax layer. In addition, the same mechanical behavior was observed in the case of pitcher plant *Nepenthes alata*, eucalyptus *Eucalyptus guinnii* and red cabbage *Brasica* (Barbakadze, unpublished results).

The desiccation greatly influences the mechanical behavior of biological materials (Gorb, 2001; Vincent and Wegst, 2004). However the effect of water loss is different for insect and plant cuticles. Fresh insect cuticles are softer and more compliant than dry ones (see chapter 3). By contrast, the hardness and the elastic modulus values of fresh plant cuticle surfaces are higher than that of dry ones.

5.4.2 Contact behavior

The figure 5.13 shows the hardness vs. displacement (A) and load-displacement (B) behavior for one of the fresh pea samples. A similar behavior can be seen for all fresh samples (fresh samples of pitcher plant *Nepenthes alata*, eucalyptus *Eucalyptus guinnii* and red cabbage *Brasica* show the same behavior as well (Barbakadze, unpublished results)). In the displacement range from 2.0 to 2.5 µm the hardness vs. displacement curves drop rapidly (figure 5.13 A). But the load-displacement curves in the same displacement range show no changes (figure 5.13 B).

The explanation could be the following: as described by the Oliver and Pharr method (1992), the indentation hardness is calculated with the formula:

$$H = F/A_c \tag{5.1}$$

where F is the applied load and A_c is the contact area, which is defined as

$$A_c = 24.5\, h_c \tag{5.2}$$

where 24.5 is the geometric constant of the Berkovich indenter;

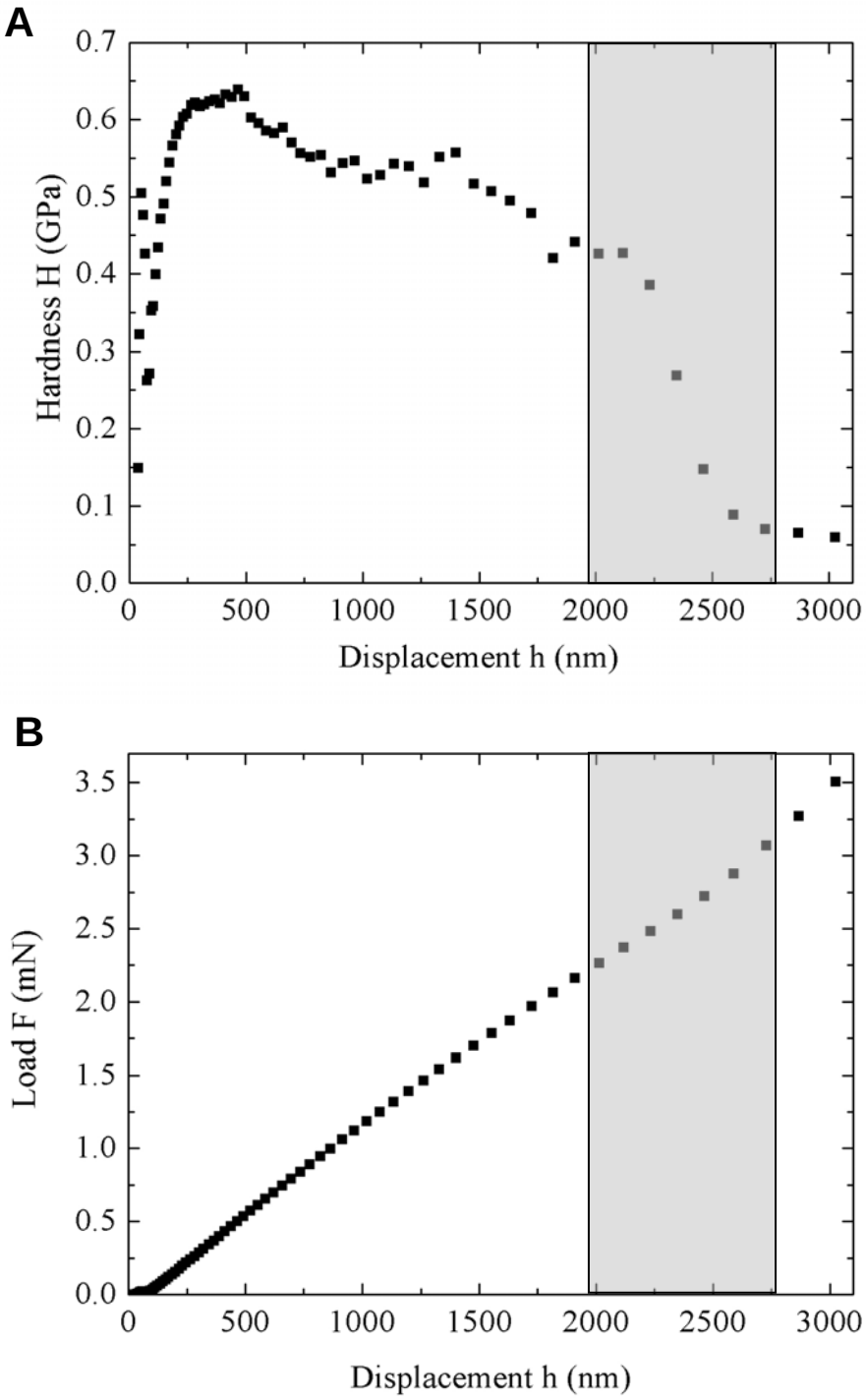

Figure 5.13: A: Hardness vs. displacement curve. In the displacement range from 2000 to 2500 nm the hardness-displacement curve drops rapidly. B: Load-displacement curve. In the displacement range from 2000 to 2500 nm the curve is linear.

h_c is the distance from the first contact point between the indenter tip and the sample to maximal contact depth and is noted as

$$h_c = h_{max} - h_s \tag{5.3}$$

The total displacement h_{max} (as shown in figure 3.4 in chapter 3) is the distance from the sample surface to maximal depth. This parameter is experimentally measured. h_s is the elastic deflection of the surface at the contact perimeter (Oliver and Pharr, 1992).

The contact depth in the displacement range of 2.0 - 2.5 µm for fresh plant samples rises rapidly (figure 5.14). Consequently, the contact area calculated using the contact depth becomes large in this displacement range. Therefore hardness values calculated with equation (5.1) are low. This causes a drop in the hardness-displacement curve. It is clear that these results are due to material properties of the fresh leaves and not to experimental errors. Further, again due to the material properties, the results can be influenced by “pile-up” effect (see chapter 2) of material around the indentation right from the start (in the first 250 nm) of the loading. In this case, the hardness will be overestimated by calculating it with an underestimated contact area (Bhushan and Li, 2003; Phillips, 2003). This effect can be the reason for the high hardness at the indentation depths until 2 µm.

The fresh plant leaves are full with water. Therefore during indentation, a water drop is thought to emerge on the surface around the indenter tip. This can influence the measurement of the experimental parameter required for the calculations of mechanical properties. However, it is difficult to estimate when the water drop occurs on the sample surface, for a 250 nm indentation depth or later at 2 µm displacement. The fracture of the cells can be excluded. This sudden occurrence is expected to change the linearity of the load - displacement curve. Because of the lack of models characterizing soft materials, it is suggested (Bhushan and Li, 2003) to perform mechanical measurements on biological systems *in situ* under optical observation.

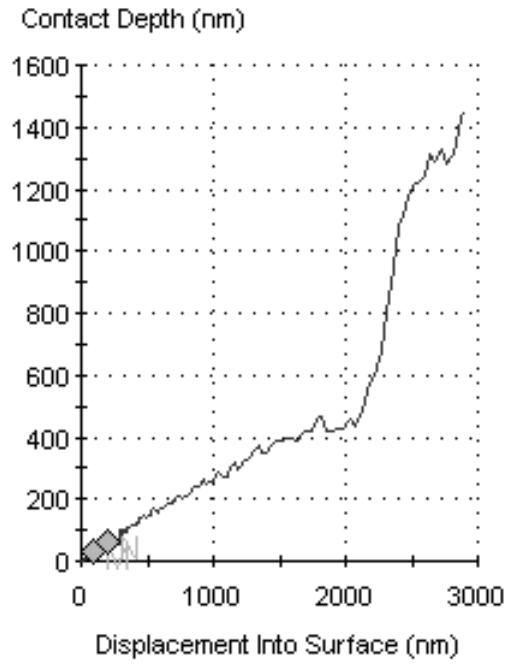

Figure 5.14: Contact depth vs. displacement into surface for the fresh pea sample. The contact depth rises rapidly in the displacement range from 2000 to 2500 nm.

There are some other events to be considered. The contact behavior during the indentation primarily depends on the surface tested and the geometry of the indenter tip. Indentations in this study were made by using a triangular diamond pyramid indenter (Berkovich-type). However, the pyramidal geometry of the indenter-tip could be the reason for erroneous results because of surface finding (or contact building) problems in the testing of the surfaces structured by wax crystalloids. A solution here could be an indentation with a tip of another geometry. The testing of the highly structured surfaces with a flat punch indenter tip could contribute to the reduction of contact problems. The contamination of the indenter tip by wax crystalloids remains a big problem as well. The wax crystals appear to easily adhere on the indenter tip. A surface treatment of the tip could prevent adhesion of wax crystals.

5.4.3 Wax coverings and insect attachment pads

The attachment abilities of insects were recently tested on the plant surfaces investigated in this study. The leaves of the wild pea (*Pisum sativum*) (Eigenbrode and Jetter, 2002) were difficult to cope for insects. While walking on these surfaces, the insects often stopped and cleaned their feet whereas they had less difficulty on the surface of the glossy mutant with reduced waxy bloom.

To elucidate the hypotheses of reduced contact area and contamination effect of the wax crystals, let us consider the results obtained in connection with the blowfly *Calliphora vicina* (Niederegger *et al*., 2002), which is the model for most studies of the structure and the attachment behavior of pads. What would the hardness and elastic modulus values obtained in this study mean for this insect? The blowfly *C. vicina* weighs about 4 mN and possesses attachment pads structured with a few thousand (4000 - 6000) flexible (1 N/m spring constant) cuticular outgrowths called seta. A single spatula (tip of the seta) has an area of 1 μm^2 (Niederegger *et al*., 2002). Thickness of the wax crystals lie in a few hundred nanometer range. By walking, three feet of the insect with one third of the whole amount of setae come in contact. However, the area of a spatula increases in contact by about 35 % (Niederegger *et al*., 2002). An estimation of the load exerted by one single seta in contact with the plant surface gives values ranging between 134 and 400 nN.

In the nanoindentation experiments, the hardness and elastic modulus values corresponding to this load range were obtained at displacements of 20-40 nm: for the wild pea, H = 50-340 MPa and E = 2.50 - 8.00 GPa (figure 5.14). With these considerations, one can assume that wax crystals remain stable under insect pads and contribute to a decrease of the contact area between the insect attachment pad and the plant surface (hypothesis 1). However, the wax crystals are not oriented perpendicularly to the surface but at different angles. The insects do not only push down the plant surface but also use lateral forces while walking. These considerations make the estimation more difficult. Regarding all these factors, contamination of the insect pads (hypothesis 2) due to the breaking and adhesion of wax crystals to the pad surface cannot be excluded. Further measurements on the isolated cuticle (without cell structure) surface are necessary.

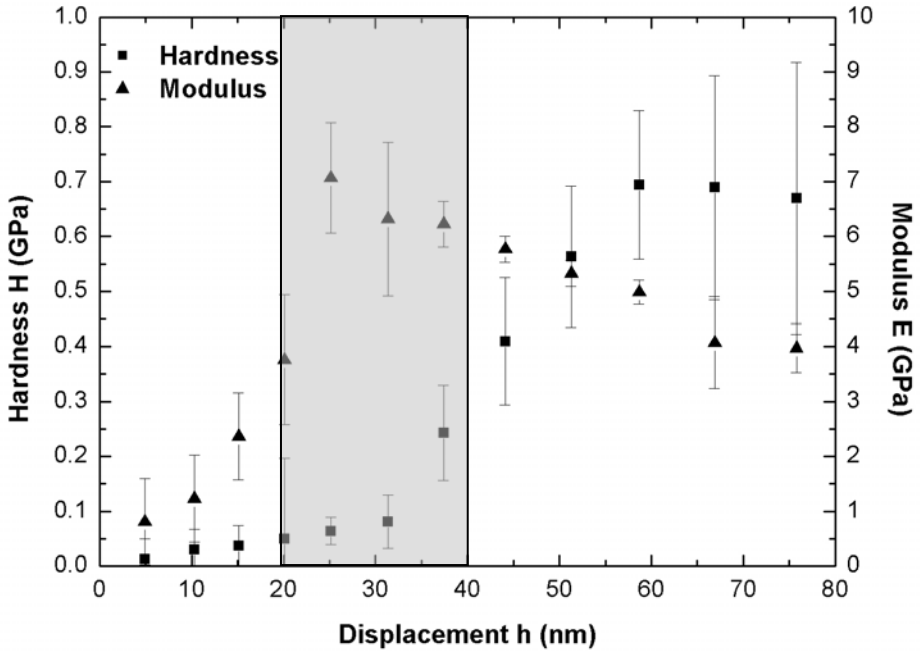

Figure 5.15: Hardness and elastic modulus of the wild pea samples (top side of the leaf) in the displacement range of 0 – 80 nm. Grey area shows the displacement area of 20 to 40 nm, corresponding to the load range of 134 – 400 nN. This load range is estimated to act during the walking of the blowfly *C. vicina* on the plant surface.

5.5 Summary and conclusion

In order to understand the role of the wax crystal layer in preventing attachment of insects on the plant surface, mechanical behavior of two pea (*Pisum sativum*) mutants (wild with normal wax covering and glossy with reduced waxy bloom) surfaces were studied by nanoindentation. Experiments were carried out on fresh and dry samples of the top and bottom side of wild and glossy pea leaves. The results can be summarized as follows:

- Desiccation of the plants influences their mechanical behavior. Contrary to insect cuticle, the fresh plants were found to be harder and stiffer than dry ones.

- There is no difference in mechanical behavior between the fresh samples with normal and with reduced wax layer. The mechanical behavior of the fresh plants is believed to be influenced by the cell structure and the pressure of the cell fluid. The occurrence of a water drop on the plant surface is thought to be the reason for the unusual contact behavior of the fresh samples.

- The amount and the density of wax crystals were found to influence the mechanical properties of the dry samples. The dry samples with normal wax layer were softer and more compliant than that with reduced wax.

- Indentation of the highly structured plant surfaces with Berkovich-indenter tip is thought to cause erroneous results. The wax crystals are found to adhere to the surface of the indenter tip. Using an indenter tip of another geometry and the treatment of the tip surface could be the solution for the contact and contamination problems.

- The anti-attachment hypotheses describing contact area reduction and contamination of attachment pads appear to be realistic. However further investigations are requires.

6 Overall summary

The mechanical behavior of various biological materials such as insect and plant cuticles was studied by applying experimental approaches of material science. A head articulation cuticle of the beetle designed for friction minimisation and the wax covered plant surfaces adapted for attachment prevention have been chosen for this study. Both insect and plant cuticles are multifunctional composite materials and have a multilayered structure. The *gula* cuticle of the beetle *Pachnoda marginata* is a part of the head articulation, which is a micromechanical device similar to a technical ball bearing. The surfaces in this system operate in contact; they must be optimised against wear and friction and must provide high mobility within the joint. The measurements on the *gula* cuticle were performed in order to understand structure and tribo-mechanical behavior of material working for friction minimizing. The plants carry amorphous wax layer which by some species is covered by wax crystals. The insects cannot attach on such plant surfaces. The location of the wax crystals on the plant cuticle increases the surface microroughness. This could decrease the real contact area between the plant surface and attachment pads of insect. Attachment can be prevented by contamination of attachment pads of insect with the wax crystalloids. In order to understand the deformation behavior of the wax layer two pea plant (*Pisum sativum*) mutants (wild type with normal wax layer and glossy with reduced waxy bloom) were studied. To observe the effect of desiccation all samples (insect and plant cuticles) were tested in fresh and dry conditions. To understand the influence of an outer wax/lipid layer, tribo-mechanical experiments on the *gula* cuticle were performed as well in a chemically treated condition. This study is believed to be one of the first for mechanically testing of insect cuticle and the very first for wax coated plant surfaces in native condition.

Mechanical properties were determined by using the Nano Indenter® SA2 (MTS Systems Corporation, Oak Ridge, USA). A high damping coefficient and a high resonant frequency of the indenter in this system allows determining mechanical properties of soft and structured materials with low contact stiffness. The biological samples can be successfully tested in native condition. Employing continuous stiffness measurement (CSM) technique allows

measuring contact stiffness continuously during indentation and obtaining the depth-dependence of the hardness and elastic modulus. This is very important for biological materials because their mechanical properties vary with depth.

The mechanical behavior of all samples was found to be greatly influenced by drying. However changes in hardness and elastic modulus were different for insect and plant cuticles. Desiccation made *gula* cuticle of the beetle harder and stiffer but the plant surface softer and more compliant. After drying, *gula* cuticles became harder and stiffer by a factor of about 5 compared to the samples in the fresh state. Chemical treatment caused further hardening of the material. Increase in stiffness could be observed only in first 1 µm of the indentation depth. There was no significant difference between elastic modulus of the dry and chemically treated samples at indentation depth higher than 1 µm.

Hardness and elastic modulus values of the fresh plant samples were significantly higher than that of the dry ones. There was almost no difference between samples with normal and with reduced wax layer in fresh condition. All fresh samples exhibited the same mechanical behavior apparently due to the influence of cell walls and especially pressure of the cell-fluid. In dry condition the effect of the cell-fluid was removed and the samples showed a great difference in mechanical properties between the plant surfaces with normal and with reduced wax layer. Dry samples with normal wax layer were softer and more compliant than with reduced waxy bloom. The pyramidal geometry of the indenter-tip (Berkovich-type) could be a reason for erroneous results because of contact problems in testing highly structured surfaces such as the plant surfaces covered with wax crystalloids. A solution could be the indentation with a tip of another geometry, e. g. a flat punch.

The changes in surface properties due to the condition influenced the friction behavior of the *gula* cuticle tested. Frictional forces were highest in fresh samples. Friction properties were influenced by different factors such as surface geometry, contact area or mechanical properties. Fresh samples were smooth, soft and compliant and exhibited higher friction coefficients than dry ones, which were rough, hard and stiff. After chemical treatment the samples were harder and stiffer than fresh and dry ones. Their surface roughness was higher than that of fresh but less than that of dry samples. Chemically treated cuticles showed the lowest friction coefficient.

7 Appendix

7.1 Contact angle of the single *gula* sample

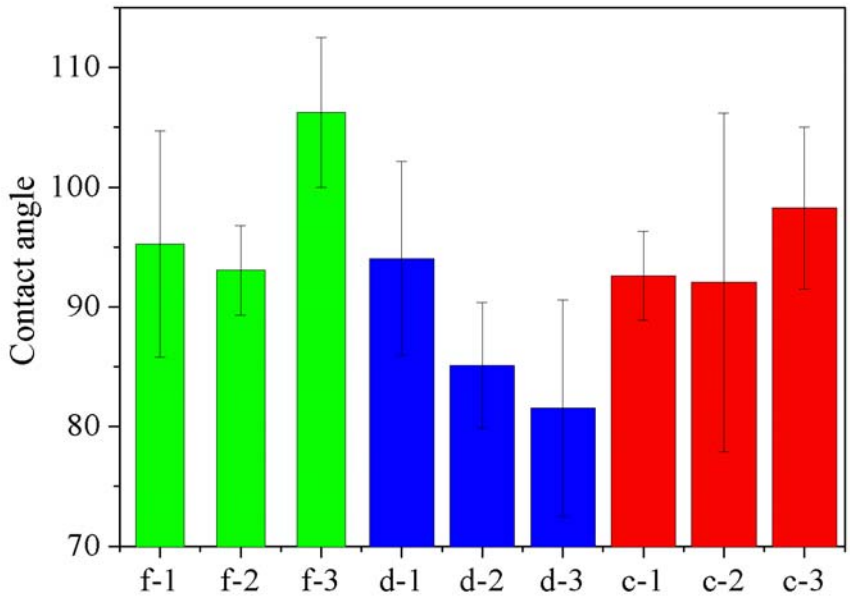

Figure 7.1: The results of the contact angle measurements on all individually tested *gula* samples. The mean values with standard deviations of 3 measurements on each sample in each condition are shown. f means fresh; d dry and c chemically treated.

7.2 Surface topography of the *gula*

Topographical investigations on the head articulation of the beetle *Pachnoda marginata* were performed using Perthometer Concept roughness and contour in Esslingen by firma Mahr (Production Measurements Technology Systems, Mahr GmbH, Göttingen, Germany).

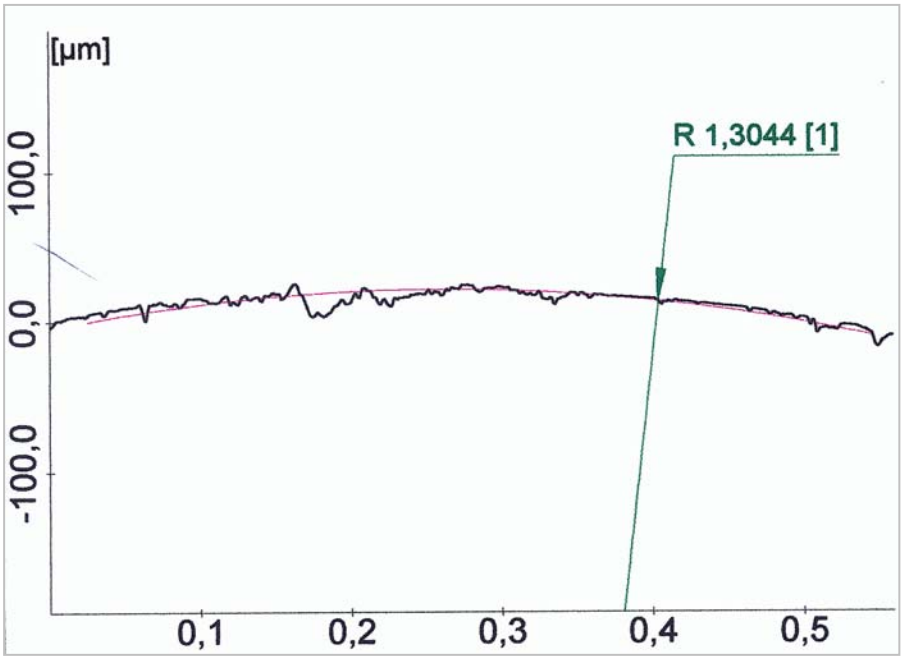

Figure 7.2: Surface roughness of the *gula* cuticle (head part of the head articulation system in the beetle *Pachnoda marginata*) with measured radius value.

8 Deutsche Zusammenfassung: Mikro/nanomechanische Messungen an Insekten- und Pflanzencuticula

8.1 Motivation und Literaturüberblick

Die Standzeiterhöhung von Werkzeugen und Bauteilen ist heute ein bedeutendes Ziel der Technik. Die Optimierung der Oberflächeneigenschaften und die Entwicklung neuer Materialien spielt eine wichtige Rolle in den verschiedenen industriellen Anwendungen. Die Miniaturisierung der technischen Systeme fordert von den Ingenieurwissenschaften die Bestimmung der Materialeigenschaften in immer kleineren Volumina.

Im Laufe der Evolution hat die Natur Strukturen und Eigenschaften verschiedenster Organismen entwickelt und für ihren Lebensraum optimiert. Das Strukturdesign, die Eigenschaften und das Funktionsprinzip der biologischen Systeme auf der Mikro- und Nanoskala zu verstehen, ist eine besondere Herausforderung für die Entwicklung neuer Materialien.

Das Strukturdesign und die mechanischen Eigenschaften der biologischen Systeme einerseits und die Entwicklung neuer Techniken zur Untersuchung der weichen Materialien im Mikro-/Nanometerbereich andererseits gelten als Motivation dieser Arbeit. Der Versuch, durch die Anwendung der modernen materialwissenschaftlichen experimentellen Technologien die mechanische Eigenschaften der natürlichen Materialien zu bestimmen, schlägt eine Brücke zwischen den Ingenieurwissenschaften und der Biologie. Das Ziel der Arbeit besteht darin, durch die Untersuchung des strukturellen und mechanischen Designs biologischer Systeme interessante Eigenschaften zu entdecken und damit eine Grundlage für die Entwicklung neuer Materialien zu schaffen.

In Rahmen dieser Arbeit wurden Oberflächen von Insekten- und Pflanzencuticulae untersucht. Das Ziel der Untersuchungen war, Informationen über die Struktur und das mechanische Verhalten der biologischen Materialien zu erhalten, um ihr natürliches Funktionsprinzip zu verstehen. Erstmalig wurden hierfür Nanoindentationsversuche mit biologischen Materialien im natürlichen Zustand durchgeführt.

Einige natürliche Oberflächensysteme ermöglichen die Erhöhung der Kontaktkräfte während der Bewegung (Reibungssysteme), andere wiederum die Minderung der Kontaktkräfte, um damit Muskelenergie zu sparen (Anti-Reibungssysteme) (Gorb, 2001). Ein interessantes Anti-Reibungssystem ist das Kopfgelenk des Rosenkäfers *Pachnoda marginata*. Das Gelenk besteht aus einem vordefinierten Oberflächenpaar, welches ein tribologisches Mikrosystem mit spezifischer Struktur und Eigenschaften bildet und dem Insekt eine freie Kopfbewegung erlaubt. Die glatte Oberfläche des Kopfteils (*Gula*) dient zur Reibungsreduzierung im Kontakt mit seinem Gegenstück (*Prothorax*), welches mit asymmetrischen Auswüchsen bedeckt ist (Enders *et al*., 2004). Die Oberflächen in diesen Systemen arbeiten im Kontakt. Sie müssen daher gegen Verschleiß und Reibung optimiert sein und gleichzeitig eine hohe Mobilität innerhalb des Gelenkes gewährleisten. Die Zusammenhänge zwischen Struktur, Eigenschaften und Funktion dieser Oberflächen sind bisher weitgehend unbekannt.

Die Pflanzenoberflächen sind mit äußeren Wachsschichten bedeckt. Auf der amorphen Wachsschicht einiger Pflanzen formieren sich die Wachskristalle. Die Wachsbeschichtungen treten auf den Blatt-, Stängel- und Fruchtoberflächen auf. Die Dicke der Wachsschicht variiert von 1 bis 20 µm (Baker, 1982; Bianchi, 1995; Barthlott *et al*., 1998; Gorb, 2001). Viele Insekten können auf der Pflanzenoberfläche, die mit dem Wachskristallen strukturiert sind, nicht laufen (Gorb und Gorb, 2002). Es existieren einige Hypothesen, warum Insekten auf der Wachsschicht nicht haften können. Zwei davon sind folgende: (1) Die Anordnung der Wachskristalle auf der Pflanzenoberflächen erhöht die Rauhigkeit und dadurch wird die reale Kontaktfläche zwischen den Pflanzenoberflächen und den Insekten Haftsystemen kleiner (Stork, 1980). (2) Durch die Wachskristalle werden die Haftsysteme von Insekten verschmutzt (Juniper und Burras, 1962). Obwohl die Struktur und die chemische Zusammensetzung der Wachse in zahlreichen Arbeiten untersucht worden sind (Hallam und Chambers, 1976; Bianchi *et al*., 1978; Baker, 1982; Avato *et al*., 1984; Jeffree, 1986; Barthlott, 1990; Bianchi, 1995; Gorb, 2001; Eigenbrode and Jetter, 2002; Gorb and Gorb, 2002), ist über die mechanischen Eigenschaften der Wachskristalle jedoch bisher nichts bekannt.

8.2 Experimentelles

Die Proben wurden vom Kopfgelenksystem des Rosenkäfers *Pachnoda marginata* und von zwei Mutanten der Erbse *Pisum sativum* hergestellt. Die Käfer wurden mit CO_2 betäubt. Der Kopf wurde vom Körper entfernt und von den inneren Substanzen befreit. Die Pflanzenproben wurden aus den Blättern eines Wildtyps mit normaler Wachsbeschichtung und des glatten Typs mit reduzierter Wachsbeschichtung der Erbse geschnitten. Die frischen Proben wurden unmittelbar nach der Vorbereitung mechanisch untersucht. Trockene Proben wurden durch Trocknen frischer Proben hergestellt. Die *Gula*-Cuticula wurde chemisch in Chloroform / Methanol (2:1) Lösung behandelt, um die Lipid- und Wachsschicht von der Probenoberfläche zu entfernen.

Das mechanische Verhalten und die Oberflächeneigenschaften wurden an frischen, trockenen und chemisch behandelten Proben der *Gula*-Cuticula untersucht, um den Einfluss des Wassergehaltes und der Wachsbeschichtungen auf ihre mechanischen Eigenschaften zu studieren. Nanoindentierungen an Proben des Wildtyps (mit natürlicher Wachsbeschichtung) und des glatten Typs (mit reduzierter Wachsbeschichtung) der Erbse wurden in frischem und trockenem Zustand durchgeführt.

Die Querschnitts- und Oberflächenstruktur der Pflanzen- und Insektencuticula wurde mittels Rasterelektronenmikroskopie untersucht. Oberflächenrauhigkeit und Hydrophobie der *Gula*-Cuticulae wurden mittels Weißlichtinterferometrie und Kontaktwinkelmessgerät studiert. Die Untersuchungen der Oberflächeneigenschaften (Rauhigkeit, Hydrophobie) wurden an drei Proben in frischem, trockenem und chemisch behandeltem Zustand durchgeführt. Die Kontaktfläche der *Gula*-Oberfläche wurde in Experimenten mit einem Mikro-Tester, einem motorisierten Mikromanipulator (DC3001R mit Controller MS314, World Precision Instruments, Sarasota, FL, USA), der mit einem Kraftsensor (100 g Kapazität, Biopac Systems Ltd, Santa Barbara, CA, USA) verbunden war, bestimmt. 10 Proben wurden in jedem Zustand getestet. Die Kontaktfläche wurde an jeder Probe für 7 verschiedene angelegte Kräfte (30, 100, 300, 1000, 3000, 5000 und 10000 µN) gemessen.

Die lokalen mechanischen Eigenschaften der Insekten- und Pflanzencuticula wurden mit dem Nano Indenter® SA2 System (Abbildung 3.2) (MTS System Corporation, Oak Ridge, USA) untersucht. Die Experimente wurden mit einer Berkovich Spitze (dreiachsige Diamant-pyramide) durchgeführt. Durch einen großen Dämpfungskoeffizient und eine hohe Resonanzfrequenz ermöglicht das Gerät (Nano Indenter® SA2) die Durchführung von Messungen an Materialien mit niedriger Kontaktsteifigkeit und kleinem Dämpfungskoeffizient. Die mechanischen Eigenschaften der meisten Materialien, insbesondere von biologischen Proben, ändern sich mit der Eindringtiefe. Die spezielle dynamische Technik, die so genannte kontinuierliche Messung der Steifigkeit (CSM) (Oliver und Pharr, 1992), erlaubt die Bestimmung der mechanischen Eigenschaften in Abhängigkeit von der Eindringtiefe. Die Härte und der Elastizitätsmodul wurden aus den während des Experimentes gemessenen Parametern (maximale Kraft (F_{max}), Eindringtiefe bei maximaller Kraft (h_{max}) und der Kontaktsteifigkeit (S_{max}) (Abb. 3.3)) nach der Methode von Oliver und Pharr (1992) berechnet. Die Indentierungen wurden an 10 Proben in jedem Zustand durchgeführt. An jeder Probe wurden 10-15 Eindrücke vorgenommen. Die Eindrücke wurden mit einem Abstand von 30 – 50 µm voneinander lokalisiert. Die maximale Eindringtiefe während der Experimente betrug 3000 nm. Die Resonanzfrequenz lag bei 75 Hz. Alle Experimente waren kraft - gesteuert.

Die Reibungsexperimente an der *Gula* Cuticula wurden mit dem Bio-Mikrotribometer Basalt-BT01 (Abb. 4.1) durchgeführt. Die Probe wurde mit einer Glasplatte in Kontakt gebracht, der Probenhalter in senkrechte Richtung mit der angegebenen Kraft (F_{AN}) von unten nach oben gedrückt und dann in die parallele Richtung zur Glasplatte gerieben. Die tangentiale Kraft (F_T) wurde als die Auslenkung des Federbalkens gemessen. Die Experimente wurden an 10 Proben der *Gula*–Cuticula in frischem, trockenem und chemisch behandeltem Zustand durchgeführt. Das Reibungsverhalten wurde an jeder Probe für 7 verschiedene (30, 100, 300, 1000, 3000, 5000 and 10000 µN) angelegte normale Kräfte (F_{AN}) gemessen.

8.3 Ergebnisse

8.3.1 Struktur und tribo-mechanische Eigenschaften der *Gula*-Cuticula

Die rasterelektronenmikroskopischen Untersuchungen haben gezeigt, dass die Oberfläche der *Gula*-Cuticula außergewöhnlich glatt für biologische Materialien ist (Abb. 3.5 A). Die getrockneten Sekretionssubstanzen (inselähnliche Stellen) und die wohl-definierten Poren können auf der *Gula*-Oberfläche gut erkannt werden (Abb. 3.5 C und 3.5 D). Die Risse auf der Oberfläche entstanden wahrscheinlich während der Austrocknung des Materials (Abb. 3.5 D). Der Querschnitt der *Gula* zeigt den Schichtaufbau des Verbundstoffes (Abb. 3.5 B). Drei Cuticulaschichten können definiert werden: (1) sehr dünne (7-8 µm) und dichte Epicuticula; (2) dichte, ungefähr 22 µm dicke Exocuticula; (3) sehr dicke (~ 50 µm) Endocuticula mit der niedrigen Dichte (Abb. 3.5 B). Die Chitinfasern orientieren sich senkrecht zur Oberfläche in der Exocuticula und parallel zur Oberfläche in Endocuticula (Abb. 3.5 B).

Die mechanischen Eigenschaften sind vom Probenzustand abhängig. Die statistischen Analysen der Härte und des Elastizitätsmoduls für verschiedene Zustände und Eindringtiefen (one-way ANOVA ($p < 0.0005$) und Tukey post tests ($p < 0.0005$) (Origin 7 SR2)) sind in Tabelle 3.1 zusammengefasst. Der Mittelwert der Härte (Abb. 3.8 A) der frischen Cuticulae ($H = 0.10 \pm 0.07$ GPa) liegt wesentlich niedriger als die Mittelwerte der trockenen ($H = 0.49 \pm 0.14$ GPa) und der chemisch behandelten ($H = 0.52 \pm 0.15$ GPa) Proben. Die Härtewerte der trockenen und chemisch behandelten Proben unterscheiden sich kaum. Für das Elastizitätsmodul kann die gleiche Tendenz beobachtet werden (Abb. 3.8 B). Die trockenen ($E = 7.50 \pm 1.80$ GPa) und die chemisch behandelten ($E = 7.70 \pm 1.90$ GPa) Proben sind wesentlich steifer als die frischen ($E = 1.50 \pm 0.80$ GPa). Durch die chemische Behandlung erhöht sich der Elastizitätsmodul leicht bis zu einer Eindringtiefe von 1000 nm.

Der Probenzustand beeinflusst die Oberflächen- und tribologischen Eigenschaften der Cuticula. Mit der Änderung des Probezustandes ändert sich die Rauhigkeit der *Gula*-Oberfläche (Tab. 4.1, Abb. 4.7). Der Einfluss des Probenzustandes auf den Kontaktwinkel ist

jedoch nicht zu erkennen (Abb. 4.9). Die *Gula*-Oberfläche bleibt in jedem Zustand hydrophob. Die frischen Cuticulae weisen höchste Kontaktflächenwerte und die trockenen niedrigste auf (Abb. 4.8). Die Reibungsexperimente zeigen, dass die tangentiale Kraft sich unabhängig vom Zustand der Probe mit der Erhöhung der anliegenden Kraft erhöht (Abb. 4.5). Der Reibungskoeffizient der frischen Proben liegt am höchsten, derjenige der chemisch behandelten am niedrigsten (Abb. 4.6). Mit zunehmender anliegender Kraft wird eine Abnahme des Reibungskoeffizienten beobachtet.

8.3.2 Struktur und mechanisches Verhalten der wachsbeschichteten Pflanzenoberflächen

Die rasterelektronenmikroskopischen Bilder wurden von beiden Seiten des Blattes aufgenommen. Die Blattoberflächen der Wilderbse (Abb. 5.2) und der Erbse mit der glatten Oberfläche (Abb. 5.3) unterscheiden sich in der Wachsbeschichtung. Die gesamte Blattoberfläche des Wildtyps ist von einer dichten Wachsschicht bedeckt, während der glatte Typ nur einzelne Wachskristalle aufweist. Wie durch den Vergleich der REM-Bilder abgeschätzt werden kann, weisen die Glatterbsenoberflächen ein Drittel der Wachsmenge des Wildtyps auf. Ein Unterschied kann auch zwischen der oberen und unteren Seite des Blattes eines Typs beobachtet werden. Die untere Seite des Wildtyps zeigt eine dichtere Wachsstruktur als die obere (Abb. 5.2 C und D). Die Wachskristalle auf der oberen Blattseite des glatten Typs erscheinen größer als auf der unteren Blattseite (Abb. 5.3 C und D). Die Abmaße der einzelnen Wachskristalle können für 1-2 µm im Durchmesser auf 100-200 nm Länge geschätzt werden (Abb. 5.2 E, F und 5.3 E, F).

Die frischen Pflanzenproben zeigen das gleiche mechanische Verhalten unabhängig vom Erbsentyp (wild oder glatt) (Abb. 5.4 und 5.5). Die trockenen Erbsenoberflächen weisen ein nachgiebigeres Deformationsverhalten auf als die frischen. Die Härte- und Elastizitätsmodulwerte der Eindringtiefen von 100 und 500 nm sind in der Tabelle 5.1 zusammengefasst. Die Härte aller frischen Blätter liegt im Bereich von 100 - 800 GPa (Abb. 5.6 und 5.7). Die trockenen Blätter des glatten Typs (H = 8 - 100 MPa für die obere Seite, H = 5 - 50 MPa für die untere Seite) sind härter als die trockenen Wilderbsenblätter (H = 210 MPa für die obere Seite, H = 0.3 - 10 MPa für die untere Seite). Im Bereich von 2-3 µm Eindringtiefe ist ein plötzlicher Abfall der Härtewerte der frischen Proben zu verzeichnen.

Der Elastizitätsmodul aller frischen Erbsenoberflächen liegt in Bereich von 25 GPa (Abb. 5.8 und 5.9). Die Pflanzen mit reduzierter Wachsbeschichtung (E = 300 - 2000 MPa für die obere Seite, E = 300 - 1500 MPa für die untere Seite) scheinen steifer als die Proben mit normaler Wachsbeschichtung zu sein (E = 200 - 600 MPa für die obere Seite, E = 100 - 500 MPa für die untere Seite).

8.4 Diskussion

Das mechanische Verhalten aller untersuchten Materialien wurde von der Austrocknung stark beeinflusst, was die einschlägige Literatur bestätigt (Andersen *et al.*, 2002; Vincent und Wegst, 2004). Der Wassergehalt ist ein entscheidender Faktor, um lokale mechanische Eigenschaften biologischer Proben mittels Nanoindentierung zu bestimmen. Jedoch sind die feuchtigkeitsabhängigen Änderungen der Härte und des Elastizitätsmoduls für die Insekten- und Pflanzencuticula unterschiedlich. Durch die Austrocknung wird die *Gula*-Cuticula härter und steifer, aber die Pflanzenoberflächen weicher und nachgiebiger.

8.4.1 Mechanisches Verhalten der *Gula* Cuticula

Die maximale Eindringtiefe in den Indentationsexperimenten betrug 3 µm. Wie in der Querschnittsstruktur (Abb. 3.5 B) der *Gula*-Cuticula ersichtlich war, betrug die Dicke der Epicuticula 7-8 µm. Daraus ist zu schließen, dass die Indentierungen innerhalb der obersten Oberflächenschicht, oder Epicuticula, durchgeführt wurden. Nach der, für die Härtemessung der dünnen Metallschichten entwickelten Modelle (Bueckle, 1965; Bhushan, 1996) zufolge, charakterisieren die Härtewerte innerhalb der ersten 700 nm die Epicuticula. Bei höheren Eindringtiefen, wird die Härte von den darunterliegenden Cuticulaschichten beeinflusst. Da die Elastizität ein weitreichender Effekt ist, wird sie größeren Bereichen des Verbundstoffes beeinflusst.

Die für die *Gula*-Cuticula gemessenen Härtewerte (0.1-0.5 GPa) und der Elastizitätsmodul (1.5 - 7.7 GPa) sind vergleichbar mit den Werten verschiedener sklerotisierter Cuticulae

(Vickers Härte 0.2 - 0.5 GPa und Elastizitätsmodul 1 - 10 GPa (Vincent and Wegst, 2004)). Jedoch liegt der Härtewert für die frische *Gula*-Cuticula (0.1 GPa) unter diesem Bereich (0.2-0.5 GPa). In der Literatur liegen Daten der Härtewerte für trockene oder rehydrierte Cuticula vor. Die lokalen mechanischen Eigenschaften der *Gula*-Cuticula sind in dieser Arbeit mittels Nanoindentation erstmals in natürlichem Zustand gemessen worden.

In diesen Untersuchungen war der Probenzustand nur eine Variable, welche die Änderungen mehrerer Oberflächeneigenschaften und folglich des tribo-mechanischen Verhaltens der *Gula*-Cuticula verursachte. Die Reibung war nicht nur von einem, sondern von mehreren Faktoren abhängig. Die tangentiale Kraft war in allen Versuchen von der anliegenden Kraft abhängig. Mit der Erhöhung der anliegenden Kraft wurden die Erhöhung der Tangentialkraft (Abb. 4.5) und die unerwartete Abnahme des Reibungskoeffizients beobachtet (Abb. 4.6). Die Mikroreibung wird durch die Adhäsion beeinflusst (Johnson *et al*., 1971; Rabinowicz, 1995; Scherge und Schaefer, 1998; Bhushan, 1999; Israelachvili, 2001; Scherge und Gorb, 2001; Hild *et al*, 2002). Mit der Erhöhung der angelegten Kraft erhöht sich die Kontaktfläche und somit die darauf wirkende Adhäsionskraft. Folglich ist eine Erhöhung des Reibungskoeffizients zu erwarten. Jedoch nimmt der Reibungskoeffizient ab. Die Reibungsversuche wurden mit zunehmender anliegender Kraft von 30 µN bis 10 mN durchgeführt. Die Oberfläche der *Gula*-Cuticula könnte beim Reiben gegen die Glasplatte beschädigt worden sein. Daher wirkt eine Adhäsionskraft bei der nächsthöheren anliegenden Kraft die Adhäsion nicht auf der gesamten, sondern nur auf der neu geschaffenen Kontaktfläche. Daraus kann man ableiten, dass die Wirkung der Adhäsion mit der Erhöhung den anliegenden Kräften abnimmt. Das kann eine Erklärung für die Abnahme des Reibungskoeffizienten sein.

Der Kontaktradius wurde aus den experimentellen und theoretischen Daten nach dem Hertz-Modell berechnet und miteinander verglichen (Abb. 4.13). Der Kurvenverlauf ist in beiden Fällen (experimentell und theoretisch) gleich, aber die experimentellen Werte liegen wesentlich höher als die theoretischen. Als Ursachen dieses großen Unterschiedes kommen einige Faktoren in Betracht. Bei den experimentellen Werten könnten die Adhäsionskräfte den Einfluss ausüben. Ein anderer Faktor könnte das Verwenden des lokalen Elastizitätsmoduls für die Berechnung der theoretischen Werte sein. Schließlich kann auch das Deformationsverhalten der Kugel (Hertz-Theorie) und der *Gula*-Curticula (kann als Shell betrachtet werden) von Bedeutung sein.

8.4.2 Mechanisches Verhalten der mit Wachs beschichteten Pflanzenoberflächen

Die Menge der Wachskristalle beeinflusst das mechanische Verhalten der trockenen Pflanzenoberflächen, aber nicht das der frischen. Die trockenen Proben mit reduzierter Wachsschicht sind härter und steifer als die mit normaler Wachschicht. Obwohl keine mechanischen Untersuchungen vorliegen, ist in der Literatur die Wachsschicht auch als "weich" bekannt (Barthlott, 1990; Barthlott *et al*., 1998). Überraschend ist es, dass die Wachsschicht keinen Einfluss auf den frischen Proben zeigt. Das bestätigen auch zahlreiche Untersuchungen mit anderen Pflanzen (unveröffentlichte Ergebnisse). Eine Erklärung könnte der Einfluss der darunterliegenden Zellstruktur sein. Auf Grund der Wirkung des Zellflüssigkeitsdruckes und der Zellwänden, weisen alle frischen Pflanzen gleiche Härte- und Elastizitätsmodulwerte auf.

Zwischen 2000 und 2500 nm Eindringtiefe wurde ein plötzlicher Abfall der Härte bei allen frischen Pflanzenproben beobachtet, obwohl auf der Kraft-Eindringtiefe-Kurve keine Änderung zu bemerken ist (Abb. 5.12). Die Härte wird mittels experimentell gemessener Kontakttiefe berechnet. Zwischen 2000 und 2500 nm Eindringstiefen erhöht sich die Kontakttiefe plötzlich (Abb. 5.13). Dadurch errechnet sich die hohe Kontaktfläche und folglich die niedrige Härte. Da die frischen Pflanzenblätter mit der Flüssigkeit gefühlt sind, könnte die Entstehung eines Wassertropfens um die Indenterspitze während des Versuches die Ergebnisse beeinflussen.

Das Kontaktverhalten zwischen der Berkovich Spitze und der mit Wachskristallen strukturierten Pflanzenoberflächen und die Verschmutzung der Indenterspitze durch die Wachskristalle kann die Ergebnisse verfälschen. Eine Lösung wäre das Verwenden der Indenterspitze von anderer Geometrie und/oder die Behandlung der Spitze.

8.5 Zusammenfassung

Das mechanische Verhalten biologischer Materialien wurde mittels materialwissenschaftlichen experimentellen Ansätzen in verschiedenen Zuständen (frisch, trocken, chemisch behandelt (nur Insektencuticula)) charakterisiert. Die Experimente wurden an der für die Reibungsreduzierung optimierten Cuticula des Kopfgelenksystems des Rosenkäfers (*Pachnoda marginata*) und an für die Haftprevention adaptierten wachsbeschichteten Pflanzenoberflächen (*Pisum sativum*) durchgeführt. Die mechanischen Eigenschaften den Insekten- und Pflanzencuticula ändern sich wesentlich in Abhängigkeit vom Feuchtigkeitsverlust. Nach der Austrocknung ist die Insektencuticula um den Faktor 4 härter und steifer als im natürlichen (frisch) Zustand, während die trockenen Pflanzenoberflächen mindestens um den Faktor 100 weicher und nachgiebiger als die frischen sind.

Tribologische Untersuchungen wiesen auf, dass die Reibung im Mikrometerbereich gleichzeitig von der anliegenden normalen Kraft und der Kontaktfläche abhängig ist. Es konnte gezeigt werden, dass die Reibung nicht nur von einem sondern von mehreren verschiedenen Oberflächeneigenschaften und Faktoren beeinflusst wird.

Die glatte Oberfläche der frischen *Gula*-Cuticula zeigte den höchsten Reibungskoeffizient. Als Gegenstück der *Gula*-Cuticula in den Reibungsexperimenten diente eine Glasplatte mit noch geringerer Rauheit, während in der Natur die *Gula*-Cuticula mit der stark strukturierten *Prothorax* Oberfläche im Kontakt ist.

Die Nanoindentierung kann für die Bestimmung der lokalen mechanischen Eigenschaften, der Härte und des Elastizitätsmoduls natürlicher Materialien mit niedriger Kontaktsteifigkeit erfolgreich verwendet werden. Mittels dieser Methode können die biologischen Proben in natürlichem Zustand untersucht werden. Da die biologischen Materialien schichtweise aufgebaut sind und ihre mechanischen Eigenschaften Tiefenabhängigkeit aufweisen, erlaubt die kontinuierliche Steifigkeitsmessung (CSM Methode) während des Versuchs die Berechnung der Härte und des Elastizitätsmoduls in jeder Eindringtiefe. Jedoch muss unter Berücksichtigung der Oberflächenrauhigkeit eine passende Geometrie der Indenterspitze gewählt werden.

9 References

Andersen, S. O. (1979) Insect cuticle. Annual Revue of Entomology, 24: 29-61.

Andersen, S. O., Peter, M. G. and Roepstorff, P. (1996) Cuticular Sclerotization in Insects. Comparative Biochemistry and Physiology, 113B (4): 689-705.

Arzt, E., Enders, S. and Gorb, S. (2002) Towards a micromechanical understanding of biological surface devices. Zeitschrift für Metallkunde, 93 (5): 345-351.

ASME (1979) Standard test method for microhardness of materials. ASME designation, E384-73: 359-379.

Avato, P., Bianchi, G. and Mariani, G. (1984) Epicuticular waxes of *Sorghum* and some compositional changes with plant age. Phytochemistry, 23: 2843-2846.

Baker, E. A. (1982) Chemistry and morphology of plant epicuticular waxes. In: The plant cuticle. Cutler, D. F., Alvin, K. L., Price, C. E. (*eds*.) Academic Press, London, pp. 139-165.

Baker, E. A. and Gaskin, R. E. (1987) Composition of leaf epicuticular waxes of *Pteridium* subspecies. Phytochemistry, 26: 2847-2848.

Ball; P. (2002) Natural strategies for the molecular engineer. Nanotechnology, 13: R15-R28.

Barber, N. H. (1955) Adaptive gene substitutions in Tasmanian Eucalyptus. I. Genes controlling glaucousness. Evolution, 9: 1-14.

Barthlott, W. (1990) Scanning electron microscopy of the epidermal surface in plants. In: Scanning electron microscopy in taxonomy and functional morphology. Claugher, D. (*ed*.) Clarendonpress, Oxford, pp. 69 - 83.

Barthlott, W. and Neinhuis, C. (1997) Purity of the sacred lotus or escape from contamination in biological surfaces. Planta, 202: 1-8.

Barthlott, W., Neinhuis, C., Cutler, D., Ditsch, F., Meusel, I., Theisen, I. and Wilhelmi, H. (1998) Classification and terminology of plant epicuticular waxes. Botanical Journal of the Linnean Society, 126 (3): 237-260.

Barwell, F. T. (1979) Bearing Systems. Oxford University Press, pp. 4-5.

Bianchi, G., Avato, P., Bertorelli, P. and Mariani, G. (1978) Epicuticular waxes of two sorghum varieties. Phitochemistry, 17: 999-1001.

Bianchi, G. (1995) Plant waxes. In: Waxes: chemistry, molecular biology and functions. Hamilton, R. J. (*ed.*). The Oily Press: Dundee, pp. 177-222.

Bhushan, B. (1996) Tribology and mechanics of magnetic storage devices. Springer-Verlag, New York.

Bhushan, B. (1999) Nanoscale tribophysics and tribomechanics. Wear. 225-229: 465-492.

Bhushan, B. (2001) Modern tribology handbook. Volumes 1 and 2. Boca Raton, FA, CRC press.

Bhushan, B. and Li, X. (2003) Nanomechanical characterization of solid surfaces and thin films. International Materials Reviews, 48 (3): 125-164.

Binnington, K. and Retnakaran, A. (1991) Physiology of the insect epidermis. CSIRO, Australia, Melbourne.

Bowden, F. P. and Tabor, D. (1950) The Friction and Lubrication of Solids. Clarendon Press, Oxford, UK.

Bueckle, H. (1965) Mikrohaertepruefung und ihre Anwendung. Stuttgart, Berliner Union.

Burnett, P. J. and Rickerby, D. S. (1987) The mechanical properties of wear-resistant coatings: I: Modelling of hardness behaviour. Thin Solid Films, 148: 41-50.

Burnett, P. J. and Rickerby, D. S. (1987) The mechanical properties of wear-resistant coatings: II: Experimental studies and interpretation of hardness. Thin Solid Films, 148: 51-65.

Ciulli, E. (2001) Friction in Lubricated Contacts: from Macro- to Microscale Effects. In: B. Bhushan (*ed*.) Fundamentals of Tribology and Bridging the Gap between the Macro- and Micro/Nanoscales. Kluwer Academic Publishers, Netherlands, pp. 725-734.

Dai, Z., Gorb, S. N. and Schwarz, U. (2002) Roughness-dependent friction force of the tarsal claw system in the beetle *Pachnoda marginata* (Coleoptera, Scarabaeidae). Journal of Experimental Biology, 205: 2479-2488.

Doerner, M. F. and Nix, W. D. (1986) A method for interpreting the data from depth-sensing indentation instruments. Journal of Materials Research, 1(4): 601 - 609.

Doerner, M. F., Oliver, W. C., Pharr, G. M. and Brotzen, F. R. (*eds*.) (1990) Thin films: stresses and mechanical properties II', MRS Symposium Proceedings, 188, Pittsburgh, PA, Materials research society.

Eigenbrode, S. D. and Espilie, K. E. (1995) Effects of plant epicuticular lipids on insect herbivores. Annual Review of Entomology, 40: 171-194.

Eigenbrode, S. D. (1996) Plant surface waxes and insect behaviour. In: Plant cuticles - an integral functional approach. BIOS Scientific Publishers Ltd, Oxford, pp. 201-222.

Eigenbrode, S. D. and Jetter, R. (2002) Attachment to Plant Surface Waxes by an Insect Predator. Integrative and Comparative Biology, 42: 1091-1099.

Enachescu, M., Van den Oetelaar, R. J. A., Carpick, R. W., Ogletree, D. F., Flipse, C. F. J. and Salmeron, M. (1999) Observation of proportionality between friction and contact area at the nanometer scale. Tribology Letters, 7: 73-78.

Enders, S. (2000) Untersuchungen der mechanischen Eigenschaften von spröden Schicht- und Kompaktsystemen durch Deformation kleiner Volumina. Dissertation, Martin-Luter-Universität Halle-Wittenberg, FB Physik.

Enders, S., Barbakadze, N., Gorb, S. N. and Arzt, E. (2004) Exploring biological surfaces by nanoindentation. Journal of Materials Research, 19 (3): 880-887.

Fraenkel, G. and Rudall, K. M. (1940) A study of the physical and chemical properties of the insect cuticle. Proceedings of the Royal Society, B 129: 1-34.

Fung, Y., C. (1993) Biomechanics, Mechanical Properties of Living Tissues. Springer-Verlag, pp. 500-544.

Gaume, L., Gorb, S. and Rowe, N. (2002) Function of epidermal surfaces in the trapping efficiency of *Nepenthes alata* pitchers. New Phytologist, 156: 479-489.

Gorb, S. N. (1997) Ultrastructural architecture of the microtrichia of the insect cuticle. Journal of Morphology, 234: 1-10.

Gorb, S. N. (1999a) Evolution of the dragonfly head-arresting system. Proceedings of the Royal Society of London, B 266: 525-535.

Gorb, S. N. (1999b) Ultrastructure of the thoracic dorso-medial field (TDM) in the elytra-to-body arresting mechanism in tenebrionid beetles (Coleoptera: Tenebrionidae). Journal of Morphology, 240: 101-113.

Gorb, S. N. and Scherge, M. (2000) Biological microtribology: anisotropy in frictional forces of orthopteran attachment pads reflects the ultrastructure of a highly deformable material. Proceedings of the Royal Society of London, B 267: 1239-1244.

Gorb, S. N. (2001) Attachment devices of the insect cuticle. Kluwer Academic Publishers, The Netherlands.

Gorb, S. N., Gorb, E. and Kastner, V. (2001) Scale effects on the attachment pads and friction forces in syrphid flies (Diptera, Syrphidae). Journal of Experimental Biology, 204: 1421-1431.

Gorb, E. V. and Gorb, S. N. (2002) Attachment ability of the beetle *Chrysolina fastuosa* on various plant surfaces. Entomologia Experimentalis et Applicata, 105: 13-28.

Gorb, E. and Gorb, S. (2002) Contact separation force of the fruit burrs in four plant species adapted to dispersal by mechanical interlocking. Plant Physiology and Biochemistry, 40: 373-381.

Gorb, S. N. and Perez Goodwyn, P. J. (2003) Wing locking mechanisms in aquatic Heteroptera. Journal of Morphology, 257 (2): 127-146.

Haberlandt, G. (1909) Physiologische Pflanzenanatomie. Engelmann, Leipzig.

Hallam, N. D. and Chambers, T. C. (1976) The leaf waxes of the genus Eucalyptus L'Heritier. Australian Journal of Botany, 18: 335-386.

Hammond, P. M. (1989) Wing-folding mechanism of beetles, with special reference to investigations of adephagen phylogeny (Coleoptera). In: Ervin, T., Ball, G. E. and Whitehead, D. R. (*eds*.) Carabid beetles: their evolution, natural history and classification. Boston, London: Junk Publishers: The Hague, pp. 113-180.

Hay, J. C., Bolshakov, A. and Pharr, G. M. (1999) A critical examination of the fundamental relations used in the analysis of nanoindentation data. Journal of Materials Research, 14: 2296-2305.

Hay, J. L. and Pharr, G. M. (2000) Instrumented indentation testing. ASM Handbook, 8.

Hepburn, H. R. and Joffe, I. (1976) On the material properties of insect exoskeletons. In: The insect integument. Hepburn, H. R. (*ed*.), Elsevier, Amsterdam, pp. 207-235.

Hepburn, H. R. and Chandler, H. D. (1976) Material properties of arthropod cuticles: the arthropodial membranes. Journal of Comparative Physiology, 109: 177-198.

Hepburn, H. R. and Chandler, D. (1980) Materials Testing of Arthropod Cuticle Preparations. In: Cuticle technologies in arthropods. Miller T. A. (*ed*.). New York, Springer Verlag, pp. 1-44.

Hertz, H. (1882) Über die Berührung fester elastischer Körper. Journal für die reine und angewandte Mathematik, 92: 156-171.

Hild, W., Schaefer, J. A. and Scherge, M. (2002) Microdynamical studies of hydrophilic and hydrophobic surfaces. In: Lubricants, Materials and Lubrication Engineering, 13th International Colloquium Tribology.

Hillerton, J. E., Reynolds, S. E. and Vincent, J. V. (1982) On the indentation hardness of the insect cuticle. The Journal of Experimental Biology, 96: 45-52.

Holmberg, K. (2001) Reliability aspects of tribology. Tribology international, 34: 801-808.

Hutchings, I. M. (1992) Tribology: friction and wear of engineering materials. Edward Arnold, A division of Hodden & Stoughton. London, Melbourn, Auckland.

Israelachvili, J. (2001) Tribology of ideal and non-ideal surfaces and fluids. In: B. Bhushan (*ed*.) Fundamentals of Tribology and Bridging the Gap between the Macro- and Micro/Nanoscales. Kluwer Academic Publishers, Netherlands, pp. 631-650.

Jeffree, C. E. (1986) The cuticle, epicuticular waxes and trichomes of plant, with references to their structure, functions and evolution. In: Insects and the plant surface. Juniper, B. E., Southwood, T. R. E. (*eds*.) Edward Arnold: London, pp. 23-64.

Jensen, M. and Weis-Fogh, T. (1962) Strength and elasticity of locust cuticle. In: Biology and Physics of locust flight. Philosophical Transactions of the Royal Society, B 245 pp. 137-169.

Joffe, I. and Hepburn, H. R. (1973) Observations on regenerated chitin films. Journal of Materials Science, 8: 1751–1754.

Johnson, K. L., Kendall, K. and Roberts, A. D. (1971) Surface energy and the contact of elastic solids. Proceedings of the Royal Society of London, Series A-Mathematical & Physical Sciences, 324: 301-313.

Jönsson, B. and Hogmark, S. (1984) Hardness measurements of thin films. Thin Solid Films, 114: 257-269.

Juniper, B. E. and Burras, J. K. (1962) How pitcher plants trap insects. New Scientist. 13: 75-77.

Juniper, B. E. and Southwood, R. (1986) Insects and the Plant Surfaces. London, UK: Edward Arnold.

Kempf, M. (2000) Biological materials, determination of Young's moduli of the insect cuticle (dragonflies; *Anisoptera*). Application note, Hysitron Inc, www.hysitron.com.

Kerner von Marilaun, A. (1898) Pflanzenleben 2. Bibliographisches Institut, Leipzig/Wien.

Klein, J. (2001) Interactions, Friction and Lubrication Between Polymer-Bearing Surfaces. In: B. Bhushan (*ed*.) Fundamentals of Tribology and Bridging the Gap between the Macro- and Micro/Nanoscales. Kluwer Academic Publishers, Netherlands, pp. 631-650.

Knoll, F. (1914) Über die Ursache des Ausgleitens der Insektenbeine an wachsbedekten Pflanzendteilen. Jahrbuch für Wissenschaftliche Botanik, 54: 448-497.

Kohane, M., Daugela, A., Kutomi, H., Charlson, L., Wyrobek, A. and Wyrobek, J. (2003) Nanoscale *in vivo* evaluation of the stiffness of *Drosophila melanogaster* integument during development. Wiley Periodicals, Inc.: 633-642.

Korsunsky, A. M., McGurk, M. r., Bull, S. J. and Page, T. F. (1998) On the hardness of coated systems. Surface Coatings Technology, 99: 171-183.

Kreuz, P., Kesel, A., Kempf, M., Göken, M., Vehoff, H. and Nachtigall, W. (1999) Mechanische Eigenschaften biologischer Materialien am Beispiel Insektenflügel. BIONA report, 14: 201-202.

Li, X. and Bhushan, B. (2002) A review of nanoindentation continuous stiffness measurement technique and its applications. Materials Characterization, 48: 11-36.

Locke, M. (1964) The structure and formation of the integument in insects. In: The physiology of Insecta. Rockstein M. (*ed*.), Academic Press, New York, pp. 123-213.

Ludema, K. (2000) Tribology at the Transition of Millennia. Lubrication Engineering, 54-57.

McGurk, M. R., Chandler, H. W., Twigg, P. C. and Page, T. F. (1994) Modelling the hardness response of coated systems: the plate bending approach. Surface Coatings Technology, 68/69: 576-581.

Neville, A. C. (1975) Biology of the arthropod cuticle. Springer Verlag, Berlin, Germany.

Niederegger, S., Gorb, S. and Jiao, Y. (2002) Contact behaviour of tenent setae in attachment pads of the blowfly *Calliphora vicina* (Diptera, Calliphoridae). Journal of Comparative Physiology, A 187: 961-970.

Nix, W. D.,Bravman, J. C., Arzt, E. and Freund, L. B. (*eds*.) (1992) Thin films: stresses and mechanical properties III', MRS Symposium Proceedings, 239, Pittsburgh, PA, Materials research society.

Oliver, W. C. and Pharr, G. M. (1992) An improved technique for determining hardness and elastic modulus using load and displacement sensing indentation experiments. Journal of Materials Research, 7 (6): 1564-1583.

Perez Goodwyn, P. J. and Gorb, S. N. (2004) Anti-frictional properties of contacting surfaces in the hemelytra-hindwing locking mechanism in the bug *Coreus Marginatus* (Heteroptera, Coreidae). Journal of Morphology (in press).

Persson, B. N. J. (1997) In: B. Bhushan (*ed*.) Micro/Nanotechnology and its Application, Kluwer, Dordrecht.

Persson, B. N. J. (1998) Sliding friction. Springer: Berlin, Heidelberg, New York.

Pethica, J. B. Hutchings, R. and Oliver, W. C. (1983) Hardness measurement at penetration depths as small as 20 nm. Philosopical Magazine, A 48: 593-606.

Phillips, M. A. (2003) Microstructure and mechanical properties of AL/AL3SC metallic multilayers – deformation mechanisms at the nanoscale. Dissertation, Stanford University, Department of Materials Science and Engineering.

Rabinowicz, E. (1995) Friction and Wear of Materials. 2nd ed. Wiley Interscience. New York, Chichester, Brisbane, Toronto, Singapore.

Rother, B. and Jehn, H. A. (1996) Coating and interface characterization by depth-sensing indentation experiments. Surface and Coatings Technology, 85: 183-188.

Scherge, M. and Gorb, S. N. (2000) Microtribology of biological materials. Tribology Letters, 8: 1-7.

Scherge, M. and Gorb, S. (2001) Biological micro- and nanotribology, natures solutions. Springer Verlag, Berlin, Germany.

Scherge, M. and Schaefer, J. A. (1998) Microtribological investigations of stick/slip phenomena using a novel oscillatory friction and adhesion tester. Tribology Letters, 4: 37-42.

Stork, N. E. (1980) Role of wax blooms in preventing attachment to brassicas by the mustard beetle, *Phaedon cochleariae*. Entomologia Experimentalis et Applicata, 28: 100-107.

Tabor, D. (1951) The hardness of metals. Oxford, Clarendon Press.

Tabor, D. (1996) Indentation hardness: fifty years on a personal view. Philosopical Magazine, A 74: 1207 -1221.

Tichy, J. A.and Meyer, D. M. (2000) Review of solid mechanics in tribology. International Journal of Solids and Structures, 37: 391-400.

Vincent, J. F. V. (1980) Insect cuticle - a paradigm for natural composites. In: The mechanical properties of biological materials. Symposium of the Society Experimental Biology, 34: 181-210.

Vincent, J. F. V. (1990) Structural Biomaterials. The University Press, Princeton.

Vincent, J. F. V. (2002) Arthropod cuticle –a natural composite shell system. Composite Part A - Applied Science and Manufacturing, 33 (10): 1311-1315.

Vincent, J. F. V. and Wegst, U.G. K. (2004) Design and mechanical properties of insect cuticle. Arthropod Structure & Development, 33: 187-199.

Wainwright, S. A., Biggs, W. D., Currey, J. D. and Gosline, J. M. (1976) Mechanical Design in Organisms. Princeton University Press.

Walton, T. J. (1990) Waxes, cutin and suberin. In: Lipids, membranes and aspects of photobiology, Dey, P. M., Harborne, J. B. (*eds*.), pp. 105-158.

Wegst, U. G. K. and Ashby, M. F. (2004) The mechanical efficiency of natural materials. Philosophical Magazine, 84, 21: 2167-2181.